INTERNATIONAL STANDARD

ISO 13232-3

Second edition
2005-12-15

Motorcycles — Test and analysis procedures for research evaluation of rider crash protective devices fitted to motorcycles —

Part 3: Motorcyclist anthropometric impact dummy

Motocycles — Méthodes d'essai et d'analyse de l'évaluation par la recherche des dispositifs, montés sur les motocycles, visant à la protection des motocyclistes contre les collisions —

Partie 3: Mannequin anthropométrique de motocycliste pour essais de choc

Reference number
ISO 13232-3:2005(E)

PDF disclaimer

This PDF file may contain embedded typefaces. In accordance with Adobe's licensing policy, this file may be printed or viewed but shall not be edited unless the typefaces which are embedded are licensed to and installed on the computer performing the editing. In downloading this file, parties accept therein the responsibility of not infringing Adobe's licensing policy. The ISO Central Secretariat accepts no liability in this area.

Adobe is a trademark of Adobe Systems Incorporated.

Details of the software products used to create this PDF file can be found in the General Info relative to the file; the PDF-creation parameters were optimized for printing. Every care has been taken to ensure that the file is suitable for use by ISO member bodies. In the unlikely event that a problem relating to it is found, please inform the Central Secretariat at the address given below.

ISO copyright office
Case postale 56 • CH-1211 Geneva 20
Tel. + 41 22 749 01 11
Fax + 41 22 749 09 47
E-mail copyright@iso.org
Web www.iso.org

Published in Switzerland

Contents

Page

Figures

Tables

Foreword

ISO (the International Organization for Standardization) is a worldwide federation of national standards bodies (ISO member bodies). The work of preparing International Standards is normally carried out through ISO technical committees. Each member body interested in a subject for which a technical committee has been established has the right to be represented on that committee. International organizations, governmental and non-governmental, in liaison with ISO, also take part in the work. ISO collaborates closely with the International Electrotechnical Commission (IEC) on all matters of electrotechnical standardization.

International Standards are drafted in accordance with the rules given in the ISO/IEC Directives, Part 2.

The main task of technical committees is to prepare International Standards. Draft International Standards adopted by the technical committees are circulated to the member bodies for voting. Publication as an International Standard requires approval by at least 75 % of the member bodies casting a vote.

ISO 13232-3 was prepared by Technical Committee ISO/TC 22, *Road vehicles*, Subcommittee SC 22, *Motorcycles*.

This second edition cancels and replaces the first version (ISO 13232-3:1996), which has been technically revised.

ISO 13232 consists of the following parts, under the general title *Motorcycles — Test and analysis procedures for research evaluation of rider crash protective devices fitted to motorcycles*:

— *Part 1: Definitions, symbols and general considerations*

— *Part 2: Definition of impact conditions in relation to accident data*

— *Part 3: Motorcyclist anthropometric impact dummy*

— *Part 4: Variables to be measured, instrumentation and measurement procedures*

— *Part 5: Injury indices and risk/benefit analysis*

— *Part 6: Full-scale impact-test procedures*

— *Part 7: Standardized procedures for performing computer simulations of motorcycle impact tests*

— *Part 8: Documentation and reports*

Introduction

ISO 13232 has been prepared on the basis of existing technology. Its purpose is to define common research methods and a means for making an overall evaluation of the effect that devices which are fitted to motorcycles and intended for the crash protection of riders, have on injuries, when assessed over a range of impact conditions which are based on accident data.

It is intended that all of the methods and recommendations contained in ISO 13232 should be used in all basic feasibility research. However, researchers should also consider variations in the specified conditions (for example, rider size) when evaluating the overall feasibility of any protective device. In addition, researchers may wish to vary or extend elements of the methodology in order to research issues which are of particular interest to them. In all such cases which go beyond the basic research, if reference is to be made to ISO 13232, a clear explanation of how the used procedures differ from the basic methodology should be provided.

ISO 13232 was prepared by ISO/TC 22/SC 22 at the request of the United Nations Economic Commission for Europe Group for Road Vehicle General Safety (UN/ECE/TRANS/SCI/WP29/GRSG), based on original working documents submitted by the International Motorcycle Manufacturers Association (IMMA), and comprising eight interrelated parts.

This revision of ISO 13232 incorporates extensive technical amendments throughout all the parts, resulting from extensive experience with the standard and the development of improved research methods.

In order to apply ISO 13232 properly, it is strongly recommended that all eight parts be used together, particularly if the results are to be published.

Motorcycles — Test and analysis procedures for research evaluation of rider crash protective devices fitted to motorcycles —

Part 3: Motorcyclist anthropometric impact dummy

1 Scope

This part of ISO 13232 specifies the minimum requirements for the:

— biofidelity of the motorcyclist anthropometric impact dummy;

— compatibility of the dummy with motorcycles, helmets, multi-directional impacts, and the instrumentation;

— repeatability and reproducibility of the dummy properties and responses.

ISO 13232 specifies minimum requirements for research into the feasibility of protective devices fitted to motorcycles, which are intended to protect the rider in the event of a collision.

ISO 13232 is applicable to impact tests involving:

— two-wheeled motorcycles;

— the specified type of opposing vehicle;

— either a stationary and a moving vehicle or two moving vehicles;

— for any moving vehicle, a steady speed and straight-line motion immediately prior to impact;

— one helmeted dummy in a normal seating position on an upright motorcycle;

— the measurement of the potential for specified types of injury, by body region;

— evaluation of the results of paired impact tests (i.e. comparisons between motorcycles fitted and not fitted with the proposed devices).

ISO 13232 does not apply to testing for regulatory or legislative purposes.

2 Normative references

The following referenced documents are indispensable for the application of this document. For dated references, only the edition cited applies. For undated references, the latest edition of the referenced document (including any amendments) applies.

ISO 13232-1, *Motorcycles — Test and analysis procedures for research evaluation of rider crash protective devices fitted to motorcycles — Part 1: Definitions, symbols, and general considerations*

ISO 13232-4, *Motorcycles — Test and analysis procedures for research evaluation of rider crash protective devices fitted to motorcycles — Part 4: Variables to be measured, instrumentation and measurement procedures*

ISO 13232-6, *Motorcycles — Test and analysis procedures for research evaluation of rider crash protective devices fitted to motorcycles — Part 6: Full-scale impact test procedures*

ISO 13232-8, *Motorcycles — Test and analysis procedures for research evaluation of rider crash protective devices fitted to motorcycles — Part 8: Documentation and reports*

ISO 6487, *Road vehicles — Measurement techniques in impact tests — Instrumentation*

49 CFR Part 572, subpart E: 1993, Anthropomorphic test dummies, United States of America Code of Federal Regulations issued by the National Highway Traffic Safety Administration (NHTSA). Washington, D.C.

3 Definitions

The following terms are defined in ISO 13232-1. For the purposes of this part of ISO 13232, those definitions apply. Additional definitions which could apply to this part of ISO 13232 are also listed in ISO 13232-1:

— abdominal foam insert;

— alternative products;

— certification, compliance;

— knee compliance element;

— load cell simulator;

— lot;

— specimen.

4 Mechanical requirements for the motorcyclist anthropometric impact dummy

4.1 Basis dummy

The basis dummy shall be the Hybrid III 50th percentile male dummy[1)]. The dummy shall be equipped with:

— the sit/stand construction[2)];

— the head/neck assembly which is compatible with the six axis upper neck load cell which is specified in 4.4.1.2 of ISO 13232-4[2)];

— standard, non-sliding knees[2)].

The basis dummy specified components shall be modified or replaced as described below.

---

1) Basis dummy as specified in 49 CFR Part 572, subpart E, or equivalent.

2) A list describing one or more example products which meet these requirements is maintained by the ISO Central Secretariat and the Secretariat of ISO/TC 22/SC 22. The list is maintained for the convenience of users of ISO 13232 and does not constitute an endorsement by ISO of the products listed. Alternative products may be used if they can be shown to lead to the same results.

4.2 Motorcyclist dummy head and head skins

The head skin components shall include the two basis Hybrid III head skins, plus two extensions which provide helmet compatibility. The geometries of the head skins and extensions are shown in Figure A.1, where 1 and 2 are the basis Hybrid III head and rear skull cap skins and 3 and 4 are the jaw and nape extensions which provide helmet compatibility. The masses of the jaw and nape skin extensions shall be 0,27 kg ± 0,05 kg and 0,15 kg ± 0,05 kg, respectively[2)]. The head-neck skin modifications to the Hybrid III head shall be attached by means of any suitable adhesive. Such an adhesive shall be shown to provide a bond between the mating parts in which the parent material will fail under tensile loading before the bond itself. Cyanoacrylate is an example of a suitable adhesive.

The complete assembly of the head, head skins, head skin extensions, head accelerometer mount, head accelerometers and cables, and neck load cell and cables shall have a mass of 5,35 kg ± 0,1 kg.

4.3 Motorcyclist dummy neck components

The complete assembly of the neck, nodding blocks, head attachment pin, bib simulator, and the upper half of the serrated lower neck mount shall have a mass of 1,55 kg ± 0,1 kg.

4.3.1 Neck shroud

The neck shroud shall be as specified in Figure A.2[2)]. The upper half of the zipper of the neck shroud shall be attached to the jaw skin extension by means of any suitable adhesive. Such an adhesive shall be shown to provide a bond between the mating parts in which the parent material will fail under tensile loading before the bond itself.

Note - “Loctite® 401”[2)] cyanoacrylate is an example of a suitable adhesive.

4.3.2 Lower neck mount

When mounting the motorcyclist neck the lower neck mount shall be set at the 5,25 degree extension position. This is appropriate for most dummy rider positioning. However, in cases of extreme dummy posture, the basis Hybrid III lower neck mount may be modified as shown in Figure A.3 to increase head position adjustability[2)].

4.3.3 Motorcyclist neck

The standard Hybrid III neck and its interfaces with the head and upper torso assembly shall be replaced by the neck shown in Figure A.4[2)].

NOTE The neck shown in Figure A.4 is designed specifically for use in motorcycle crash testing. Use and limitation information is contained in B.2.5.

4.3.4 Replacement nodding blocks

The standard Hybrid III nodding blocks shall be replaced with the pair of nodding blocks shown in Figure A.4[2)].

4.3.5 Neck initial conformity of production

For certification of a new neck and nodding block production design, material specification or manufacturing process which otherwise meet the specifications given in Figure A.4, one neck shall be dynamically tested according to the procedures described in 6.8. The neck responses shall be within the corridors described in 6.8 and shown in figures 1, 2, 3, 4, 5, 6, and 7.

4.3.6 Neck subsequent conformity of production

Once a production design, material specification or manufacturing process has been certified according to 4.3.5, each manufactured neck and nodding block assembly produced thereafter shall be tested according to the procedures in 6.9 to verify the characteristics specified in Table 1.

Table 1 — Neck subsequent conformity of production specifications

Static Test	Characteristics	Required average value	% Required standard deviation
Flexion	Flexion angle	17,6 ± 2,6 °	10% of average value
Flexion	Slider displacement	14,0 ± 3,0 mm	10% of average value
Extension	Extension angle	30,9 ± 4,6 °	10% of average value
Lateral	Lateral angle	28,7 ± 4,3 °	10% of average value
Torsion	Torsion angle	41,5 ± 6,2 °	10% of average value

4.4 Motorcyclist dummy upper torso components

4.4.1 Replacement thoracic spine

Either a standard Hybrid III thoracic spine, or a replacement thoracic spine[2)] shall be used. If a replacement spine is used, then the replacement thoracic spine shall be compatible with the internal data acquisition system described in ISO 13232-4. When combined with the internal data acquisition system, the replacement thoracic spine shall:

— maintain the same interface geometry and overall height as the standard Hybrid III spine box, including the shoulder, rib, lower neck mount, and lumbar spine attachment points;

— not interfere with the motion of the shoulders;

— provide at least 75 mm of sternum deflection in the sagittal plane, measured perpendicularly, relative to the front surface of the spine box;

— not exceed 125 mm in lateral width;

— result in the same upper torso mass and centre of gravity as specified for a standard Hybrid III upper torso except that the centre of gravity tolerance shall be ± 30 mm.

4.4.2 Modified chest skin

With the chest skin properly installed on the upper torso, the back of the chest skin may be modified with four holes which expose the two upper and two lower rib attachment screws in order to enable measurement of the upper torso angle, using a torso inclinometer such as the example shown in ISO 13232-6, Figure C.1.

4.5 Motorcyclist dummy lower torso components

When fully assembled, the lower torso assembly shall result in the same lower torso mass as specified for the standard Hybrid III lower torso[3)].

4.5.1 Modified straight lumbar spine

For use with either the six-axis or three-axis lumbar load cell, the straight lumbar spine and cable shall be FTSS part numbers 1260004 and 1260005[4)]. The lower lumbar spine transducer mount and ballast block shall be replaced with the part shown in Figure A.5 for a six-axis load cell[2)] and in Figure A.6 for a three-axis load cell[2)]. An

---

3) Refer to General Motors Hybrid III drawing numbers 78051-70 and 78051-338 in 49 CFR Part 572.

4) Parts 1260004 and 1260005 are products supplied by First Technology Safety Systems, Plymouth, Michigan, USA. This information is given for the convenience of users of ISO 13232 and does not constitute and endorsement by ISO of the product named. Alternative products may be used if they can be shown to lead to the same results.

abdomen reaction plate, as shown in Figure A.7 revision 1 for the six-axis load[2)] cell or Figure A.8 for the three-axis load cell[2)], shall be mounted to the lower lumbar spine transducer mount and ballast block.

When assembling the pelvis and ballast block, if hard contact interference prevents the proper positioning of the parts either part may be trimmed as required to facilitate the assembly.

When using the dummy without either of the permissible lumbar load cells described in 4.4.1.4 of ISO 13232-4, the load cell shall be replaced with a lumbar load cell simulator[2)].

4.5.2 Motorcyclist dummy abdominal insert

The basis Hybrid III abdominal insert shall be replaced with a frangible solid abdominal insert, as shown in Figure A.9. The replacement insert shall have a mass of 53 g ± 3 g.

When tested according to the method described in 6.7, the specified values of force shall be as given in Table 2[2)].

Table 2 — Specified values for certification of replacement abdominal insert

Deflection mm	Force N
20	1 040
40	1 875
60	2 810

4.5.3 Sit/stand pelvis

The internal data acquisition system may be contained within a sit/stand pelvis which has been suitably modified to accommodate it[2)]. Whether modified or not, the sit/stand pelvis shall:

— maintain the same interface geometry and external dimensions as the standard Hybrid III sit/stand pelvis;

— not interfere with the motion of the legs.

4.6 Arms and modified elbow bushing

The Delrin elbow bushing, Hybrid III part number 78051-199[5)], shall be modified with scribe marks, as shown in Figure A.10.

The masses of the upper and lower arms shall be as specified for a standard Hybrid III.

4.7 Motorcyclist dummy hands

The basis Hybrid III hands shall be replaced with the Itoh-Seiki Co. part number 065-322048[6)].

4.8 Motorcyclist dummy upper leg components

The mass of the upper leg assembly shall be 4,89 kg ± 0,2 kg.

---

5) Refer to General Motors Hybrid III drawing number 78051-199 in 49 CFR Part 572.

6) Part number 065-322048 is a product supplied by Itoh-Seiki Co., Tokyo, Japan. This information is given for the convenience of users of ISO 13232 and does not constitute an endorsement by ISO of the product named. Alternative products may be used if they can be shown to lead to the same results.

4.8.1 Frangible femur bone and mounting hardware

The frangible femur bone shall be mounted to the knee joint using the adaptor shown in Figure A.11[2)]. The frangible femur bone shall meet the interface and size requirements shown in Figure A.12, and have a mass 85 g ± 10 g. The frangible bone materials and design shall remain constant in the axial direction along the minimum frangible length, as shown in Figure A.12.

When statically tested according to the methods described in 6.1, 6.2, and 6.5, the specified values of the static deflection and strength of the bone shall be as given in Table 3. When dynamically fractured according to the methods described in 6.3 and 6.4, the specified values of the peak strength of the bone shall be as given in Table 3[2)].

Table 3 — Specified values for certification of frangible femur components

	Static deflection	Dynamic peak strength	Static strength
Bending	5,1 mm	360 N·m	-
Torsion	5,8°	205 N·m	-
Axial loading	-	-	34 680 N

4.8.2 Femur load cell simulator

When using the dummy without the permissible femur load cells described in 4.4.1.5 of ISO 13232-4, the load cell shall be replaced with an upper femur load cell simulator, as shown in Figure A.13[2)].

4.9 Motorcyclist dummy frangible knee assembly

The frangible knee assembly and the interface with the knee clevis assembly shall be as shown in Figure A.14. The knee assembly shall have a mass of 1,00 kg ± 0,05 kg.

When statically tested according to the methods described in 6.6, the specified values of the rotational angles for the defined moments shall be as given in Table 4. The specified values of the rotational angles and moments which indicate peak strength at shear pin failure shall be as given in Table 4[2)].

Table 4 — Specified values for certification of frangible knee assembly components

Degree of Freedom	Condition	Specified value
Valgus	Rotation at 89 N·m (pre-failure)	20,0°
	Maximum torque	132 N·m
	Rotation at maximum torque	25,0°
Torsion	Rotation at 35 N · m (pre-failure)	20,0°
	Maximum torque	87 N·m
	Rotation at maximum torque	40,0°

4.10 Leg retaining cables

Each frangible leg bone shall be installed together with leg retaining cables to prevent the loss of portions of the dummy leg when the frangible bone fractures. The total cable mass shall not exceed 200 g for each frangible bone. The cables shall be installed with at least 5 mm of slack[2)].

4.11 Motorcyclist dummy lower leg components

The mass of the lower leg and foot assembly shall be 5,29 kg ± 0,2 kg.

4.11.1 Frangible tibia bone and mounting hardware

The frangible tibia bone shall be mounted to the ankle joint using the adaptor shown in Figure A.15[2)]. The bone shall meet the interface and size requirements shown in Figure A.16 and have a mass of 120 g ± 10 g. The frangible bone materials and design shall remain constant in the axial direction along the minimum frangible length, as shown in Figure A.16.

When statically tested according to the methods described in 6.1 and 6.2, the specified values of the static deflection of the bone shall be as given in Table 5. When dynamically fractured according to the methods described in 6.3 and 6.4, the specified values of the peak strength of the bone shall be as given in Table 5[2)].

Table 5 — Specified values for certification of frangible tibia components

	Static deflection	Dynamic peak strength
Bending	3,8 mm	280 N·m
Torsion	7,0°	171 N·m

4.11.2 Modified lower leg skin

The basis Hybrid III lower leg skins shall be modified according to Figure A.17, to:

— include a vertically aligned rear surface zipper to permit installation and removal of the skin from the leg;

— conform to the frangible knee structure.

The mass shall be 1,05 kg ± 0,10 kg.

4.12 Complete motorcyclist dummy

When fully assembled the complete motorcyclist dummy shall have a mass of 75,84 kg ± 1,64 kg.

4.13 Certification documentation

The manufacturers of dummies or dummy components which are intended to meet ISO 13232, shall provide with the supplied dummies or dummy components, certification that the dummies or dummy components meet the requirements specified below.

5 Sampling of frangible components

5.1 Initial conformity of production

For certification of any new design, material specification, or manufacturing process of any frangible component and for each of the test methods described in clause 6, ten unused components shall be tested to establish estimates of the sample's mean and standard deviation. For example, certification of three different test methods would require 30 components to be tested.

The sample mean value shall be within ± 5% of the specified value for all strengths and abdominal insert static forces. The sample mean value shall be within ± 20% of the specified value for all static deflections. The sample standard deviation shall be less than 7% of the sample mean value for all strengths and abdominal insert static forces. The sample standard deviation shall be less than 10% of the sample mean value for all static deflections.

5.2 Subsequent conformity of production

Once a specific design, material specification, and manufacturing process have been certified, three components from each lot which is identically manufactured shall be tested to verify the applicable characteristics specified in Table 6.

Table 6 — Frangible component subsequent conformity of production characteristics

Component	Characteristic
Frangible abdominal insert	Forces at 40 mm deflection
Frangible leg bone	Dynamic bending strength
Knee shear pin	Failure moments given in Table 4
Knee compliance element	Pre-failure rotations given in Table 4

If none of the components deviates by more than two standard deviations, as defined in 5.1, from the established mean value for the specified characteristic, the lot shall be considered acceptable for full-scale impact testing, according to ISO 13232-6. If one or more of the tested components deviate by more than two standard deviations, as defined in 5.1, from the established mean value for the specified characteristic, a different sample of three components from the same lot shall be tested. If more than two of the total sample of six components deviate by more than two standard deviations, as defined in 5.1, from the established mean values, the said lot shall not be used for full-scale impact testing.

5.3 Condition of sampled frangible components

For the testing specified in 5.1 and 5.2, such sampling shall be performed using new, unused frangible components.

6 Test methods

6.1 Frangible bone static bending deflection test

Using pins, attach rigid extensions of equal length, as shown in Figure A.18, to each end of the frangible bone such that the minimum combined length of the bone and extensions is as given in Table 7. Support the specimen radially at both ends, at the distances given in Table 7. Place a 25 mm diameter solid rigid cylindrical bar at the mid-span location, perpendicular to the specimen axial axis with the curved surfaces of the bone and bar in contact with each other. Apply a radial load as given in Table 7.

Table 7 — Frangible bone static bending deflection test specifications

	Minimum combined length mm	Distance between supports mm	Applied radial load N
Femur	355	341	1 350 ± 25
Tibia	300	286	1 450 ± 25

Measure the perpendicular linear deflection at the mid-span location of the specimen relative to the supported ends.

6.2 Frangible bone static torsional deflection test

Apply a torsional load of 69 N · m to the femur and 48 N · m to the tibia. Measure the torsional deflection of one end of the bone relative to the other end.

6.3 Frangible bone dynamic bending fracture test

Using pins, attach rigid extensions and support the specimen as described in 6.1, using the bone extensions shown in Figure A.18 and the specimen supports shown in Figure A.19. Align the specimen so that it is perpendicular to both the cylindrical bar and the direction of motion of the impactor head, shown in Figure A.20. Attach the impactor head to the impactor device, which is shown in Figures A.21 through A.24. Impact the specimen at 7,5 m/s ± 0,2 m/s at mid-span, using the impacting mass shown in Figure A.21.

Measure the impactor linear acceleration from just before bone contact until just after bone fracture, with an Endevco accelerometer, model 2262A-1000[7)] rigidly mounted to the impactor at the location shown in Figure A.21. Filter the data with an analog filter such that the data is attenuated by at least 40 dB at and above a frequency of 7 kHz. Sample the data at 10 kHz and filter the digital data such that the frequency response of the data output to the unfiltered analog input is in accordance with ISO 6487, CFC 600. Determine the peak linear acceleration related to the impact with the bone. Calculate the maximum bending moment as shown for this example:

$$M_{x,max} = (0{,}25)\,(9{,}807)\,d_s\ \mathrm{m}\ a_{m,max}$$

where

$M_{x,max}$ is the maximum bending moment, in Newton-metres;

d_s is the distance between supports, in metres;

m is the mass of the impactor, in kilograms;

$a_{m,max}$ is the maximum linear acceleration of the impactor mass, in g units;

9,807 is a conversion factor from g units to newtons.

6.4 Frangible bone dynamic torsional fracture test

Attach a rigid extension to each end of the frangible bone and restrain one end of the resulting specimen with a Denton load cell, model B-2193[8)]. Attach a rigid moment arm to one of the rigid extensions, such that it extends

7) Model 2262A-1000 is a product supplied by Endevco Corp., San Juan Capistrano, California, USA. This information is given for the convenience of users of ISO 13232 and does not constitute an endorsement by ISO of the product named. Alternative products may be used if they can be shown to lead to the same results.

8) Load cell model B-2193 is a product supplied by Robert A. Denton, Inc., Rochester Hills, Michigan, USA. This information is given for the convenience of users of ISO 13232 and does not constitute an endorsement by ISO of the product named. Alternative products may be used if they can be shown to lead to the same results.

perpendicularly from the axial axis of the specimen. Impact the moment arm at 7,5 m/s ± 0,2 m/s at a distance 0,150 m ± 0,005 m from the axial axis of the specimen. Impact with a solid rigid cylindrical bar with a diameter of 0,025 m ± 0,003 m and a total impacting mass greater than 50 kg. Orient the cylindrical bar to be perpendicular to the direction of travel and to the moment arm.

Measure the bone torque using the load cell and filtering and sampling according to the method described in 6.3. Determine the maximum torsional moment.

6.5 Frangible femur bone static axial load fracture test

Attach a rigid fixture to each end of the frangible bone such that any compressive load is transferred to the bone through the bone mounting bolt. Place the specimen in a hydraulic press, as shown in Figure A.25, such that the centre line is aligned with the centre line of the hydraulic plunger and the lower end fixture is centred on a Denton load cell, model B-2193[8)] . Apply a continually increasing load at a rate of 6 500 N/s $\pm$ 2 000 N/s until failure occurs. Electronically record the applied load until the time of failure.

6.6 Frangible knee static strength and deflection test

6.6.1 Apparatus

Use either the apparatus shown in Figure A.26, or the equivalent, including a

— lever arm with minimum length of 0,5 m;

— load cell located at the load application point;

— rotational potentiometer.

6.6.2 Procedure

Apply a continually increasing moment to the frangible knee valgus or torsional axis, at a rate of 30 N · m/s ± 5 N · m/s. Record the rotational angle and applied moment until shear pin failure occurs.

6.7 Frangible abdomen test

Use the apparatus shown in Figure A.27, or the equivalent. Apply a continually increasing load to the centre of an unused frangible abdominal insert at a rate of 450 N/s ± 150 N/s. Record the crush deflection and applied load up to a load greater than 3 300 N.

6.8 Motorcyclist neck dynamic test for initial conformity of production

6.8.1 Dynamic extension test

Assemble a Hybrid III lower neck mount (set at 5,25 degrees extension), the motorcyclist neck to be tested (with nodding blocks and without the shroud), a Denton upper neck load cell (model 1716[9)]) and a standard Hybrid III head. Set the mid neck angle adjustment to the full forward (flexion) position.

Mount the assembly on an acceleration sled and apply an acceleration to the base of the neck which meets the criteria of Table 8. Measure the upper neck M_y moment with the Denton 1716 load cell[9)] and the change in head pitch angle.

9) Load cell model 1716 is a product supplied by Robert A. Denton, Inc., Rochester Hills, Michigan, USA. This information is given for the convenience of users of ISO 13232 and does not constitute an endorsement by ISO of the product named. Alternative products may be used if they can be shown to lead to the same results.

Table 8 — Neck extension sled pulse criteria

Peak acceleration	5,8 ± 0,5 G
Average acceleration above 1.0 G	4,3 ± 0,5 G
Overall velocity change	4,5 ± 0,3 m/s

Measure the change in head pitch angle directly with an external goniometer, or by high-speed photographic means.

Use high-speed film or video with a minimum frame rate of 1 000 frames per second. Use target decals on the dummy head for this measurement, correcting for parallax error. Synchronize the time-base of this data recording with that of the M_y data.

Process the moment data according to SAE J211, CFC600. Process the electronic angle measurement according to SAE J211, CFC180.

Plot the neck moment (M_y) versus change in head pitch angle on a graph, along with the corridor described in Table 9, and shown in Figure 1.

Table 9 — Neck extension bending corridor

Change in head angle (degrees)	**Extension moment, M_y (Nm)**
0	0
0	7
-10	7
-60	-15
-60	-34
0	0

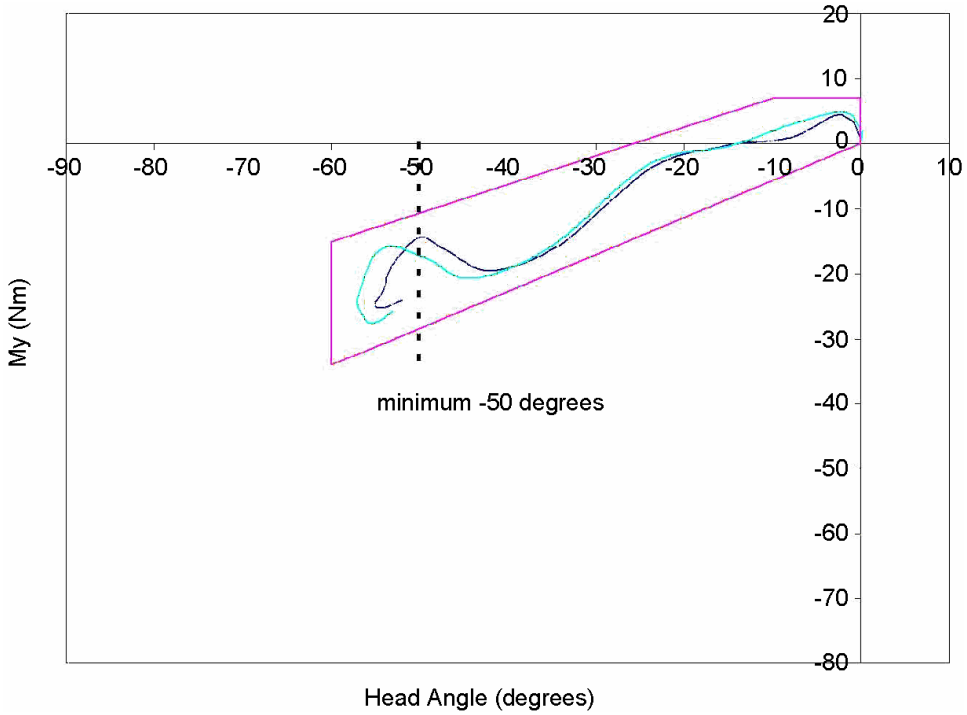

Figure 1 — Extension moment vs. head angle

6.8.2 Dynamic flexion test

Assemble a Hybrid III lower neck mount (set at 5,25 degrees extension), the motorcyclist neck to be tested (with nodding blocks and without the shroud), a Denton upper neck load cell (model 1716[9]) and a standard Hybrid III head. Set the mid neck angle adjustment to the full forward (flexion) position.

Mount the assembly on an acceleration sled and apply an acceleration to the base of the neck which meets the criteria of Table 10.

Table 10 — Neck flexion sled pulse criteria

Peak acceleration	24,0 ± 1,5 g
Average acceleration above 1.0g	12,4 ± 1,0 g
Overall velocity change	16,8 ± 0,3 m/s

Measure the following variables:

— upper neck M_y moment with the Denton 1716 load cell,[9]

— change in head pitch angle,

— *x* and *z* position of occipital condyle pin,

— *x* and *z* position of head centre of gravity.

Measure the change in head angle directly with an external goniometer, or by high-speed photographic means.

Use high-speed film or video with a minimum frame rate of 1 000 frames per second. Use target decals on the dummy head for this measurement, correcting for parallax error. Synchronize the time-base of this data recording with that of the M_y data.

Process the moment data according to SAE J211, CFC600. Process the electronic angle measurement according to SAE J211, CFC180.

Measure the neck angle based on a virtual line connecting the occipital condyle coordinates and T1 (virtual location of anterior tip of first thoracic vertebra). Consider T1 to be a fixed point located nominally 129,5 mm below and 11,3 mm behind the initial coordinate of the occipital condyle. Consider that the change in angle of this line to be the change in neck angle.

Plot the neck moment (M_y) versus head pitch angle, head centre of gravity and occipital condyle Z position versus X position, and neck angle versus head pitch angle on graphs, along with the corridors described in Tables 11 to 14, and shown in Figures 2 to 4.

Table 11 — Neck flexion bending corridor

Change in head angle (degrees)	Flexion moment, M_y (Nm)
0	11,5
17,5	11,5
50	45
65	57
65	0
35	0
20	-20
0	-25

Table 12 — Neck flexion head centre of gravity corridor

Head c. of g. (*x* mm)	Head c. of g. (*z* mm)
11	148
80	121
130	23
115	7
68	98
6	124
11	148

Table 13 — Neck flexion occipital condyle corridor

Occipital condyle (*x* mm)	Occipital condyle (*z* mm)
30	195
108	167
183	66
169	46
96	144
23	172
30	195

Table 14 — Neck flexion change in neck angle vs. change in head angle corridor

Change in head angle (degrees)	Change in neck angle (degrees)
0	21
20	40
40	50
55	77
65	77
65	62
45	38
15	20
5	0

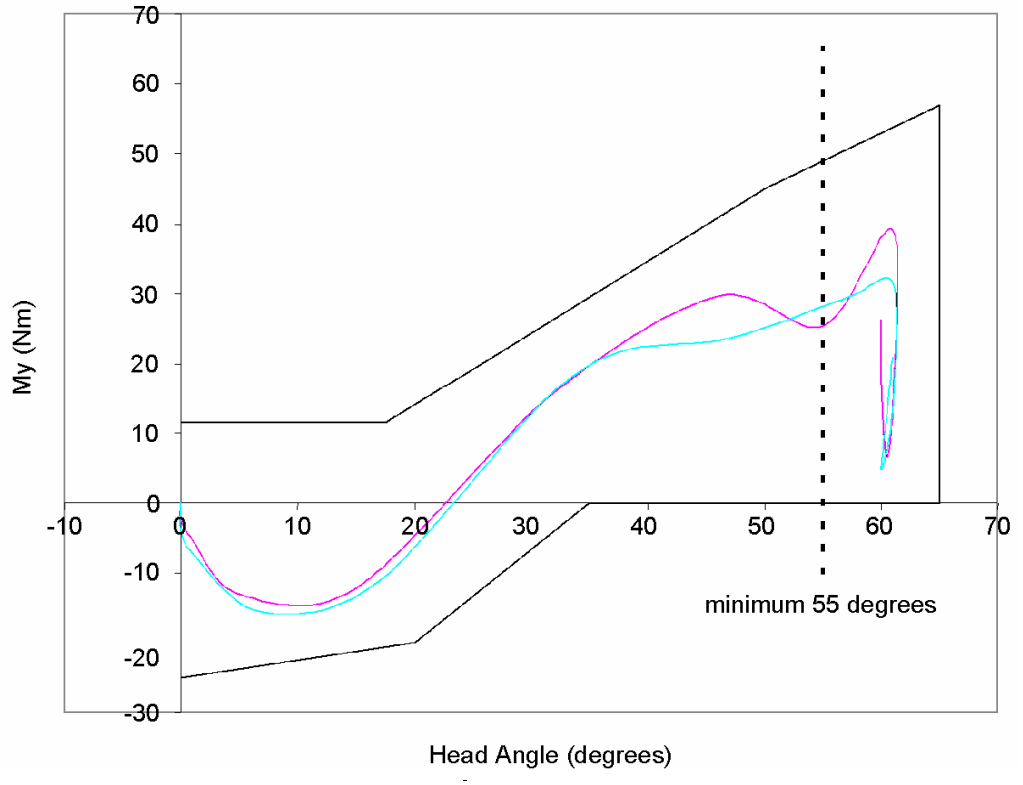

Figure 2 — Neck flexion bending moment vs. head angle

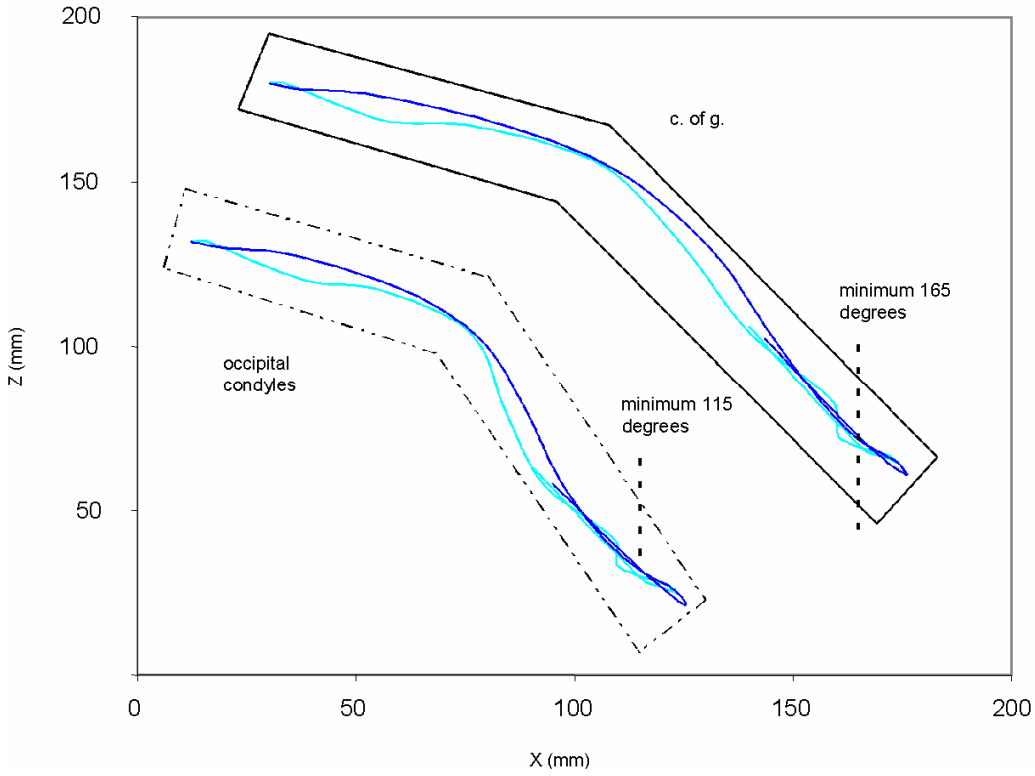

Figure 3 — Neck flexion occipital condyle and head centre of gravity position

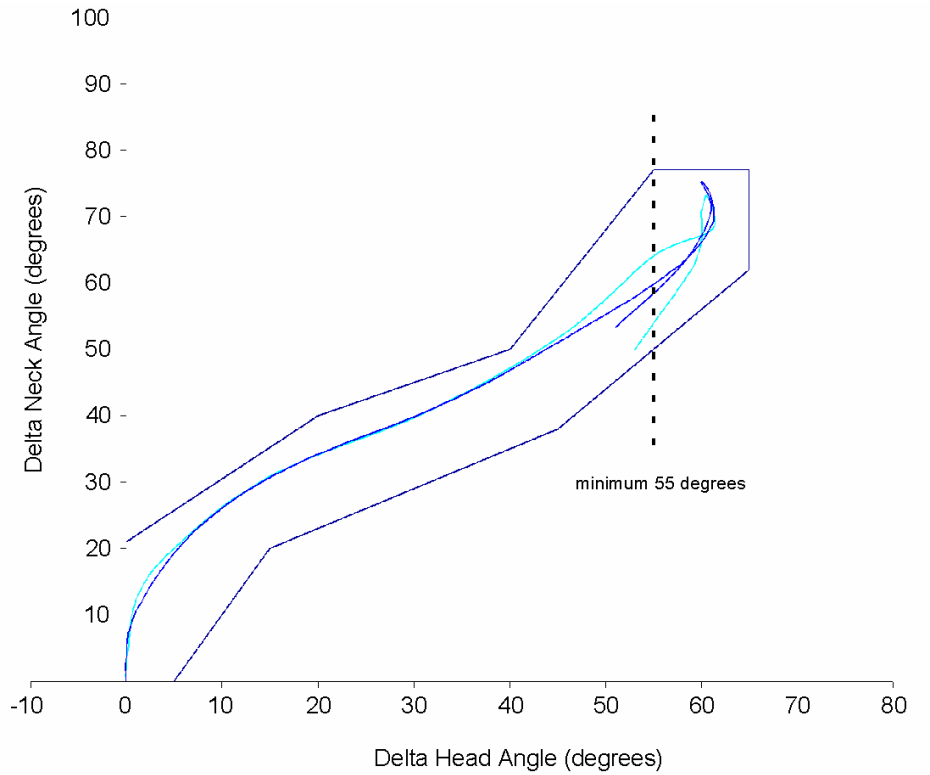

Figure 4 — Flexion neck angle vs. head angle

6.8.3 Dynamic lateral test

Assemble a Hybrid III lower neck mount (set at 5,25 degrees extension), the motorcyclist neck to be tested (with nodding blocks and without the shroud), a Denton upper neck load cell (model 1716[9)]) and a standard Hybrid III head, set the mid neck angle adjustment to the full forward (flexion) position.

Mount the assembly on an acceleration sled and apply an acceleration to the base of the neck which meets the criteria of Table 15.

Table 15 — Lateral sled pulse criteria

Peak acceleration	13,5 ± 1,0 G
Average acceleration above 1.0 G	5,9 ± 1,0 G
Overall velocity change	7,4 ± 0,5 m/s

Measure the head roll angle, and the y position and z position of the head centre of gravity.

Measure the head angle and centre of gravity position by high speed photographic means. Do not use an external goniometer for displacement measurement due to the non-planar motion of the neck in lateral bending. Do not use external targets on the head for locating the centre of gravity due to large amounts of head twist during this event. Insert a slender metal rod (nominally 350 mm long and 1,5 mm diameter) laterally through the centre of gravity holes in the skull, centre the rod, and affix targets to each end. Ensure that both targets remain visible to the camera throughout the test, such that the centre of gravity position may be resolved as a mid-point between the targets. Measure head angle by referencing a line between the targets.

Use high-speed film or video with a minimum frame rate of 1 000 frames per second. Correct for parallax error.

Plot the head the head roll angle vs. time and z position vs. head y position on graphs, along with the corridors described in Tables 16 and 17, and shown in Figures 5 and 6.

Table 16 — Lateral head angle vs. time corridor

Time (sec)	Head angle (degrees)
0	0
0,098	77
0,128	77
0,157	70
0,157	32
0,12	60
0,098	60
0,025	0

Table 17 — Lateral head centre of gravity corridor

Head c. of g. (*y* mm)	Head c. of g. (*z* mm)
0	10
50	6
90	-10
120	-29
140	-53
150	-71
135	-84
120	-57
100	-37
60	-17
0	-7

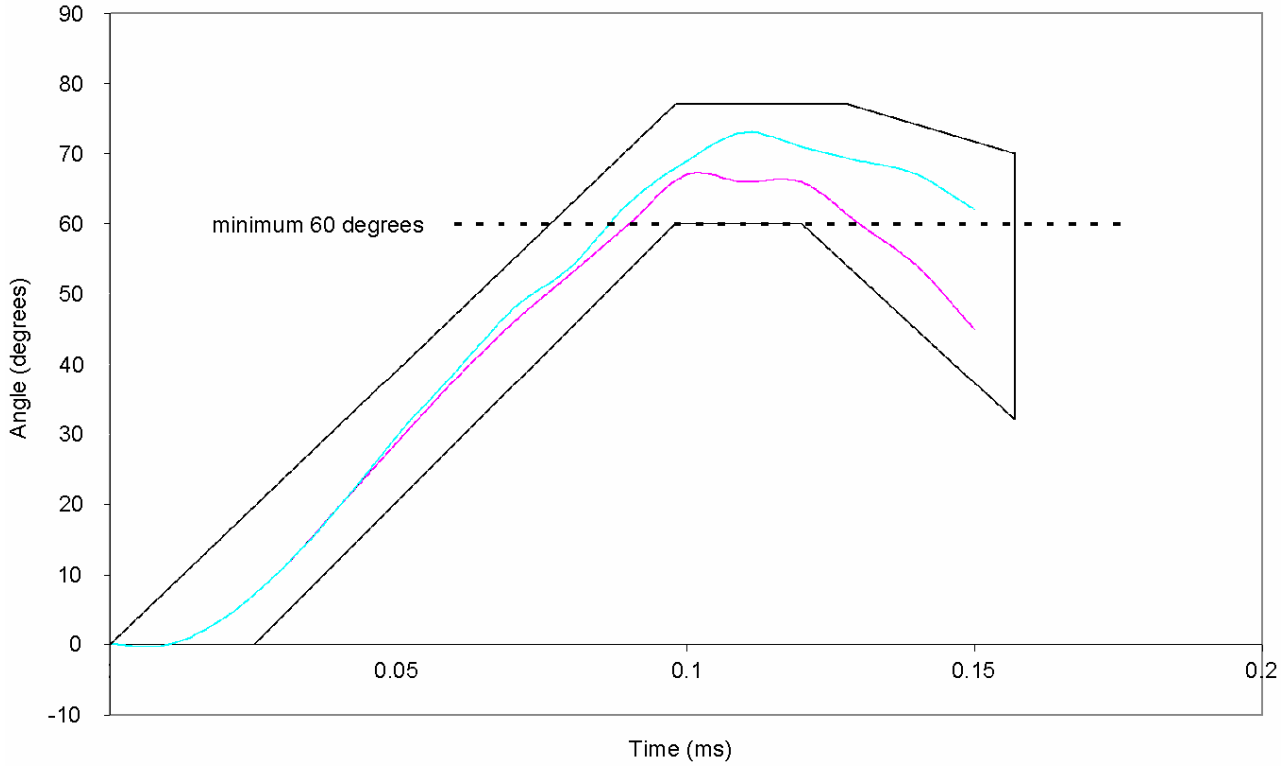

Figure 5 — Lateral head angle vs. time

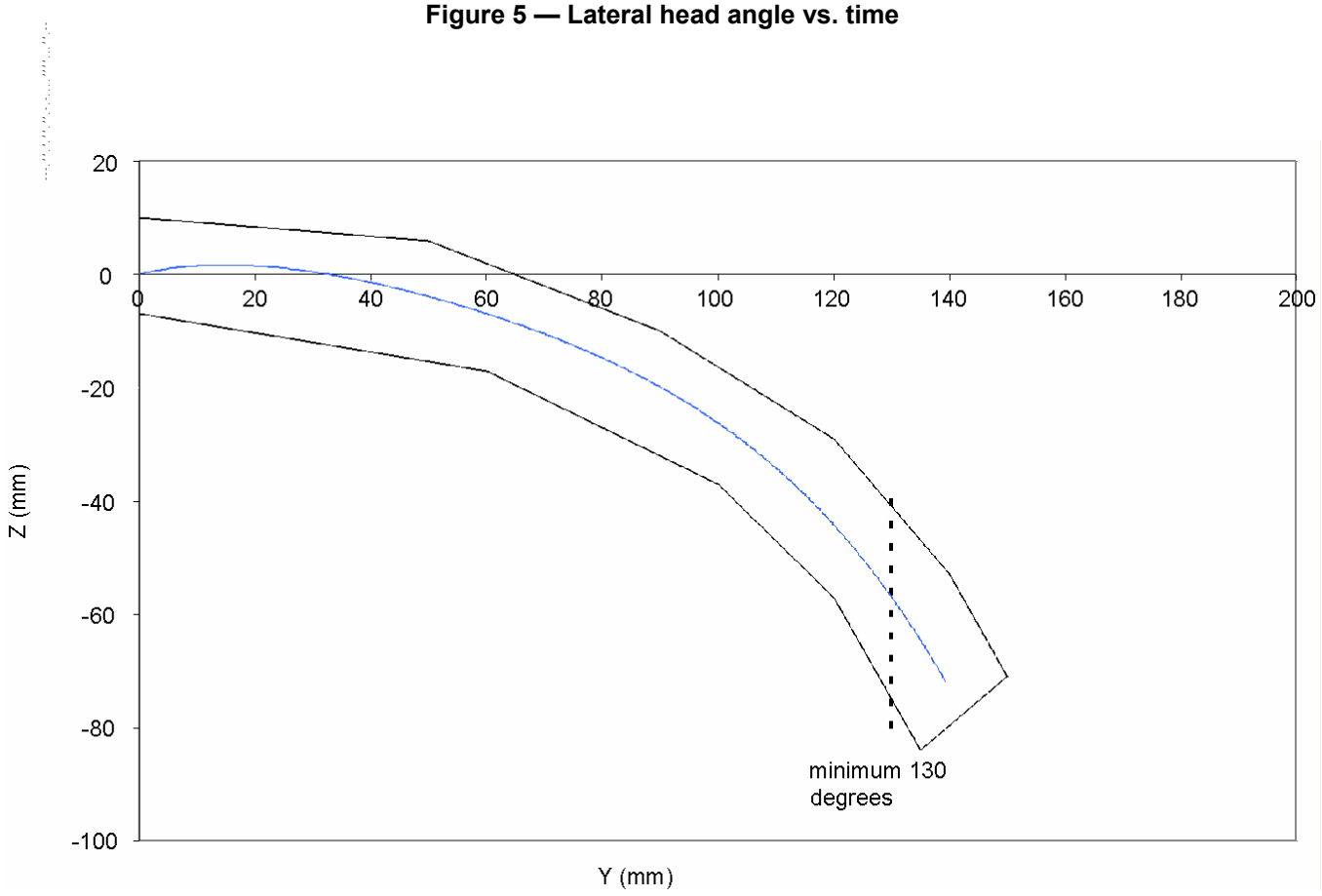

Figure 6 — Lateral head centre of gravity position

6.8.4 Dynamic torsion test

Assemble a Hybrid III lower neck mount (set at 5,25 degrees extension), the motorcyclist neck to be tested (with nodding blocks and without the shroud), and a Denton upper neck load cell (model 1716[9)]). Do not use a dummy head. Set the mid neck angle adjustment to the full forward (flexion) position.

Use either the pendulum fixture shown in Figure A.28 or equivalent. Release the pendulum so that its velocity at the bottom of the swing is 4,2 m/s ± 0,2 m/s. Measure the pendulum velocity in the last 10° before the vertical position. Measure the torque at the top of the neck, using a Denton load cell, model 1716[9)]). Measure the rotation of the neck mount using a potentiometer or other suitable device.

Process moment data according to SAE J211, CFC600. Process electronic angle measurement according to SAE J211, CFC180.

Plot the neck torque vs. the rotation angle of the lower neck mount on a graph, along with the corridor described in Table 18, and shown in Figure 7.

Table 18 — Neck torsion stiffness corridor

Rotation (degrees)	Neck torque M_z (Nm)
0	10
125	55
140	44
13	0

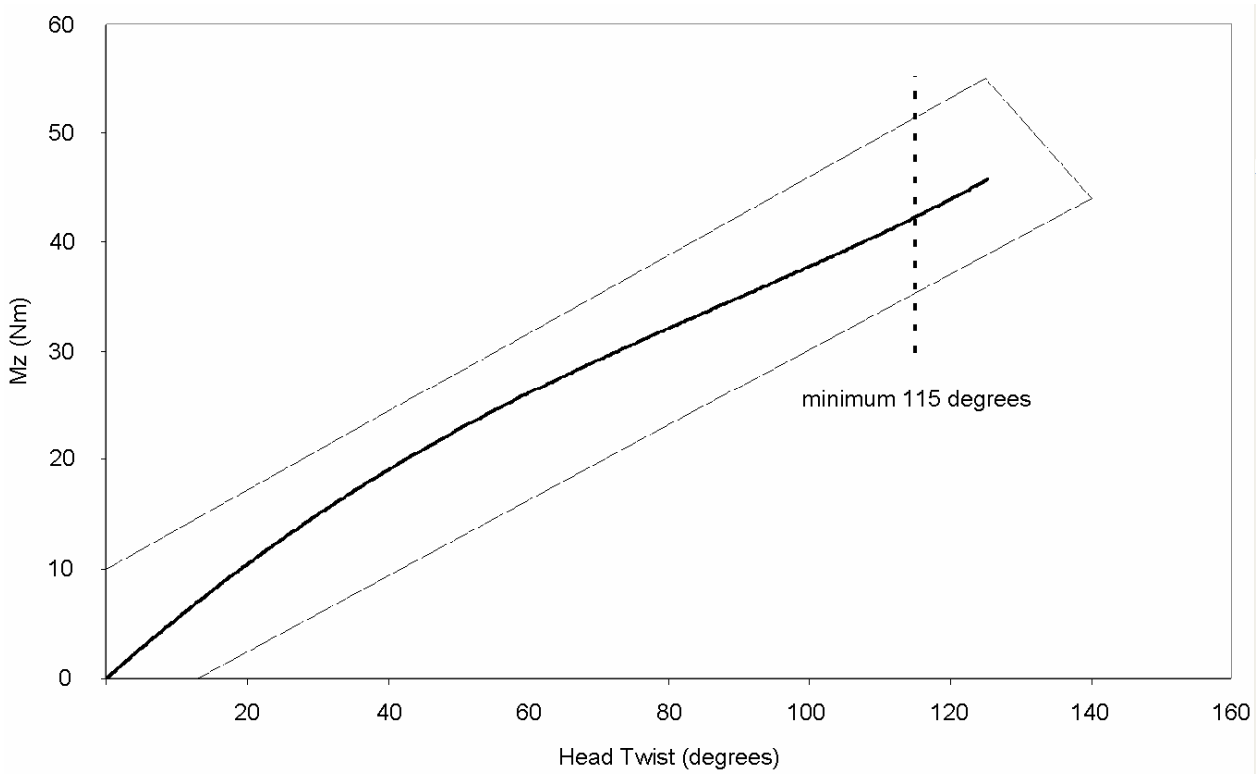

Figure 7 — Neck torsion stiffness

6.9 Motorcyclist neck static tests for subsequent conformity of production

Perform the motorcyclist neck subsequent conformity of production tests using the procedures described in Annex C.

7 Marking and documentation of frangible components

7.1 Marking

All frangible components shall be marked by their manufacturer with some designation of their lot number, in an area not likely to be damaged during testing.

7.2 Documentation

The manufacturer of each frangible part shall supply, with the frangible part, test data showing initial and subsequent conformity of production according to clauses 4, 5, and 6. The test data shall be included in the full-scale impact test documentation (see ISO 13232-8). The test data shall show the manufacturer and lot number designation of the part.

Annex A
(normative)

Drawings for motorcyclist anthropometric impact dummy special components

Drawings and specifications of special components for replacement of or modification to basis Hybrid III components.

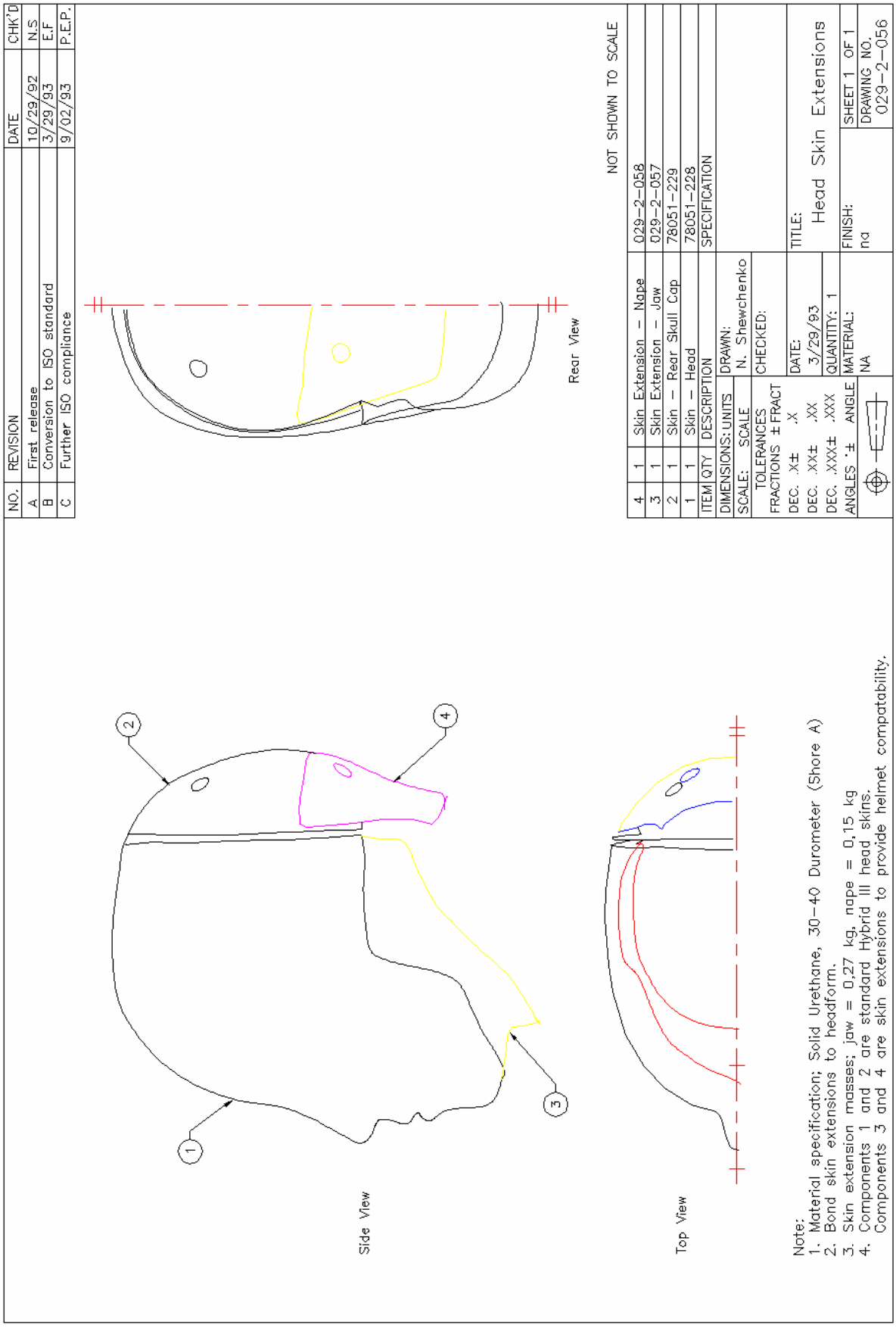

Figure A.1 — Motorcyclist head skins and extensions

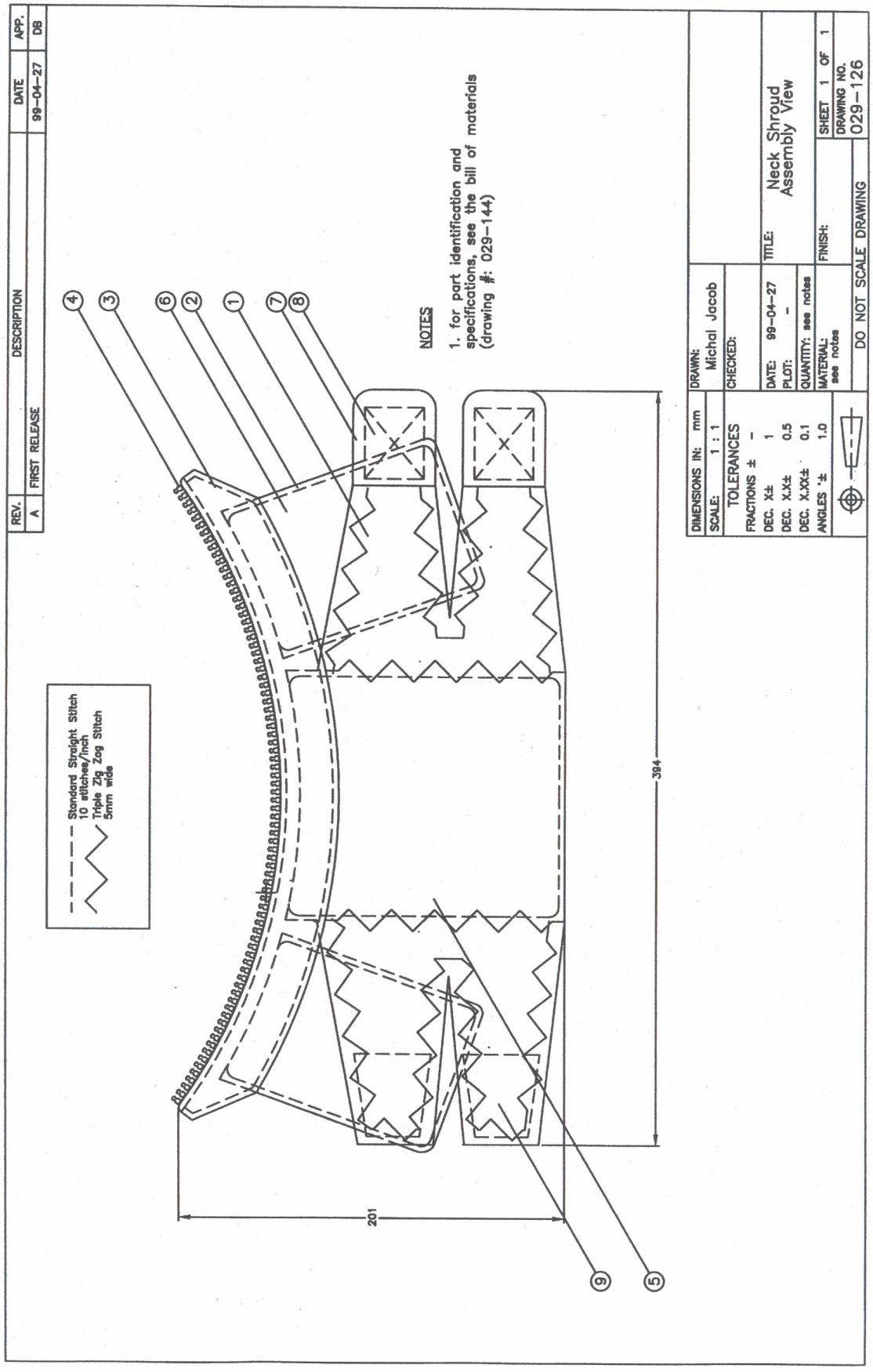

Figure A.2 — Neck shroud specifications

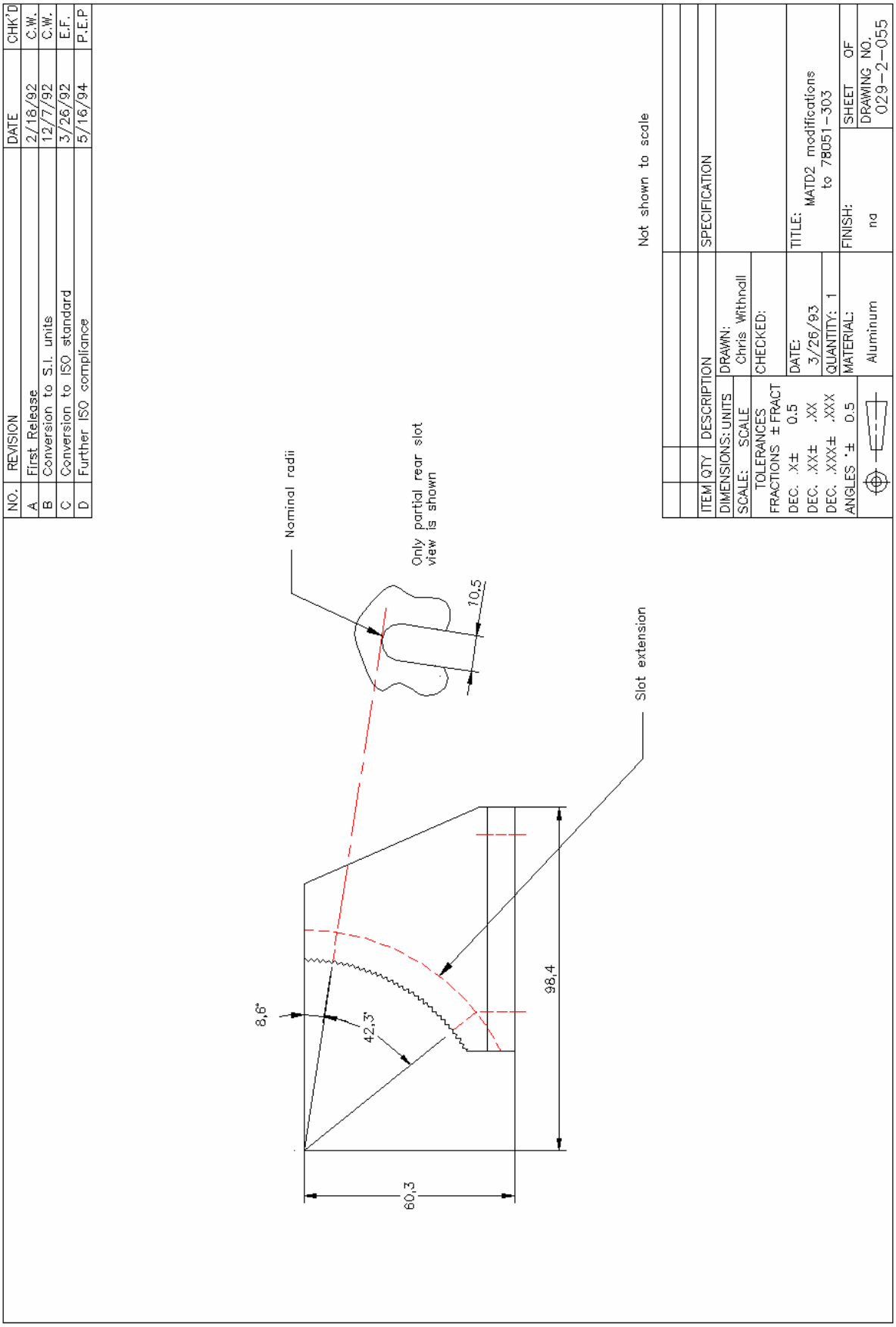

Figure A.3 — Hybrid III modified lower neck mount

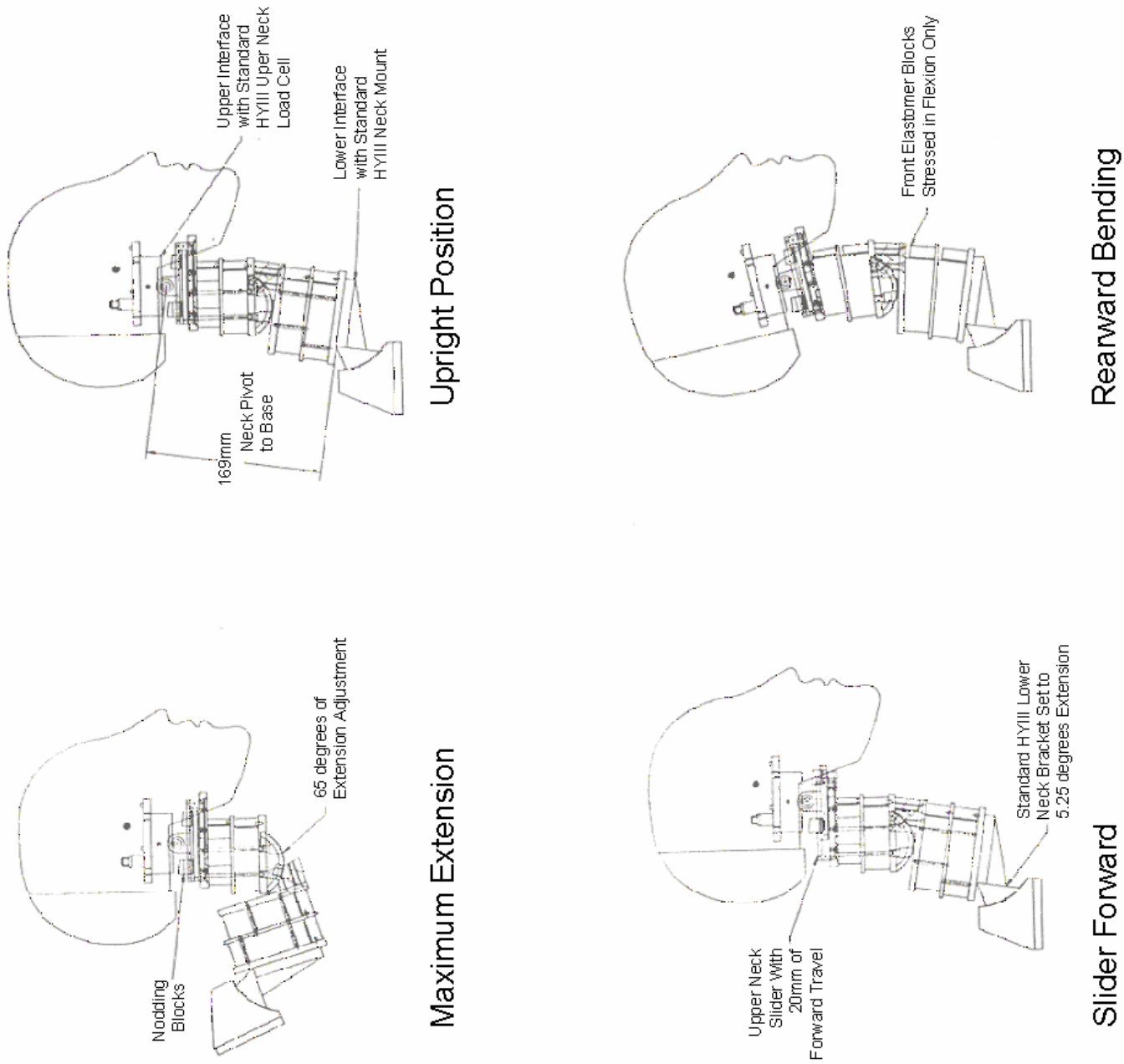

Figure A.4 — Motorcyclist neck and interface requirements

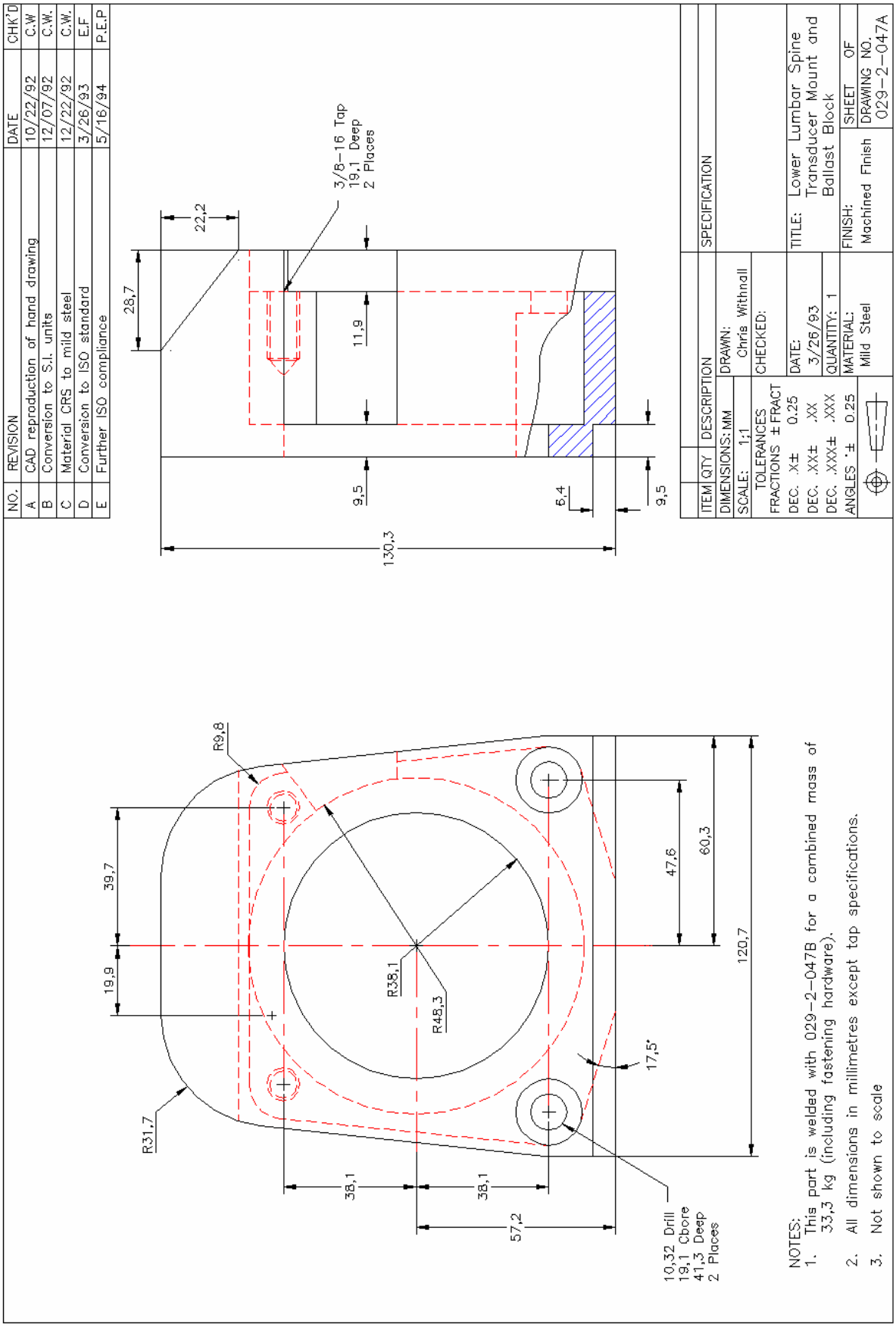

Figure A.5 — Lower lumbar spine transducer mount and ballast block for the six-axis load cell

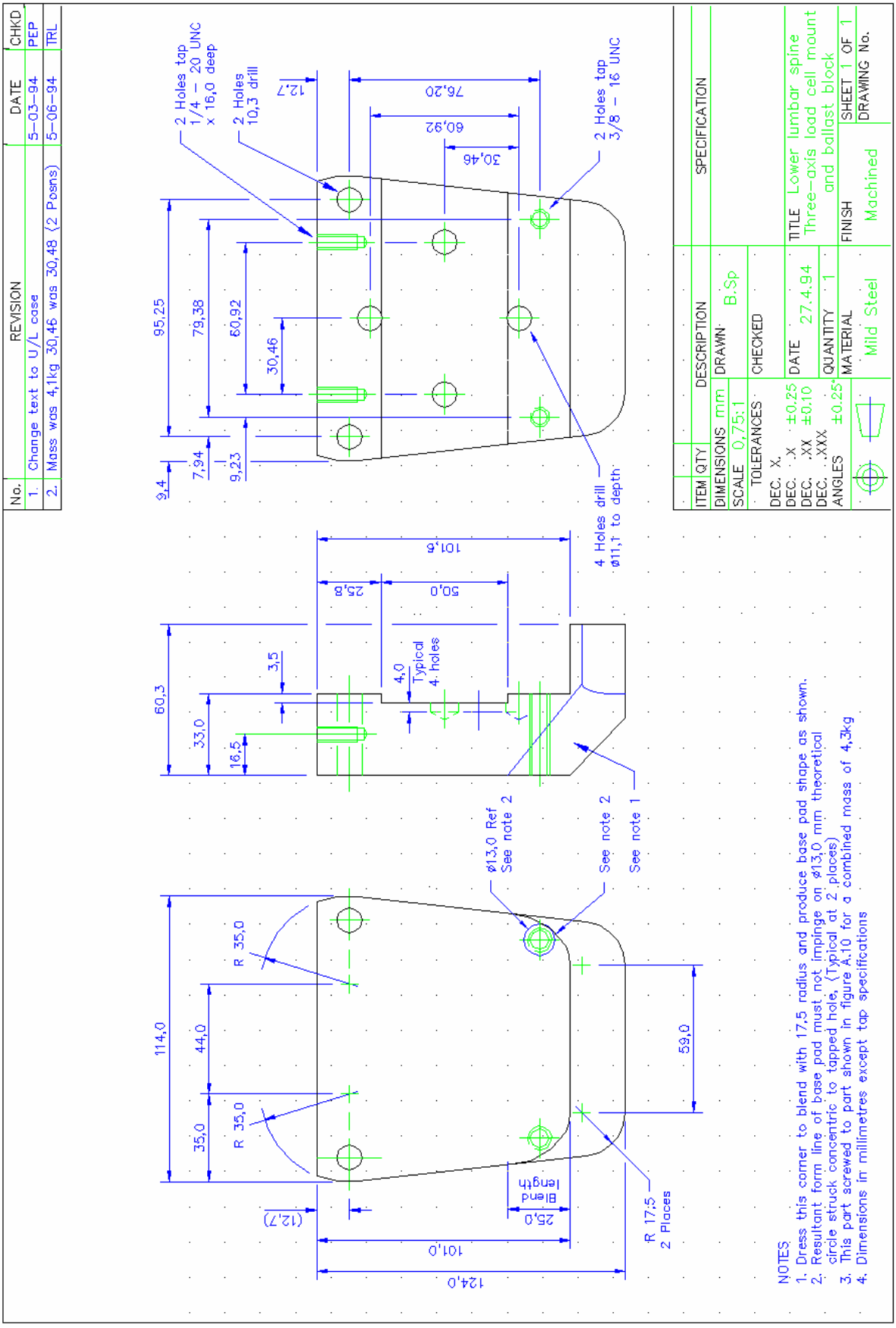

Figure A.6 — Lower lumbar spine transducer mount and ballast block for the three-axis load cell

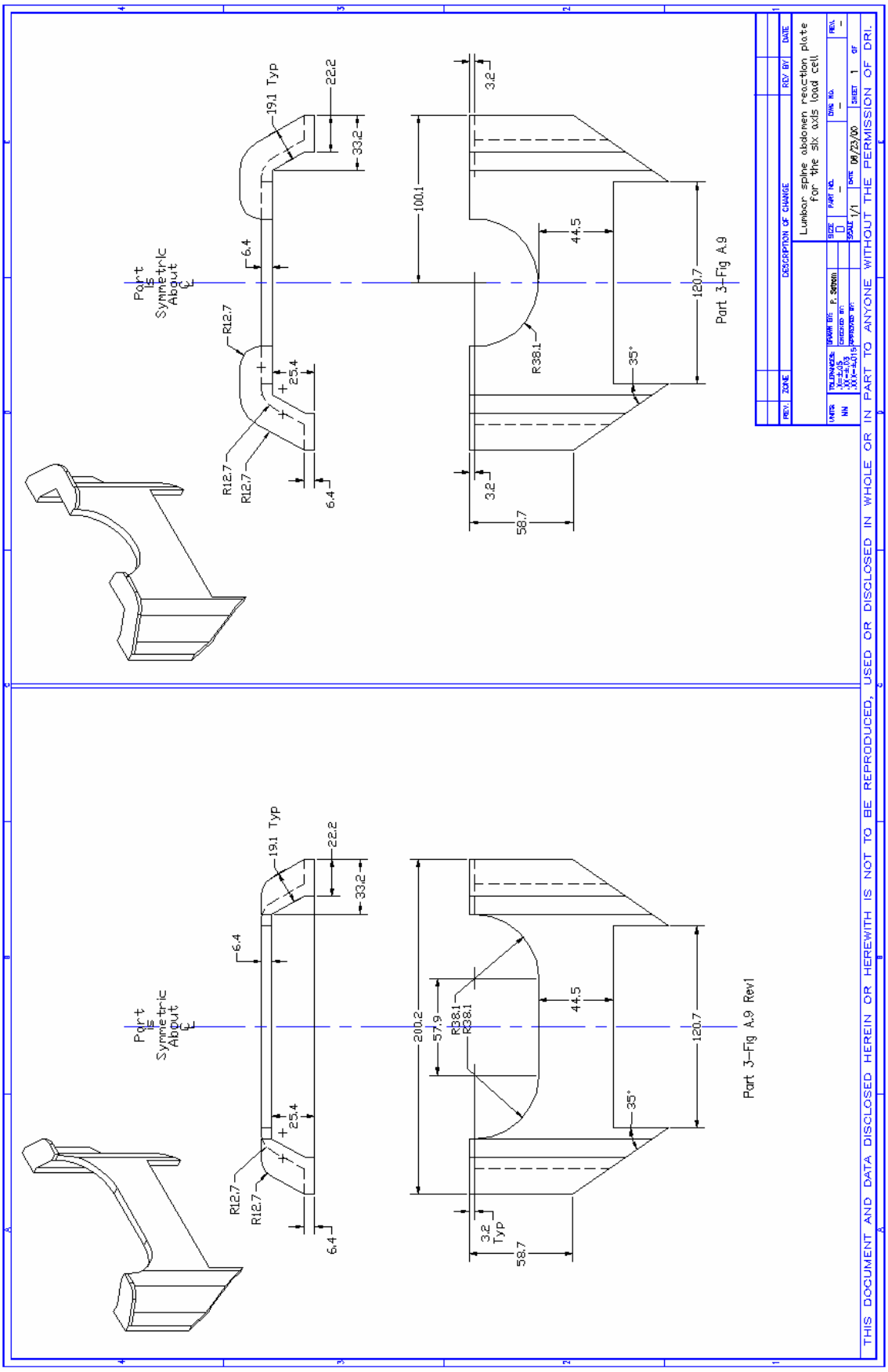

Figure A.7 — Lumbar spine abdomen reaction plate for the six-axis load cell

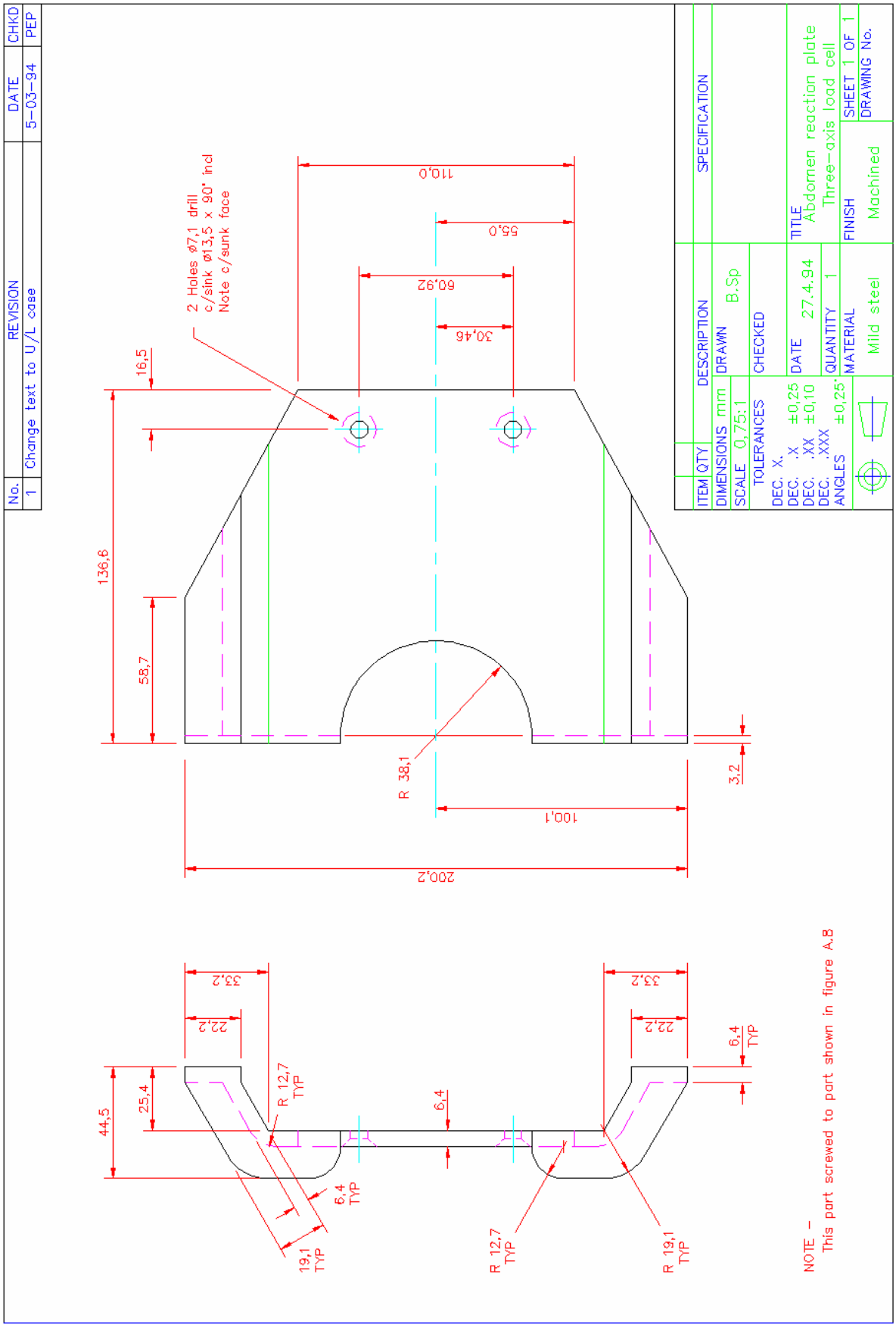

Figure A.8 — Lumbar spine abdomen reaction plate for the three-axis load cell

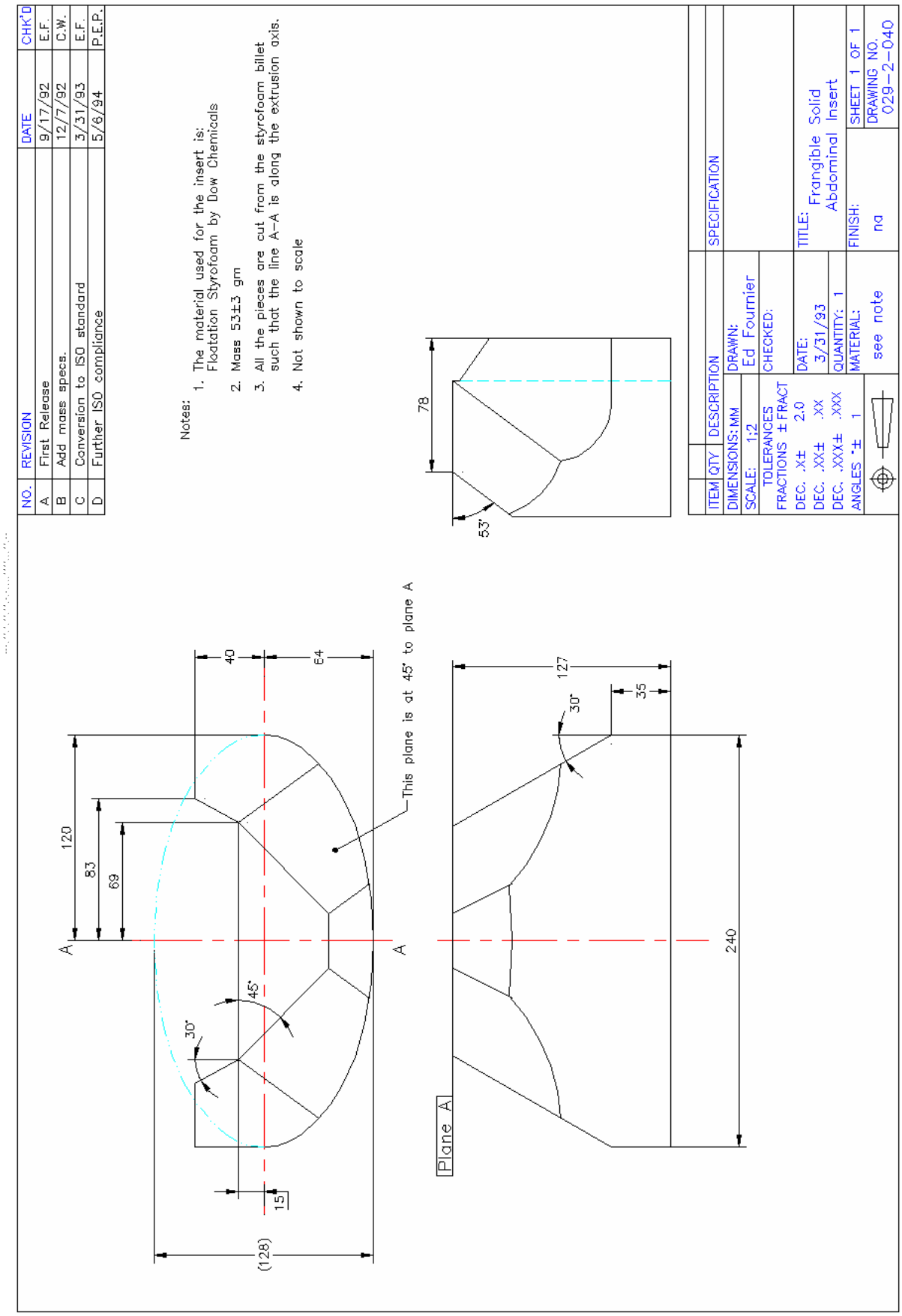

Figure A.9 — Replacement frangible solid abdominal insert

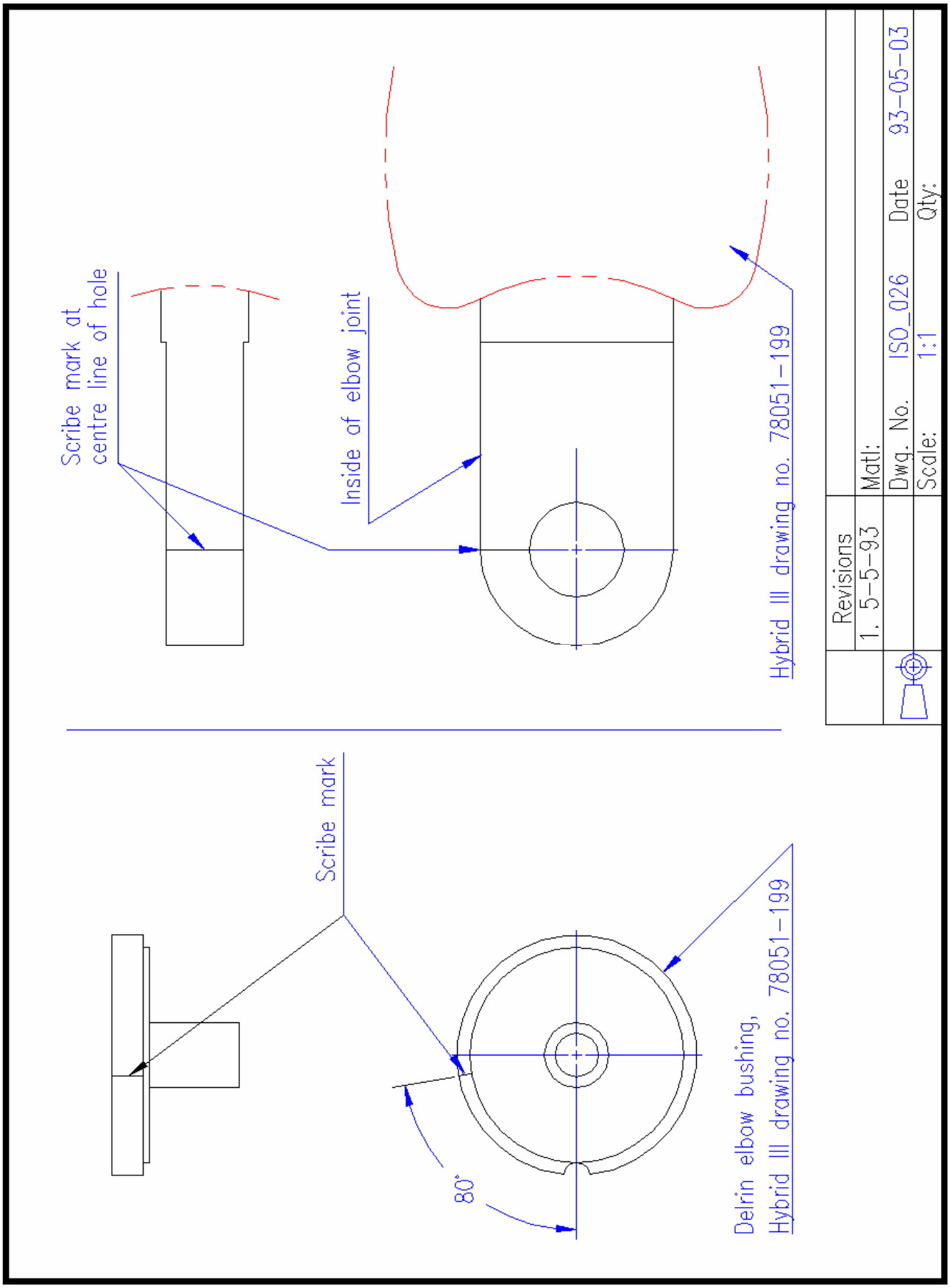

Figure A.10 — Elbow joint scribe marks for 10° arm pivot

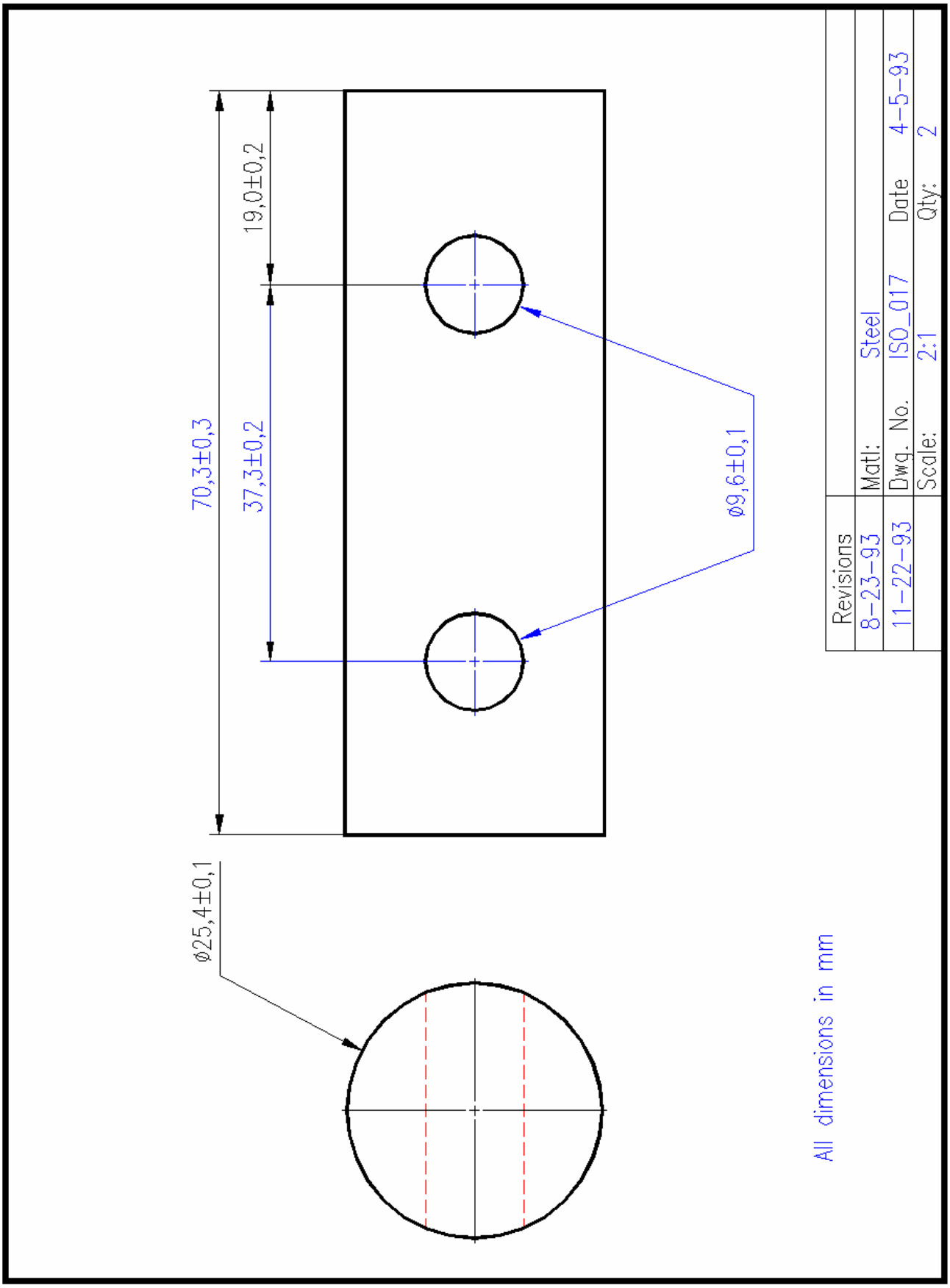

Figure A.11 — Frangible femur bone to knee adaptor

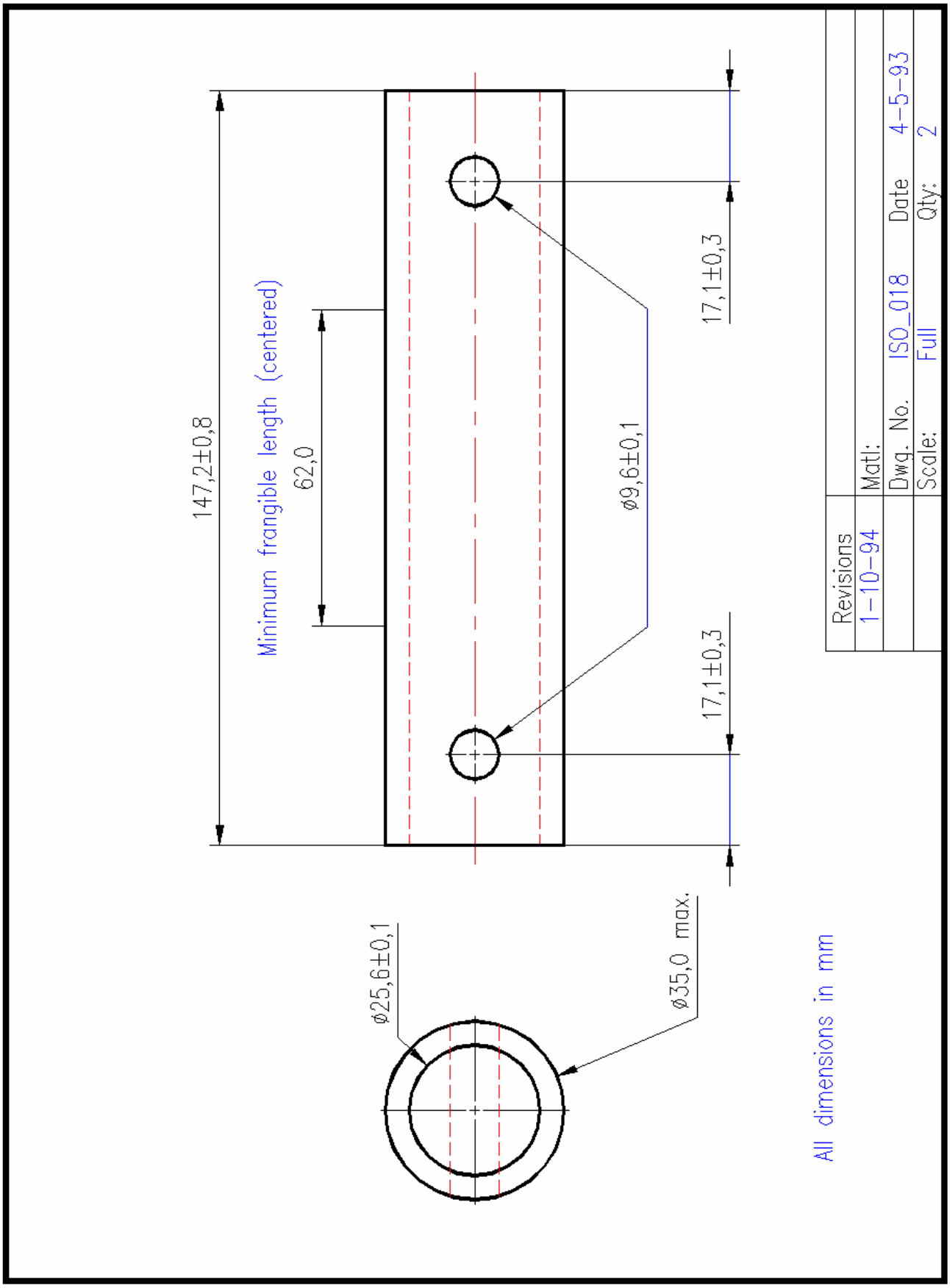

Figure A.12 — Frangible femur bone interface and size requirements

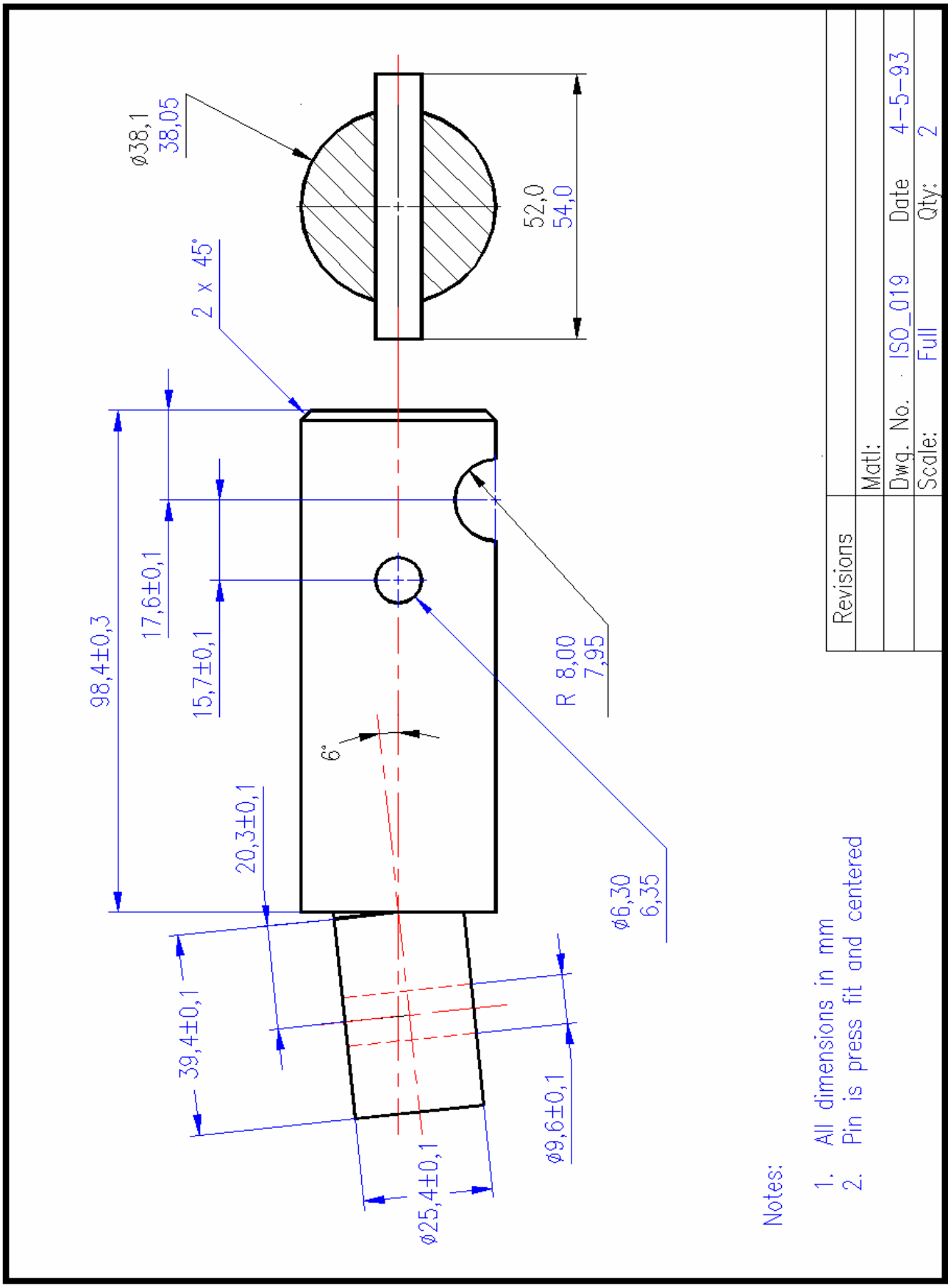

Figure A.13 — Upper femur load cell simulator

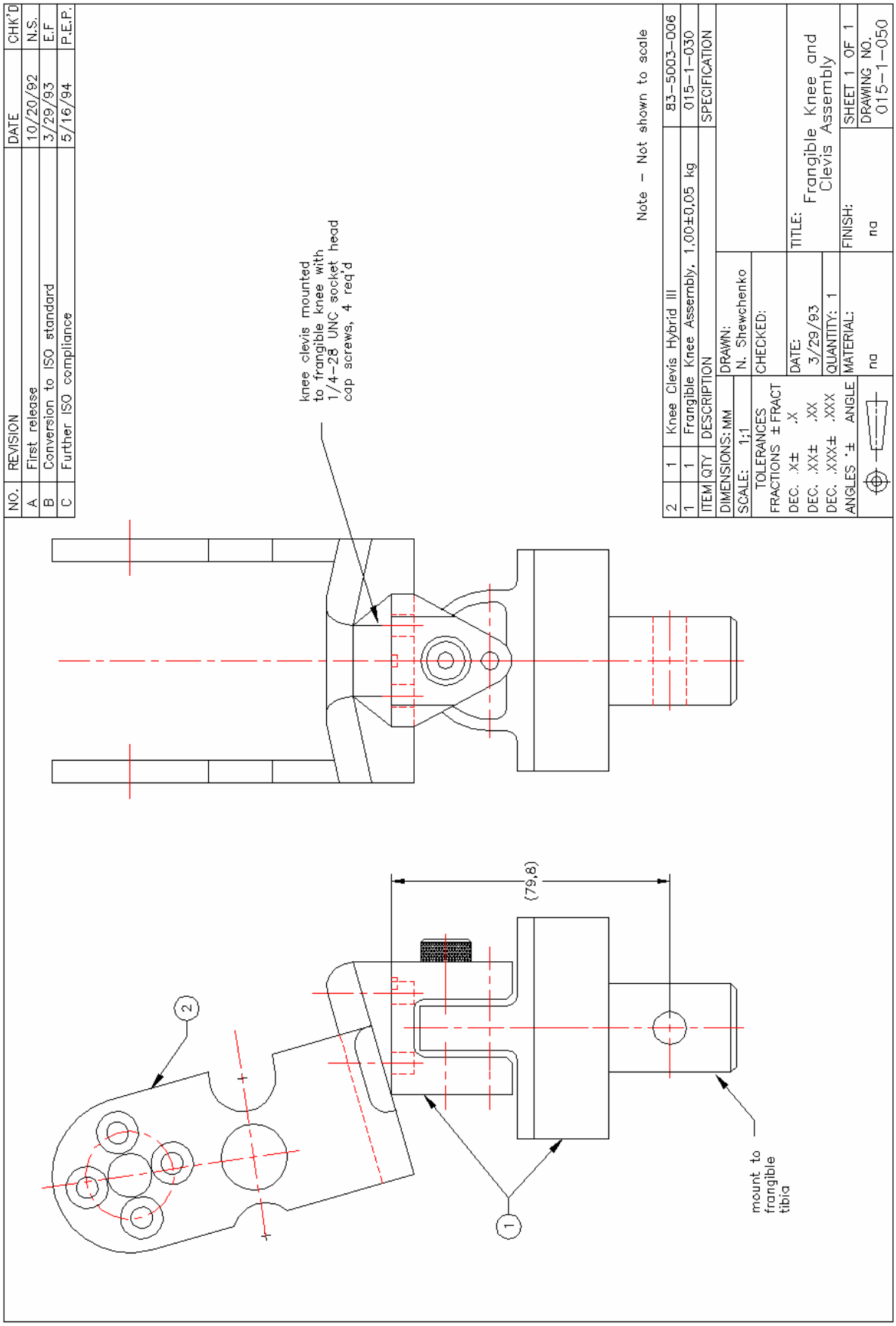

Figure A.14 — Frangible knee and knee clevis assembly

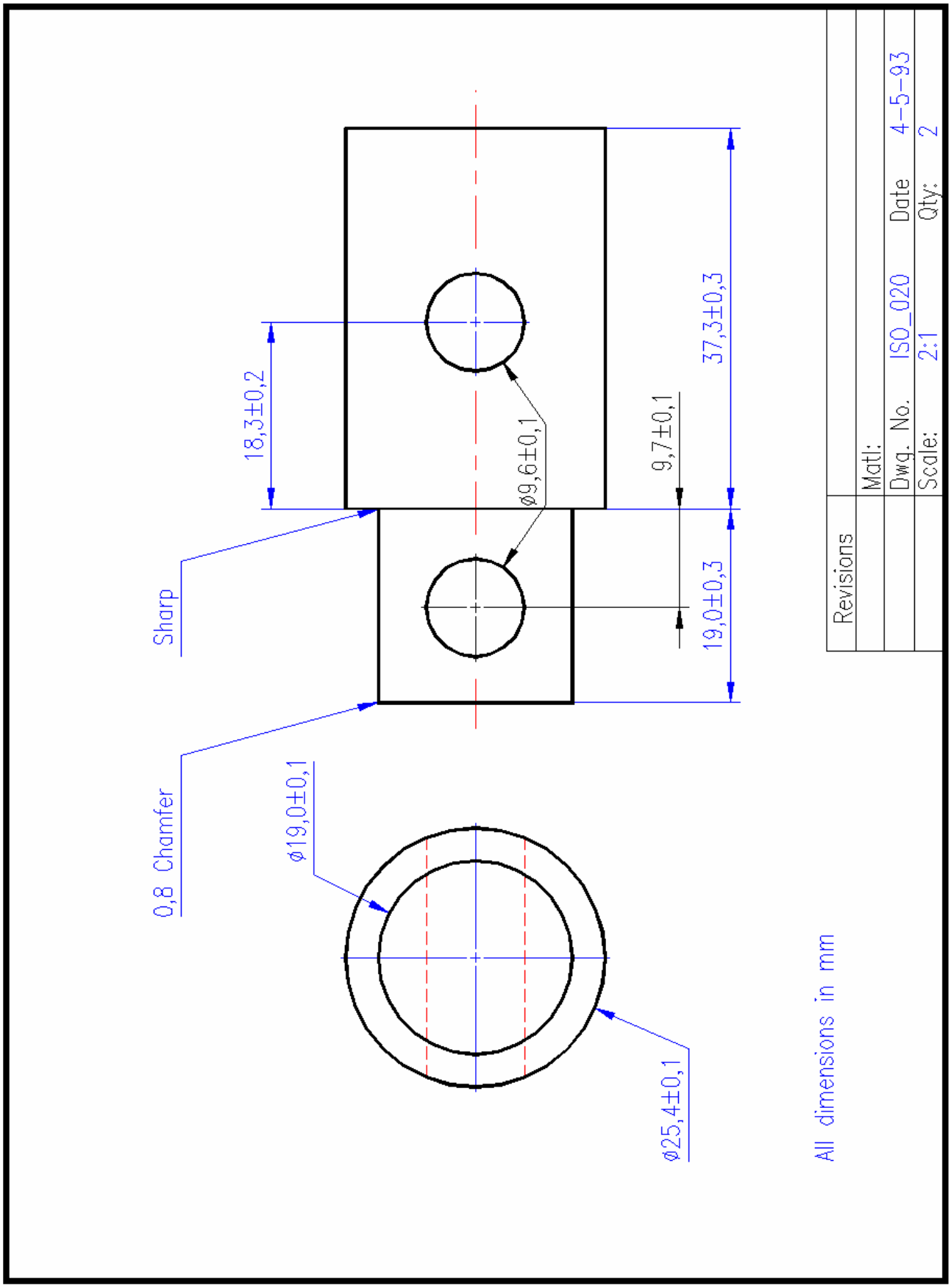

Figure A.15 — Frangible tibia bone to ankle joint adaptor

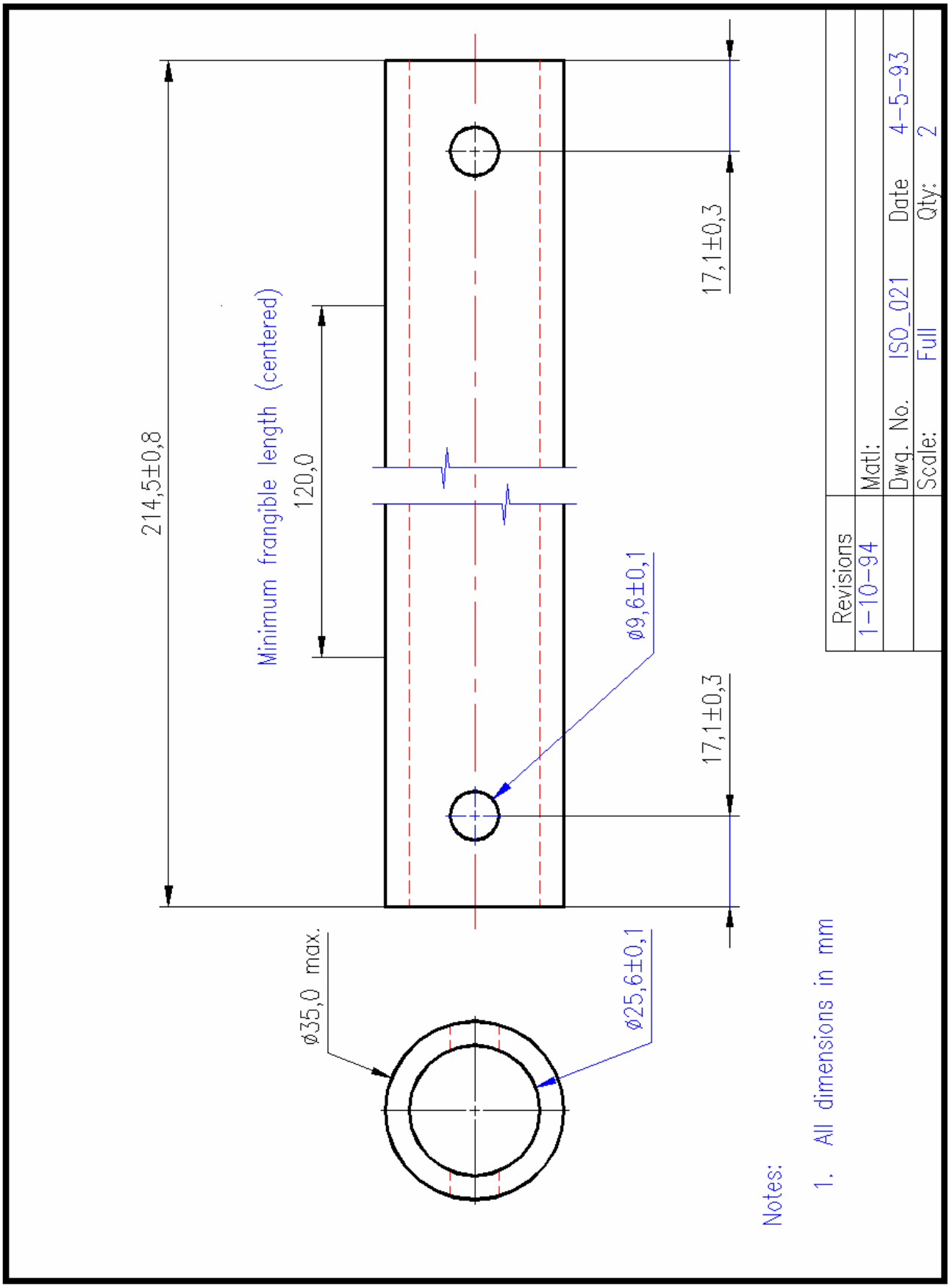

Figure A.16 — Frangible tibia interface and size requirements

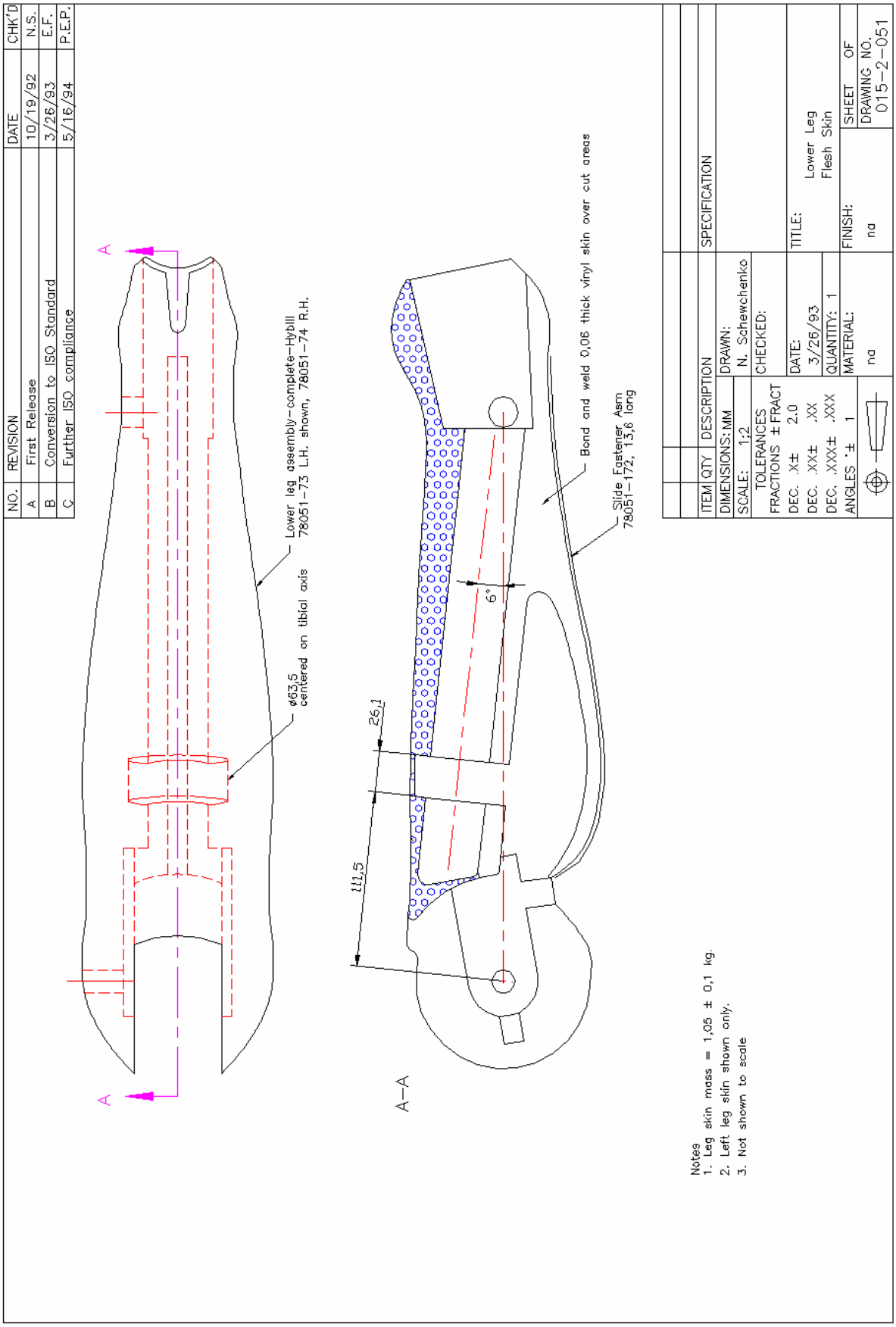

Figure A.17 — Modified lower skin

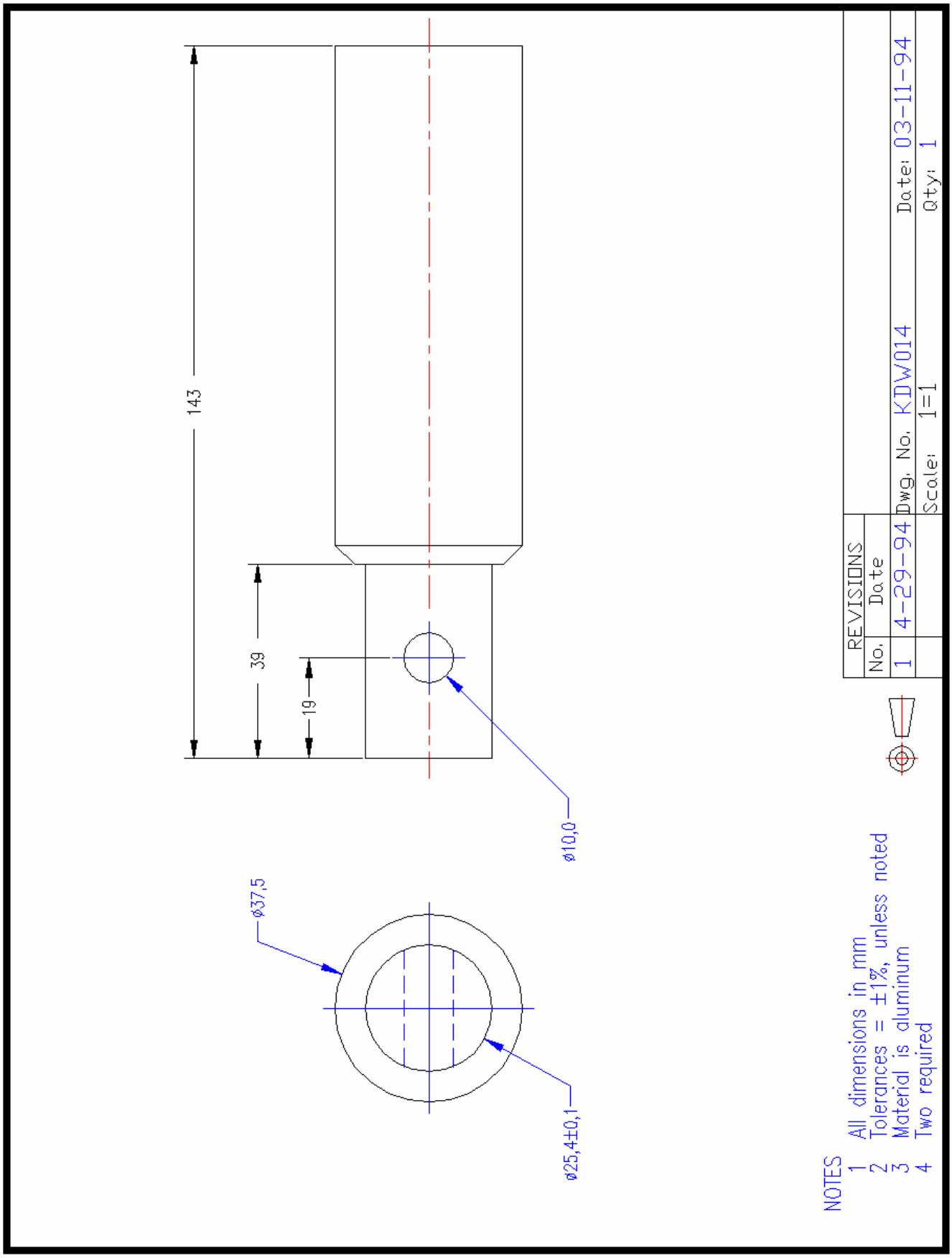

Figure A.18 — Frangible leg bone extensions for the bone bending tests

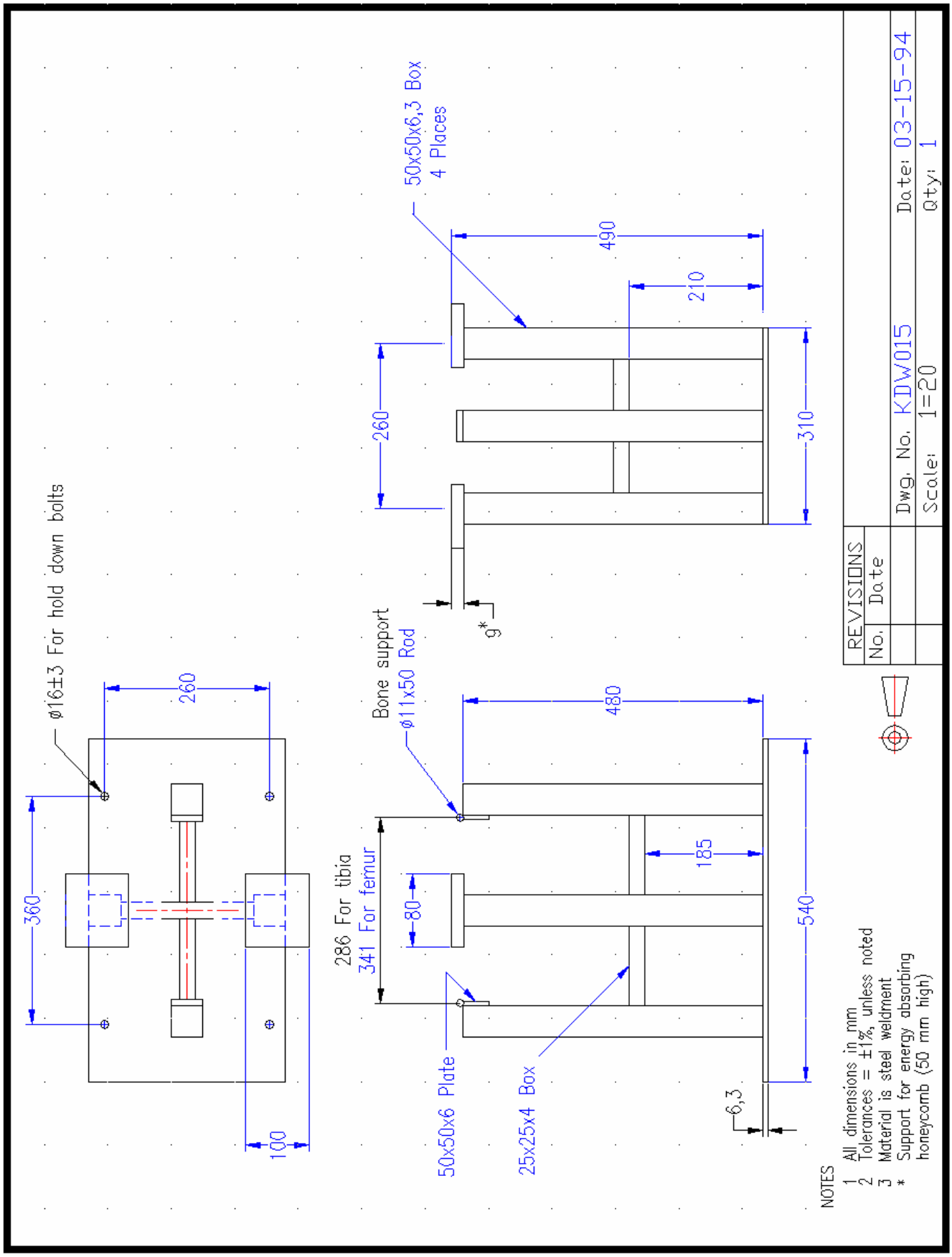

Figure A.19 — Specimen supports for the bone dynamic bending fracture test

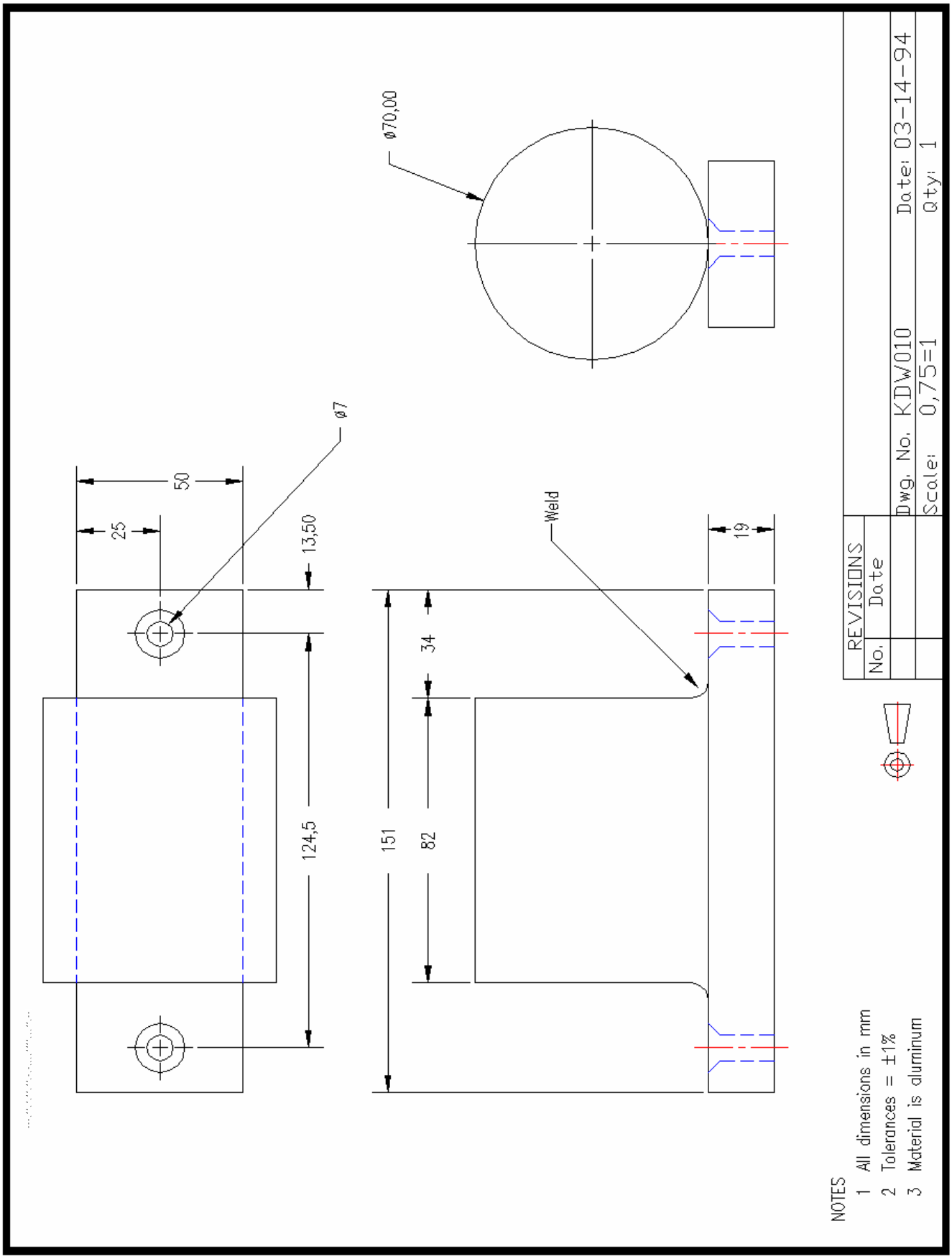

Figure A.20 — Impactor head for the bone dynamic bending fracture test

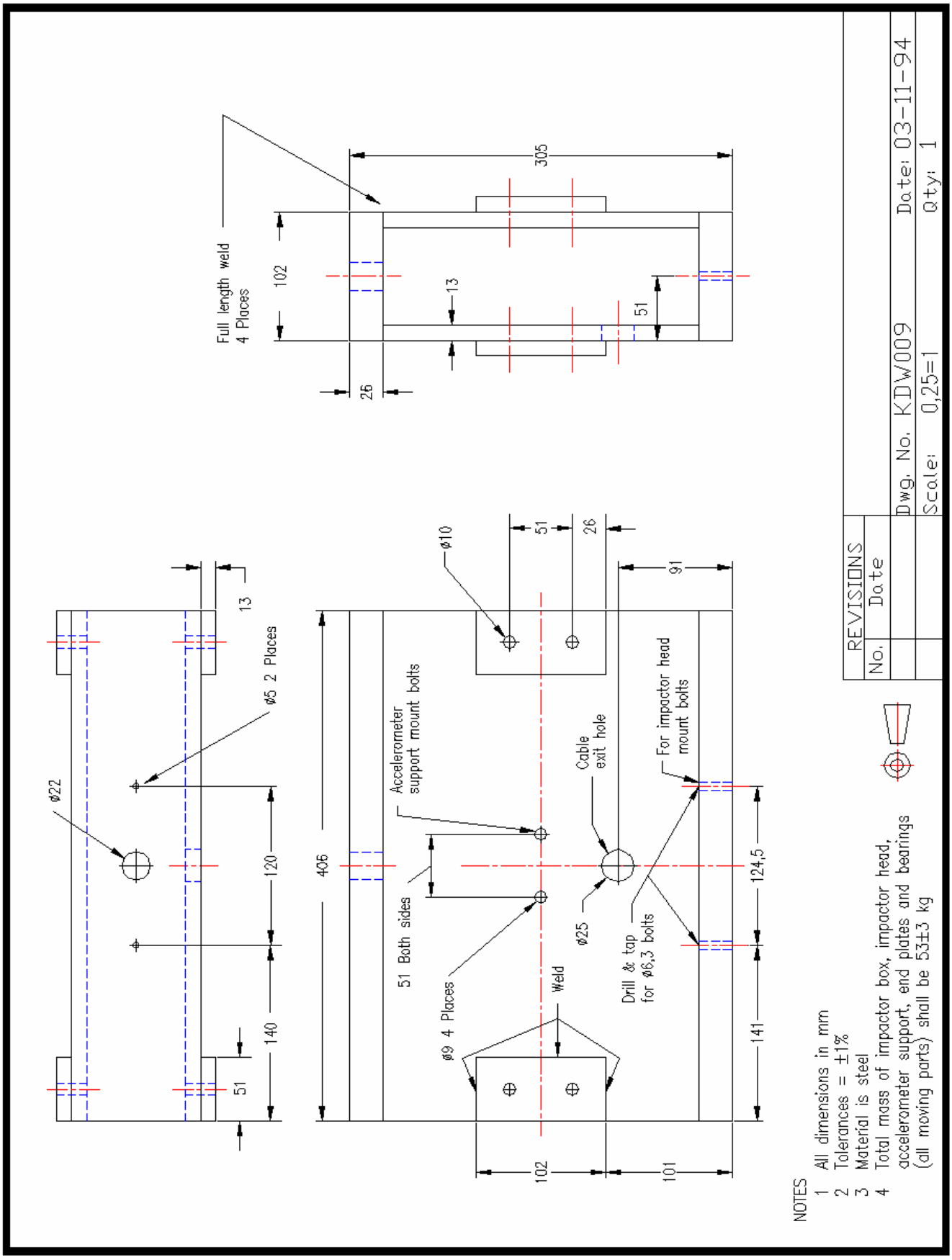

Figure A.21 — Impactor box for the bone dynamic bending fracture test

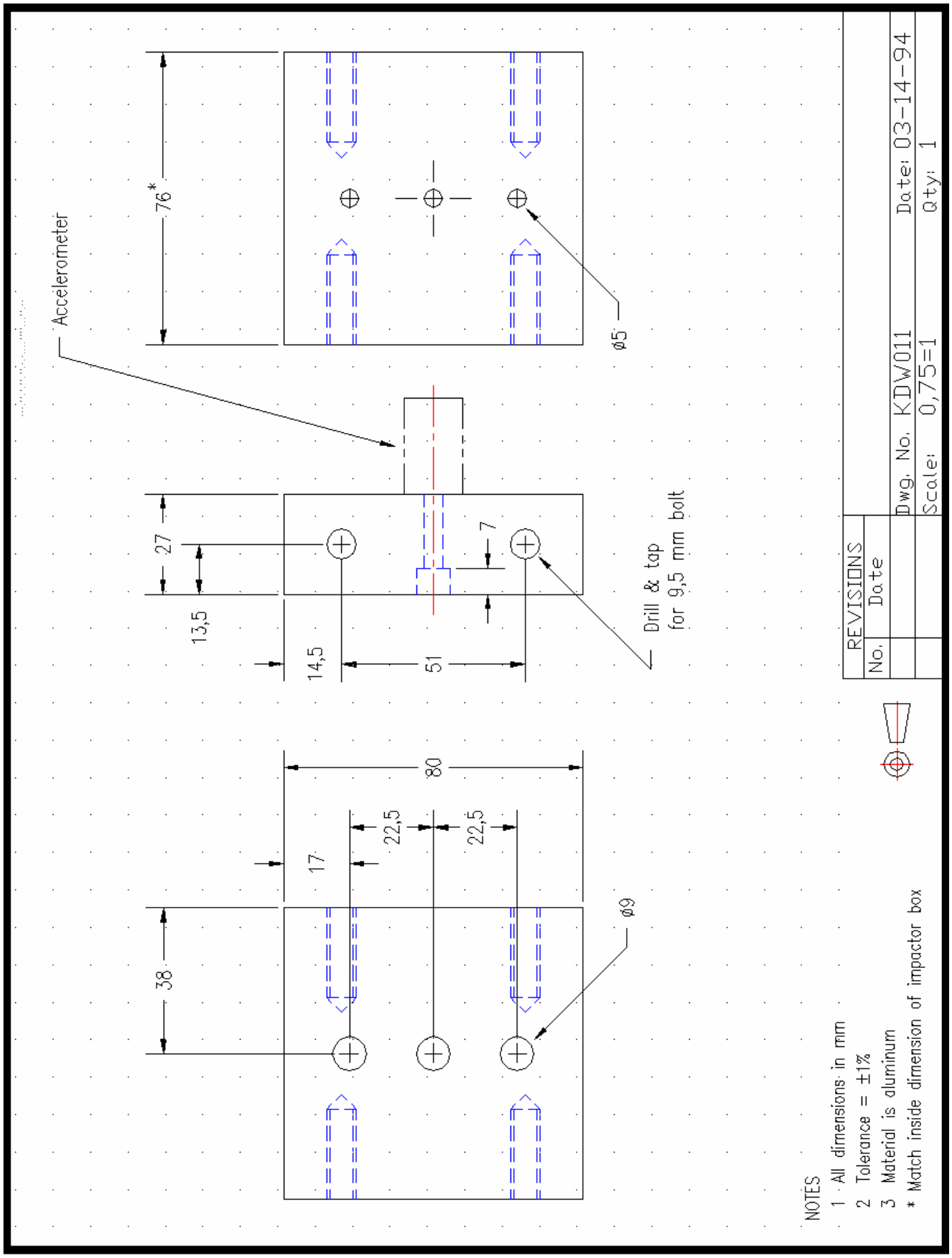

Figure A.22 — Impactor accelerometer support for the bone dynamic bending fracture tests

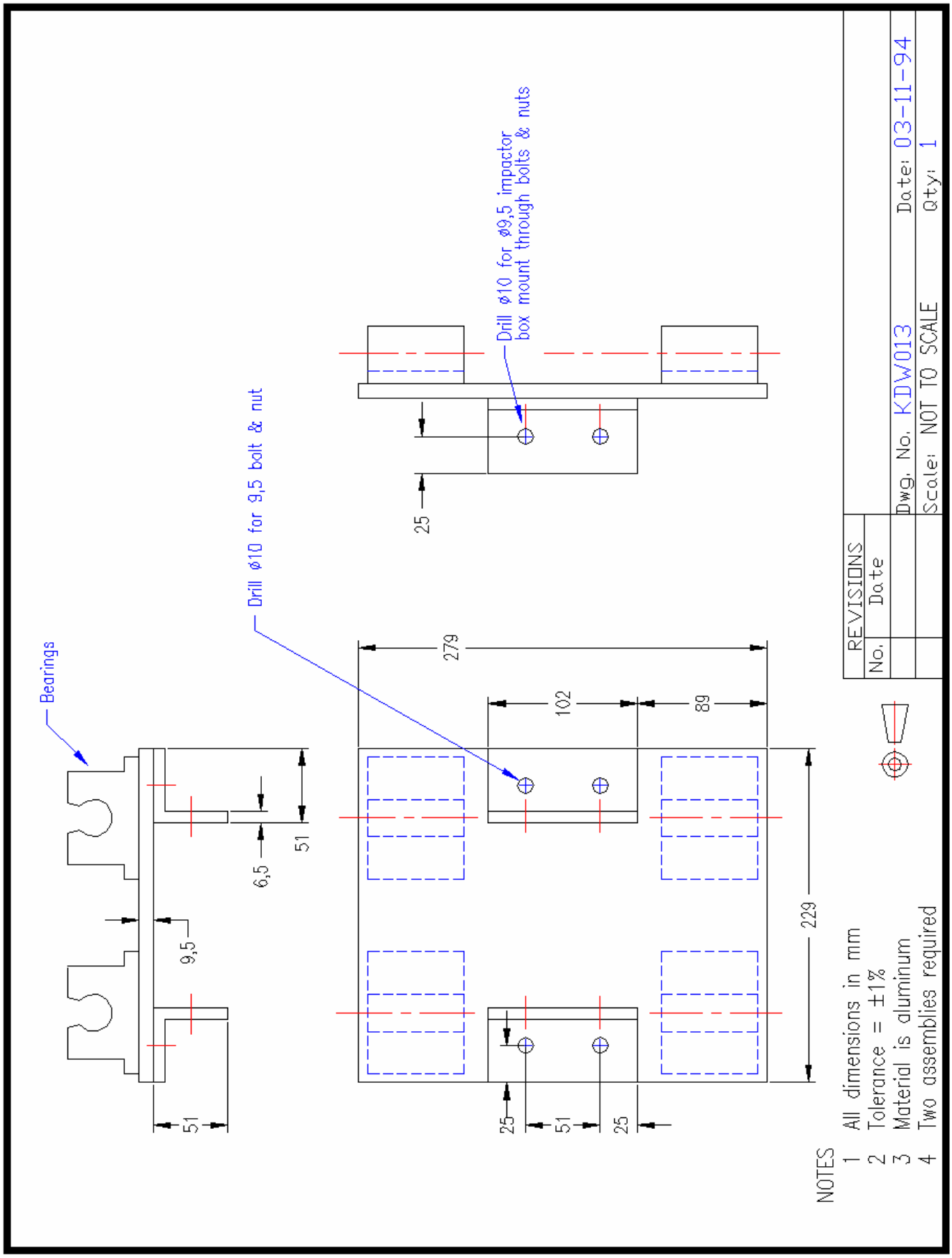

Figure A.23 — Impactor end plate and bearing mount for the bone dynamic bending fracture test

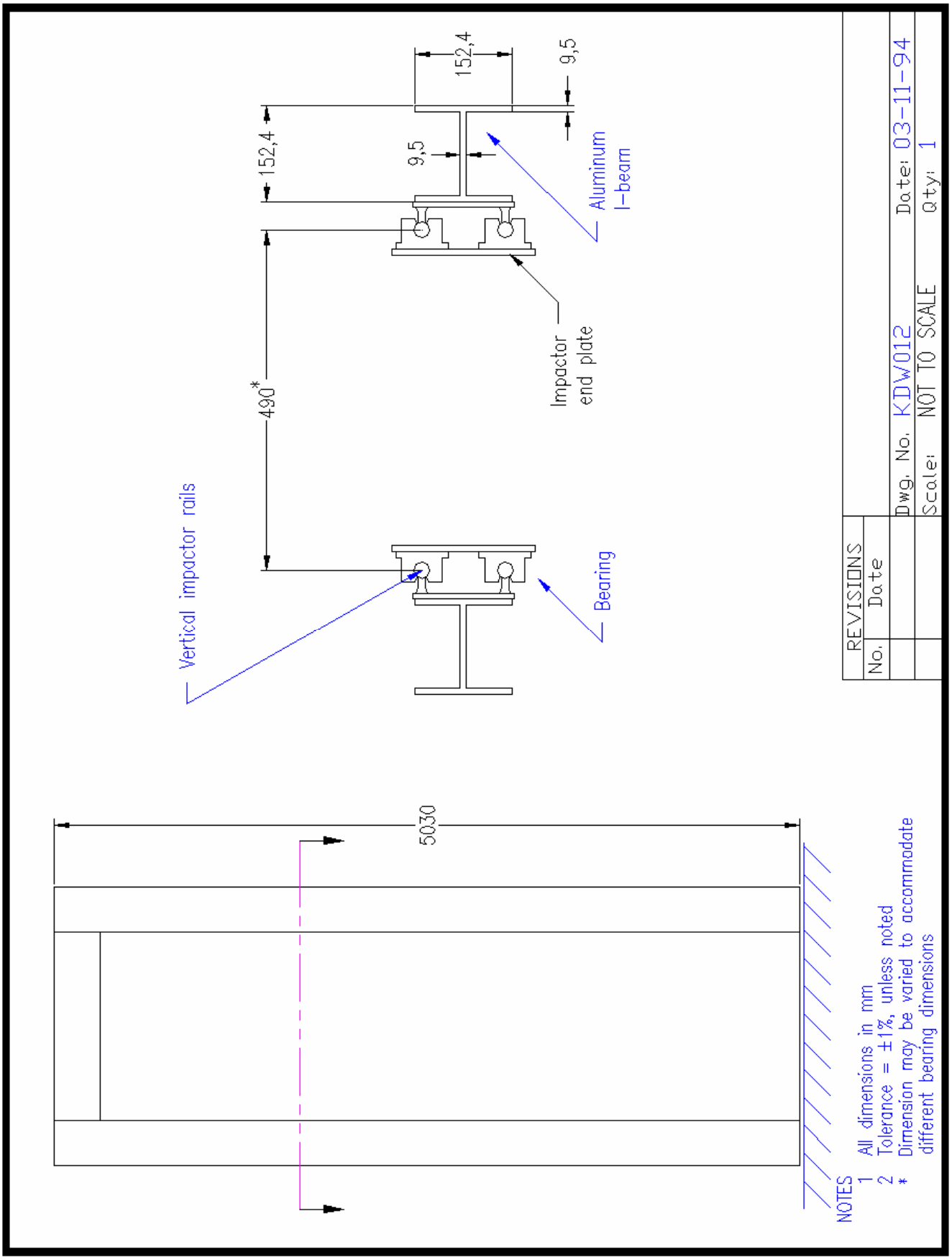

Figure A.24 — Impactor rail support for the bone dynamic bending fracture test

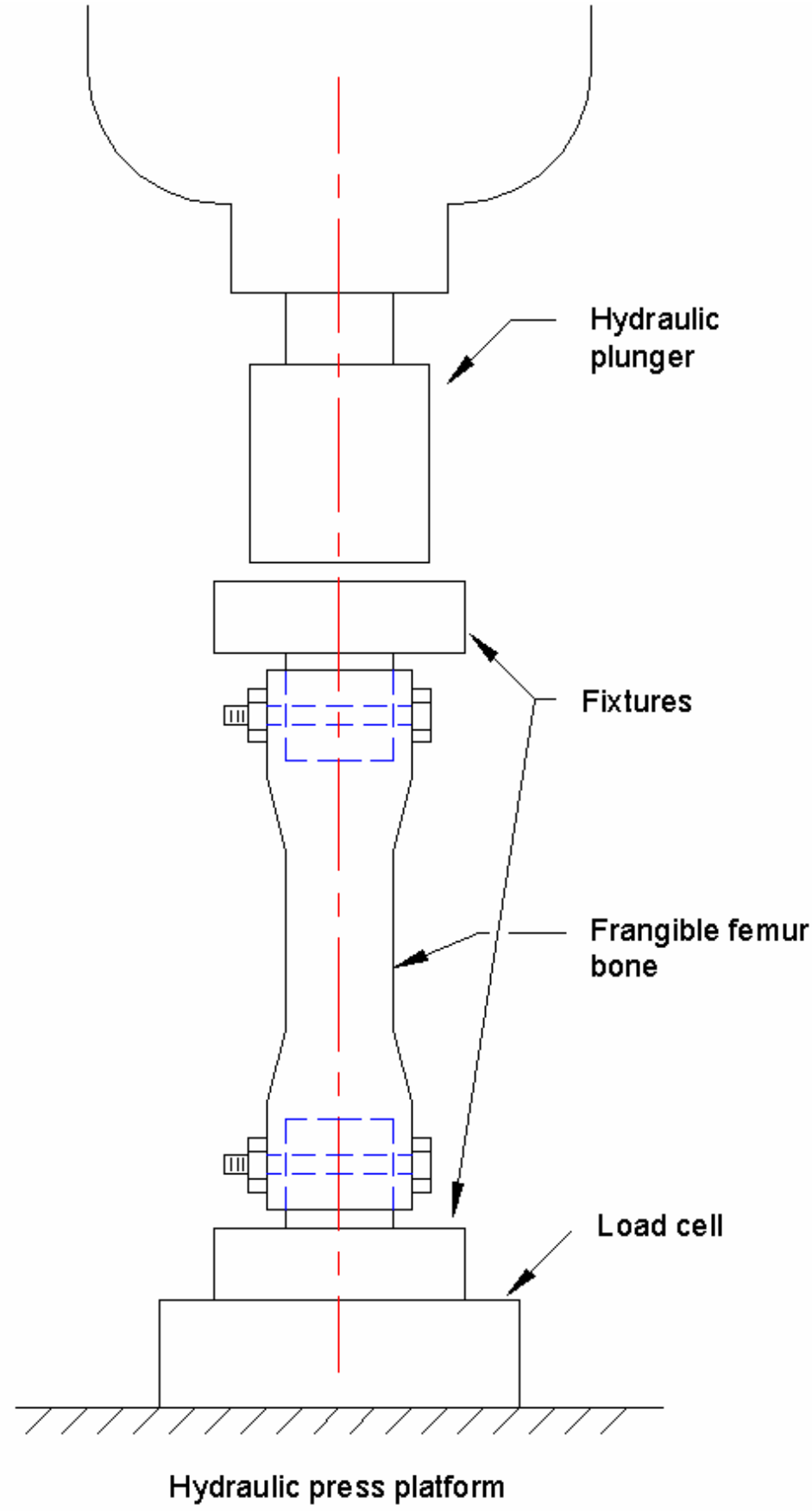

Figure A.25 — Frangible femur bone static axial load fracture test apparatus

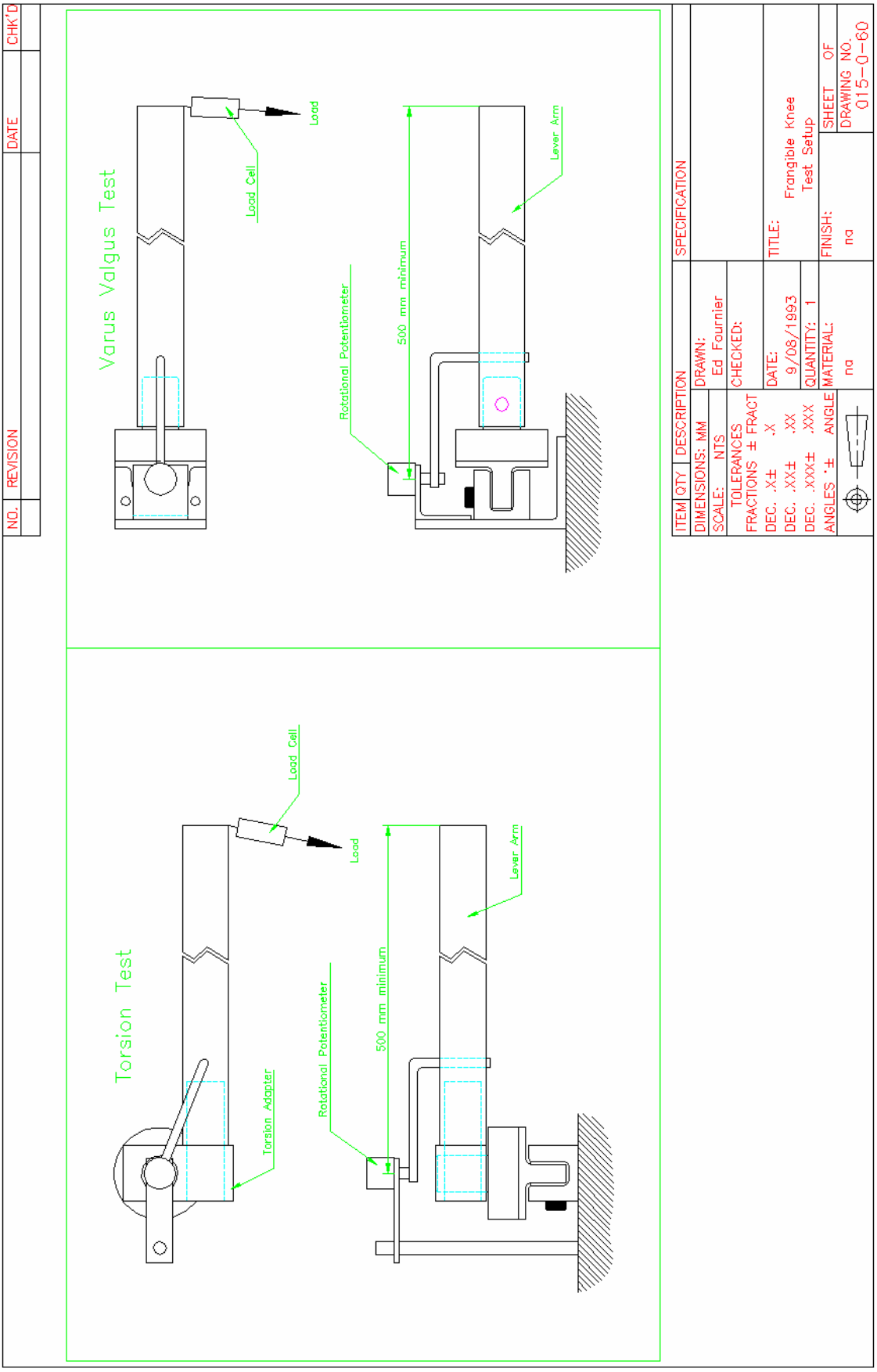

Figure A.26 — Frangible knee test apparatus

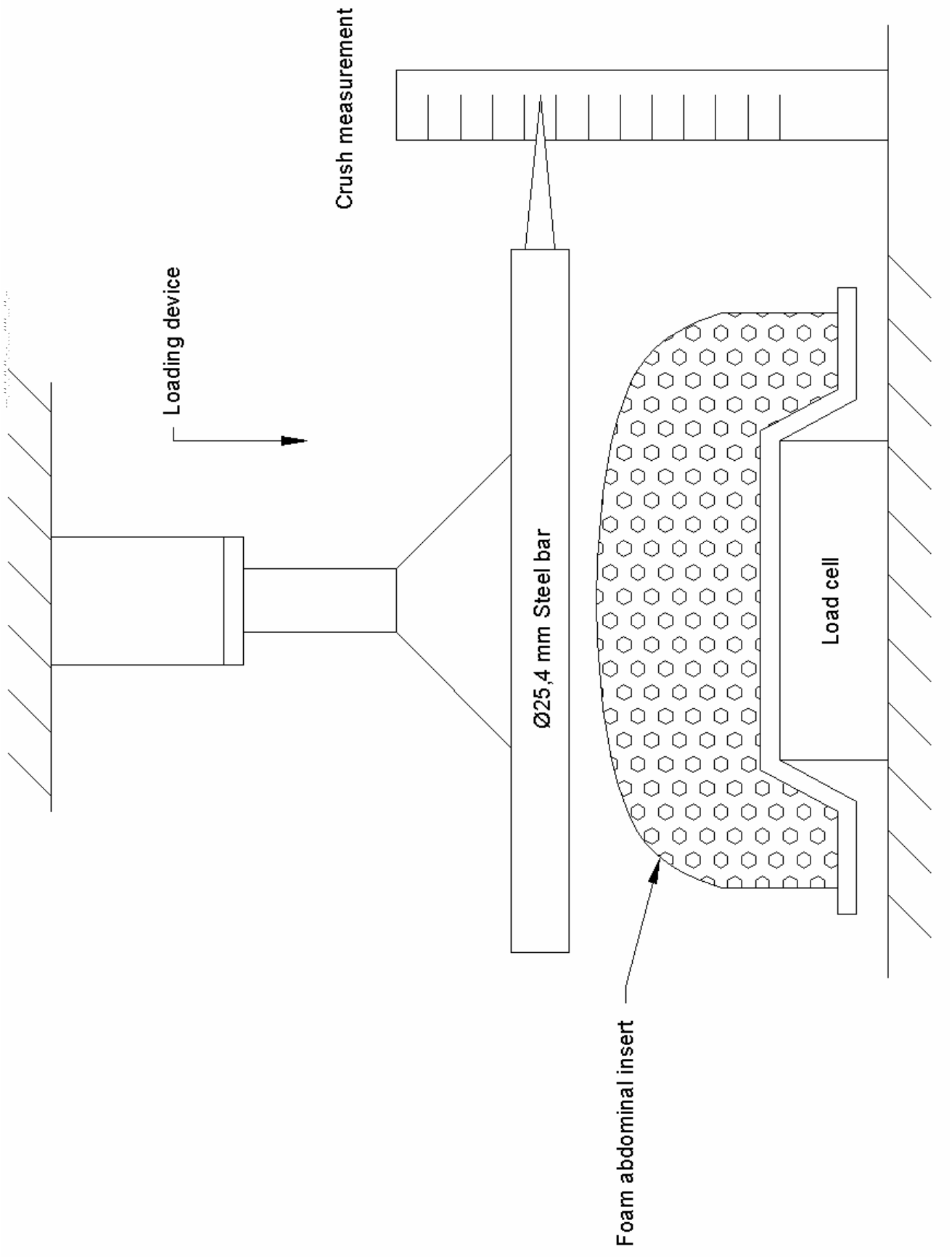

Figure A.27 — Frangible abdomen test apparatus

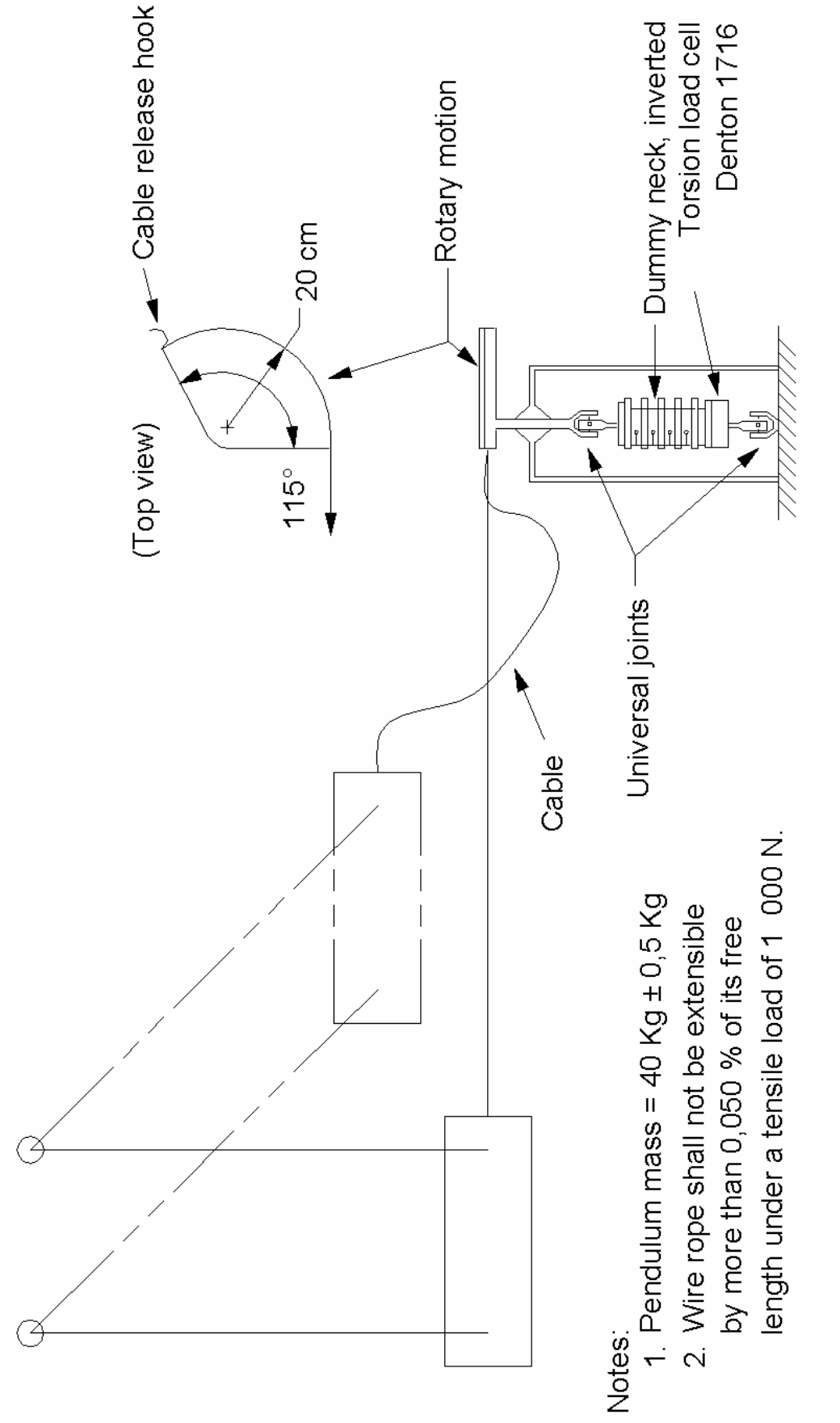

Figure A.28 — Neck torsion test schematic

Annex B
(informative)

Rationale for ISO 13232-3

The references cited in Annex B are listed in Annex B of ISO 13232-1.

B.1 Specific portion of the Scope

"Biofidelity" refers to the human like response to impacts and other forces, of an impact dummy, in comparison to existing human measurements. This is reflected in the sensed forces, deflections, and motions of various dummy parts, which are used for injury assessment. In general, it is necessary to have as high a level of biofidelity as practicable, in order to be able to infer that the measured responses are indicative of human response and injury potential.

"Compatibility" refers to the physical fitment of, for example: the helmet on the dummy head; the dummy on actual motorcycle seats and fuel tanks; the instrumentation system and sensors within the dummy structure; and the exposure of the dummy to various directions, speeds, and objects of impact, bearing in mind that existing car occupant dummies have been designed for a limited range of these variables.

B.2 Mechanical requirements for the motorcyclist anthropometric impact dummy

B.2.1 Basis dummy (see 4.1)

The selection of a basis dummy for motorcycle impact testing must consider a comprehensive list and analysis of factors (Biokinetics, 1990). This includes: anthropomorphic accuracy, impact response biofidelity, multi-directionality of response (in view of large vehicle roll, pitch, and yaw motions in motorcycle impacts), compatibility with motorcycles and helmets, availability of documentation, repeatability, reproducibility, durability, repairability, etc. A comprehensive review of available anthropometric test dummies was done, using these criteria.

As a result, in 1989, the Hybrid III 50th percentile male dummy was identified as being the most thoroughly researched, contemporary, biofidelic, well documented, available dummy as a starting point for a motorcyclist dummy, on a worldwide basis. In addition, however, a number of modifications to it were needed, in order for it to be useable in motorcycle impact research, and these are further described below.

B.2.1.1 Motorcycles are quite different from passenger cars in the relatively unrestrained and exposed position of the rider; the large yaw, pitch, and roll motions of the vehicle during impact; and the multiplicity of impact objects, directions, and speeds. In view of the fact that passenger car dummies, including the Hybrid III, were designed for a relatively narrow range of these variables, it was recognized that modifications would be needed, and that the Hybrid III provided the best available basis at that time, for what might be considered a first attempt at a specialized multi-directional impact dummy.

A 50th percentile male dummy was considered to be appropriate for the target rider population.

The Hybrid III is a public domain design provided by a number of manufacturers, for example, First Technology Safety Systems.

B.2.1.2 The sit/stand (pedestrian) construction allows the dummy to be mounted astride a conventional motorcycle. In the passenger car (sitting) version of the Hybrid III the upper legs do not rotate sufficiently with respect to the pelvis in view of the large range of motion encountered in motorcycle impacts.

B.2.1.3 A head/neck assembly which is compatible with an upper neck load cell is necessary in view of the potential importance of the neck in motorcycle air bag feasibility research and because not all Hybrid III head forms are compatible with such load cells.

B.2.1.4 Non-sliding knees are specified because the passenger car occupant sliding knees tend to bind in lateral impacts, which are common in motorcycle accidents.

B.2.2 Motorcyclist dummy head skins (see 4.2)

Head skin extensions are required because the standard Hybrid III head skin does not provide surfaces for the helmet retention strap (under the chin) or for rear helmet seating.

The addition of the head accelerometers and mounting block may require the removal of some of the head ballast. A specified mass for this assembly will eliminate a potential difference between test dummies. The 5,35 kg mass is based on the existing feasible design.

B.2.3 Motorcyclist dummy neck components (see 4.3)

A specified mass for this defined assembly will eliminate a potential difference between test dummies. The 1,55 kg mass is based on the existing feasible design.

B.2.4 Neck shroud (see 4.3.1)

The introduction of a new neck design which is significantly different than the current Hybrid III-based design, requires a new neck shroud. A neck shroud is required to promote a more realistic interaction between a deploying airbag and the dummy's neck and jowl regions. It is desirable for a neck shroud to extend from the dummy's jaw, in order to cover the void experienced in instances of neck extension.

The new neck design articulates at its mid-length, requiring a shroud design that can accommodate. Also, because the new neck can simulate a highly extended posture, the void beneath the jaw must be covered. For this reason, the new shroud design connects directly to the jaw extension of the dummy's head skin via a zipper. One side of the zipper is permanently affixed to this jaw extension, and the other side is sewn permanently to the shroud. Velcro straps wrap around the neck and affix the shroud in place.

B.2.5 Lower neck mount (see 4.3.2)

In previous Hybrid III-based design, much of the head angle adjustment was accomplished through the lower neck mount. To this end, a modification was introduced to allow a further range of neck extension. However, the new neck design accomplishes all of its adjustment at its mid-length, such that the lower neck mount may be permanently set to 5,25 degrees of extension. No additional modification is required of the standard Hybrid III part, but any previously modified part may still be used.

B.2.6 Motorcyclist neck (see 4.3.3)

Research (Rogers, 1991c; Zellner, Newman and Rogers, 1993) into motorcycle air bags has indicated that the potential exists for serious neck injury as a result of motorcycle air bag deployment. For example, the necks of out-of-position cadaver subjects were observed to be fractured by air bags deployed from the fuel tank region of a motorcycle. This may relate to the significantly different seating and air bag positions on motorcycles, as contrasted with cars and, in particular, the more fully extended angle of the head relative to the torso. For these and other reasons, it is considered to be very important to measure and to evaluate neck forces and moments in a realistic manner, in researching the feasibility of motorcycle air bag systems.

The new neck design for motorcycle crash testing is a departure from previous Hybrid III-based design. The neck is designed to meet simultaneously biofidelity criteria in frontal flexion and extension, lateral bending and torsion, as described in Table B.1.

Table B.1 — Neck biofidelity criteria

Loading Direction	Performance Target
Frontal flexion	Mertz modified moment-angle corridors (Biokinetics R95-26B) Thunnissen, et al., head-neck angle relationship (Thunnissen, et al., 1995) Thunnissen, et al., c. of g. and o.c. position relationship (Thunnissen, et al., 1995)
Lateral flexion	ISO TC22/SC12/WG5 c. of g. maximum trajectory ISO TC22/SC12/WG5 peak lateral head angle
Rearward extension	Mertz modified moment-angle corridor (Biokinetics R95-26B)
Torsion	Biokinetics torque-angle relationship (ISO 13232-3:1995)

For reference, the sled test acceleration time histories used in the initial design and conformity of production are given in Figures B.1, B.2 and B.3. These were designed to be similar to the calculated T1 accelerations in the NBDL volunteer study.

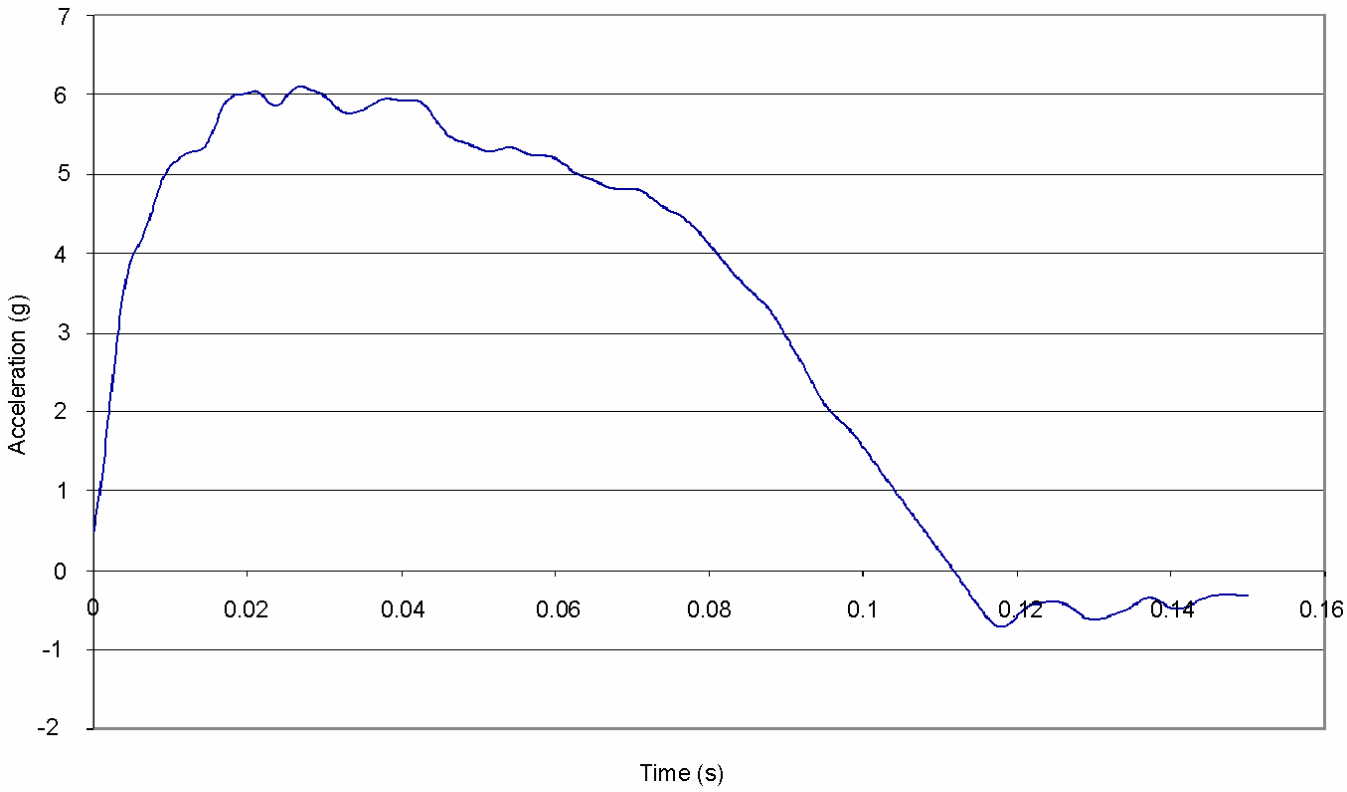

Figure B.1 — Sample extension acceleration pulse

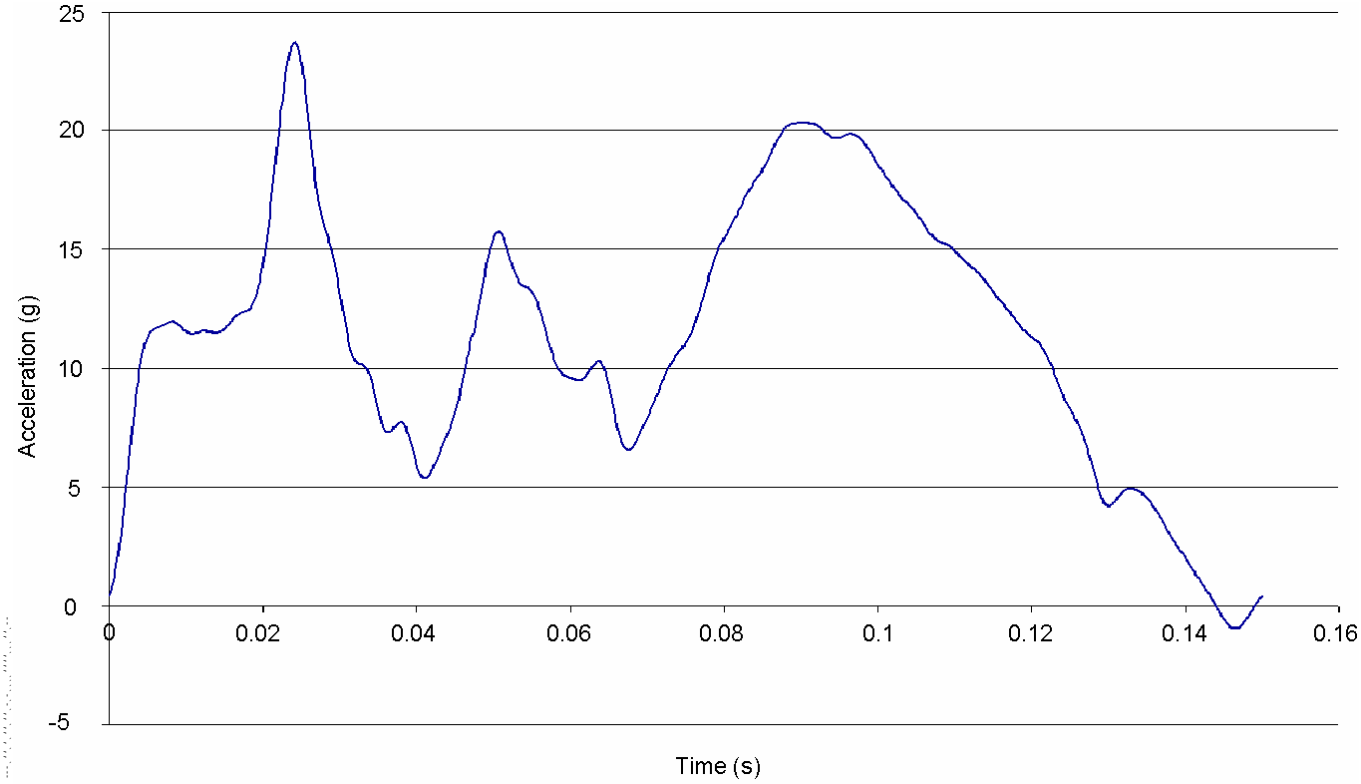

Figure B.2 — Sample flexion acceleration pulse

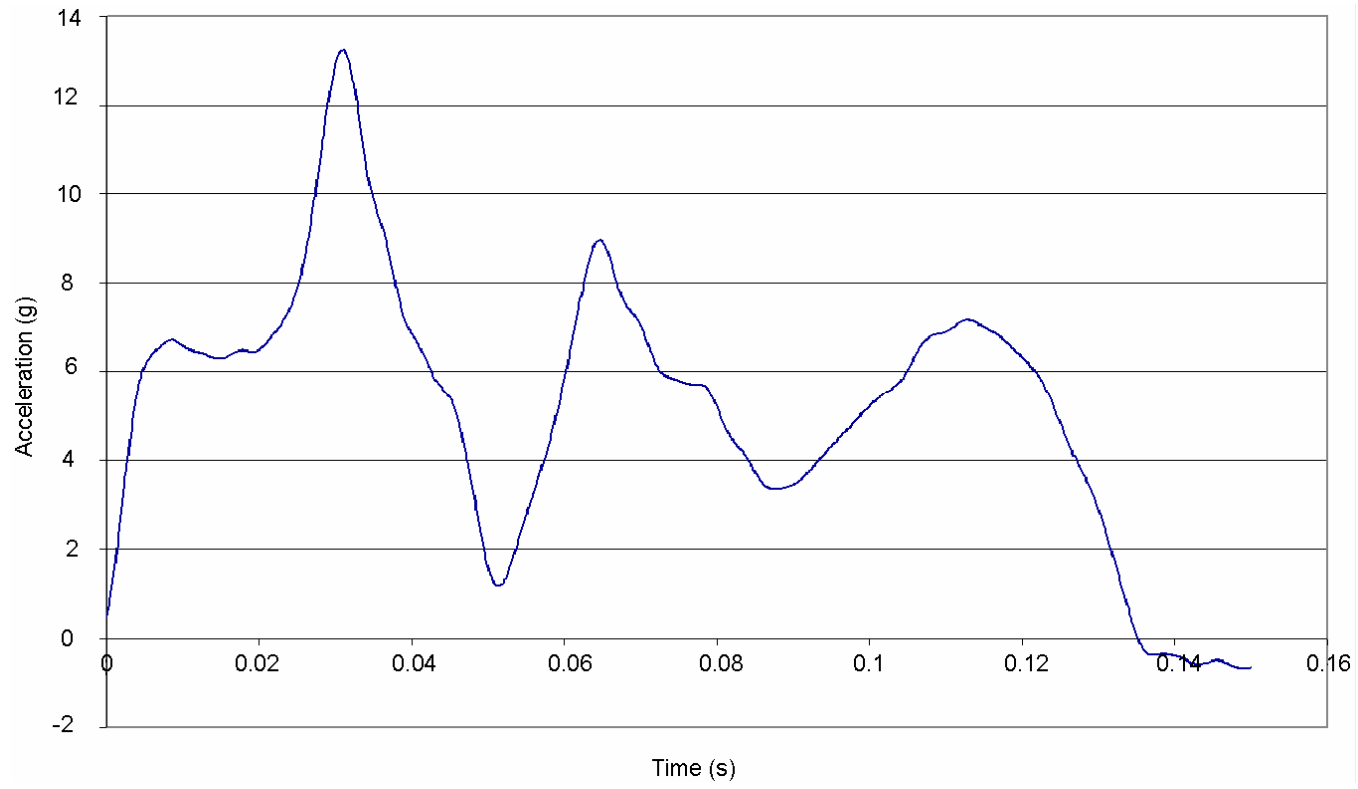

Figure B.3 — Sample lateral acceleration pulse

The aim of the neck is threefold. First, the head-lag phenomenon, described by analysts of Naval Biodynamics Lab volunteer data (Wismans and Spenny, 1984), was duplicated via an upper neck slider mechanism. This phenomenon was observed in frontal flexion, where the volunteer's torso underwent a rearward acceleration, causing the head to translate forwards initially as the neck began to rotate. Physiologically, the nature of this behavior is likely due to the straightening of the neck's natural lordosis, as well as contribution from neck musculature. However, to duplicate this physiology in a mechanical neck is prohibitively complex. The spring-return slider system mimics this phenomenon, such that head kinematics are correct, in a simple and rugged design.

Second, the range of dummy posture adjustment has been widened to accommodate a range of 65 degrees. A brief study was conducted of riders on various styles of motorcycles, in various riding postures, ranging from upright cruising style to aggressively inclined sport style (Withnall et al., Biokinetics report R97-01, 1997). The position of the rider's head relative to their torso was recorded as a function of back angle. As the rider's neck was more extended, the effective length shortened, as the centre of gravity moved rearwards. For a dummy neck, a single angle adjustment at the neck's mid-length was sufficient to position the head properly relative to the torso. The new dummy neck design adopts this mid-length adjustment via a toothed interface between the upper and lower neck. This is the only adjustment feature required for proper head orientation.

The third aim was to incorporate torsional compliance via the entire neck structure, rather than adding a separate torsional module. However, it was discovered that the required frontal and lateral bending stiffness dictated sizes and shapes of the neck elements that were incompatible with that needed for proper torsional stiffness. This was overcome by introducing additional deformable elements to the front of each elastomeric disk. These elements were only bonded on their bottom surface, such that in torsion or neck extension, the elements played no role. However, in flexion, the elements would be compressed, contributing to the higher stiffness needed in this bending mode.

The deformable elements of the neck design are made of a very tough and reliable cast urethane rubber. This material displays minimal damping and excellent hysteresis properties, even at high strains, which result in very good repeatability. Four elements are present, which increase in size from top to bottom, to account for the higher bending loads lower in the neck. Each element, or disk, is bonded to adjacent surfaces of aluminum by a specialized multi-stage adhesive. This adhesive was found to be stronger than casting the urethane rubber in place, and the material will fail before the bond.

The conformity of production, dynamic response in a full scale test, structural durability, and dynamic response durability of the new neck were tested using a series of tests.

The ability to fabricate multiple copies of the neck, with each copy having similar stiffness properties (conformity of production) was investigated by fabricating four necks. The first neck was subjected to initial conformity of production sled testing to verify the dynamic responses of the design. Three additional necks were fabricated some months later using the same manufacturing processes. All four necks were then tested using the subsequent conformity of production test procedures.

The results of the subsequent conformity of production testing are shown in Table B.2. Note that for each neck each test is repeated three times with the average of the three tests reported.

Table B.2 — Subsequent conformity of production test results

Neck	Average flexion angle (deg)	Average slider displacement (cm)	Average extension angle (deg)	Average lateral bending angle (deg)	Average torsion angle (deg)
First neck	17,5	13,0	30,9	28,7	41,5
Copy 1	16,3	12,4	27,7	26,4	37,9
Copy 2	17,1	12,2	28,5	26,3	36,9
Copy 3	18,0	14,7	29,7	27,1	38,2
Average of 4 necks	17,2	13,1	29,2	27,1	38,6
% Standard deviation of 4 necks	4,2%	8,7%	4,7%	4,1%	5,1%

The results of these tests showed close agreement between the stiffness properties of all four necks and thus verified that the design and production processes are repeatable.

The dynamic response of the new neck (copy 1) in a 413-0/30 full scale test (FST) was tested at JARI. The neck was mounted to an ISO 13232 motorcyclist dummy which was mounted on a Kawasaki GPZ 500 equipped with a UKDS leg protector. This test configuration was chosen because previous testing with the initial ISO 13232 neck, the Kawasaki GPZ 500 and UKDS leg protector, and this impact configuration resulted in a direct impact between the helmet and the side of the OV which produced large neck loads. The primary impact (0 -500 ms) neck loads for the two different necks are shown for comparison in Table B.3.

Table B.3 — Neck FST loads comparison

	F_x (kN)		F_y (kN)		F_z (kN)		M_x (Nm)		M_y (Nm)		M_z (Nm)	
	+	-	+	-	+	-	+	-	+	-	+	-
Old	4,02	-1,32	0,59	-0,09	1,81	-5,57	27,06	-15,74	62,19	-87,71	34,51	-4,50
New	0,53	-1,48	0,30	-0,22	1,58	-1,29	10,47	-33,21	23,45	-67,78	16,77	-14,20

For this MC frontal impact the primary measures were F_x, F_z, and M_y. The data shown above indicate that using the new softer neck resulted in reduced F_x, F_z, and M_y loads. An inspection of the new neck after the FST showed no visible damage to the neck. After the FST the neck was tested using the subsequent conformity of production test procedures. The results shown below in Table B.5 show that the neck met all stiffness criteria after the FST.

During the pre-test set up of the Kawasaki GPZ 500 and dummy the new neck was found to be very easy to work with. The neck shroud was easy to install and the neck angle adjustment allowed the head angle to be set at 0 degrees which was not possible with the old neck and the Kawasaki GPZ 500 equipped with a UKDS leg protector which results in a 28 degree torso angle.

In order to further test the structural and dynamic response durability of the new neck design, after the FST the new neck (copy 1), assembled with a head and upper neck load cell, was subjected to a series of dynamic bending tests using a Part 572 neck test pendulum. The test process involved subjecting the neck to about 15 pendulum tests followed by a physical inspection for damage and a check of the neck stiffness properties using the subsequent conformity of production test procedures. This process was repeated until the neck had been subjected to 100 pendulum tests. The drop heights and pendulum deceleration values were chosen to produce neck moments (Table B.4) which were equivalent to those experienced in a severe crash tests.

Table B.4 — Neck moments produced by pendulum drop tests

Primary motion	Flexion	Extension	Lateral bending
Peak moments (Nm)	90 to 110	70 to 85	40 to 50
Drop angle (deg)	120	90	90

After the 24th pendulum test a small (6 mm) crack was noticed on the back of the second disk from the top of the neck. Testing continued with careful examination of the crack after each test. The crack slowly grew to a length of about 10 mm. After 60 pendulum tests the crack was glued together using a cyanoacrylate based adhesive. This closed the majority of the crack and kept it partially closed until testing was stopped after 100 tests.

The history of subsequent conformity of production test results is shown in Table B.5.

Table B.5 — History of subsequent conformity of production test results

Time of test	Average flexion angle (deg)	Average slider displacement (cm)	Average extension angle (deg)	Average lateral bending angle (deg)	Average torsion angle (deg)
Before use	16,3	12,4	27,7	26,4	37,9
After FST	15,5	13,0	27,5	26,4	37,9
After 7 E, 10 F, 0 L[a]	17,7	15,3	30,7	29,4	41,1
After 14 E, 10 F, 0 L	16,9	15,5	29,8	28,7	39,8
After 16 E, 16 F, 0 L	18,1	16,3	31,6	30,0	41,3
After 23 E, 23 F, 0 L	18,3	16,3	31,0	30,2	41,3
After 30 E, 30 F, 0 L	18,4	17,3	31,7	30,4	41,8
After 30 E, 30 F, 10 L	17,8	16,9	30,9	31,1	41,6
After 30 E, 30 F, 25 L	17,8	17,2	31,1	31,5	41,5
After 30 E, 30 F, 40 L	18,1	17,0	31,0	31,9	41,9
[a] 7E, 10 F, 0 L, indicates 7 extension, 10 flexion and 0 lateral pendulum tests					

The subsequent conformity of production test results show that the neck met the flexion, extension, lateral, and torsion specifications through out the entire test program. This included testing while the small crack existed. The slider displacement requirement (14 $\pm$ 3 mm) was met until after 60 tests. It should be noted that the cost of replacing the slider spring would be small and in addition, spare slider springs could be purchased and kept with the dummy and replaced in the field if needed. In addition it should also be noted that if needed a single urethane disk could be replaced for much less than the cost of a new neck.

Note that it may be possible that dynamic characteristics might change without changes in static characteristics. Users should check necks for age and use-related changes in dynamic properties and report any relevant results to WG22.

Based on this series of tests it is concluded that the new neck design:

— can be manufactured in a repeatable manner,

— can be successfully used in full scale tests,

— includes adequate angle adjustment to properly position the head,

— is not critically affected by small cracks,

— continues to meet calibration specifications until after about 60 severe impacts,

— and can be field repaired if small cracks occur.

When considering the demonstrated service life of the neck and the low cost of replacing or repairing urethane parts as needed, the life cycle cost of the new neck should be somewhat less than the existing neck design.

B.2.6.1 Neck use and limitations (see 4.3.3)

The neck shown in Figure A.4 is designed specifically for use in motorcycle impact research. Users should review the following information.

B.2.6.1.1 The MATD neck stiffness is based on head and neck motions measured in the Navy volunteer tests (Ewing, 1973). For more severe conditions relatively large elongations may be observed in comparison to other

dummy neck designs (e.g., Hybrid III, which has a longitudinally mounted steel cable which limits elongation). Note that as shown in Figure B.4, the Navy volunteer's neck elongation (in addition to "craning" motion) was relatively large.

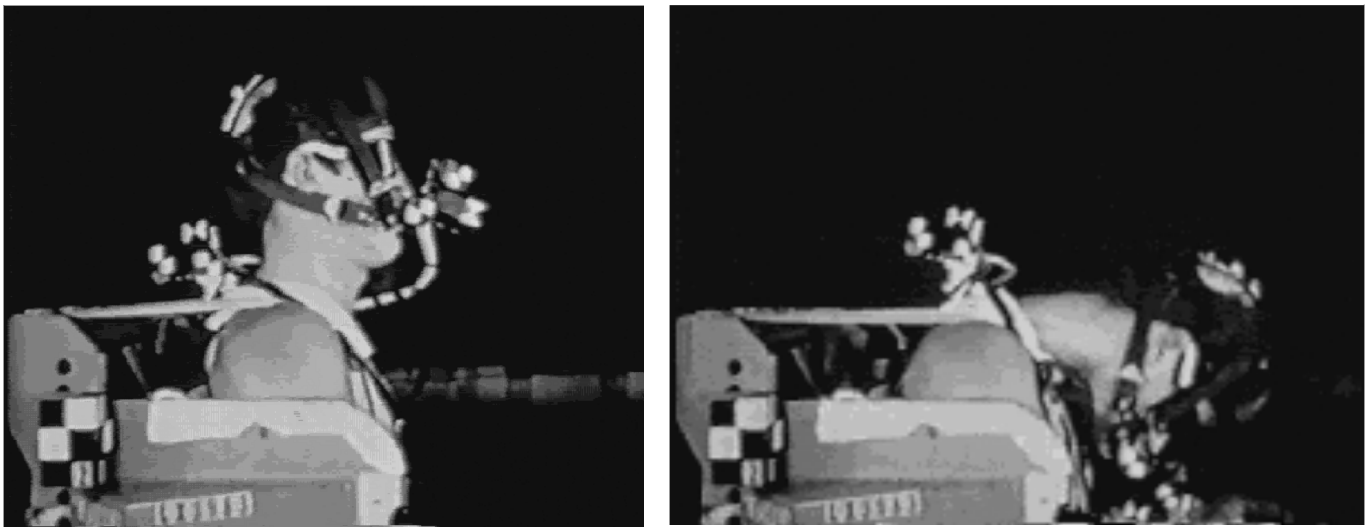

Figure B.4 — Human neck elongation observed in Navy volunteer testing

B.2.6.1.2 The MATD neck static length was based on a posture study performed with three 50th percentile adult males and three different motorcycle styles. The study quantified the location of a rider's head with respect to the rider's chest for torso angles ranging from about 12° forward to about 86° forward. The MATD neck static length, segment lengths, and rotation point location were designed such that the MATD head position relative to the chest for different motorcycle riding torso angles would be representative of human riders (Shewchenko, 2001).

B.2.6.1.3 HIII and MATD neck lengths are different because the curved length of the human cervical, thorax, and lumbar spines depend on posture. Thus, the neck length for the forward leaning MATD cannot be directly compared to the neck length for the rearward leaning HIII.

B.2.6.1.4 In sled tests with a ΔV of 9,4 m/s and 45 g the MATD neck has shown flexions which resulted in "nose to chest" contact rather than "chin to chest contact". This unexpected result could be caused by differences between the MATD (HIII) chest design and a human chest. Also, no human data is available to indicate if "nose to chest" contact might occur in humans subjected to the same sled pulse, as this sled pulse may be injurious to humans.

B.2.6.1.5 The MATD neck was designed and tested for compliance with sled test induced inertial loading response data. Further validation of neck response to impact conditions, such as actual helmetted head impact, should be considered in the future.

B.2.7 Replacement nodding blocks (see 4.3.4)

The nodding blocks are not used for head orientation. One set of blocks is supplied, for all dummy postures. All head levelling is accomplished by the mid-length neck adjuster.

B.2.8 Replacement thoracic spine (see 4.4.1)

In general, a replacement thoracic spine box is needed which is compatible with the internal data acquisition system specified in ISO 13232-4. It is intended that it maintain the same neck and lumbar structural attachment points and the same fore/aft sternum deflection capability as the standard Hybrid III component, and that it is compatible with standard Hybrid III ribs. The 120 mm width is suggested as a boundary that would be compatible with the existing feasible design of an internal data acquisition system. With regard to mass and inertial properties, the Hybrid III specification only specifies mass and cg location for the upper torso assembly as a whole. The mass,

cg, and moments of inertia of the spine box assembly are not specified and may vary as long as the upper torso mass and cg specifications are met.

An existing feasible design meets the specified upper torso mass and cg requirements. A tighter tolerance can not be met with current feasible designs.

B.2.9 Modified chest skin (see 4.4.2)

The modified chest skin is required to allow use of the upper torso inclinometer, specified in ISO 13232-6, to measure the upper torso angle during motorcycle test set up.

B.2.10 Modified straight lumbar spine (see 4.5.1)

A modified straight lumbar spine is required in order to: provide an upright seating position on a motorcycle; be compatible with the Hybrid III total height specification; provide proper biofidelity with respect to published human force-displacement properties; provide a mounting system for the abdominal insert described below; and provide appropriate weight for maintaining the proper Hybrid III mass. The static moment vs. thoracic angular displacement curve of this modified lumbar spine and cable assembly (FTSS Part numbers 1260004 and 1260005), falls within the corridors for human volunteers (Melvin and Weber, 1985). See Figure B.5.

The lumbar load cell simulator is specified in order to provide the proper lower torso dimensions and weight when the optional lumbar load cell is not used.

B.2.11 Motorcyclist dummy abdominal insert (see 4.5.2)

The frangible abdominal insert is based upon research by General Motors (Rouhana, et al., 1989). It allows quantification of potential abdominal injuries as a result of penetration into the polystyrene material. Compared to the original Rouhana design the specified component is of single piece construction without fins (which would not be biofidelic in lateral impacts), and has twice the force/deflection stiffness of the original design, in order to account for the space available in the dummy lower thorax. The very light mass lies within the limits of the Hybrid III mass and centre of gravity specifications. This specification of a test method provides a performance standard for this component.

B.2.12 Sit/stand pelvis (see 4.5.3)

Part of the internal data acquisition system described in ISO 13232-4 may be contained in the pelvis, and if so, then the requirement is that the listed Hybrid III sit/stand pelvis characteristics remain unchanged. Note that the Hybrid III pelvis moments of inertia are not specified, and may vary within and among manufacturers.

B.2.13 Modified elbow bushing (see 4.6)

The Delrin elbow bushing requires a score mark on the outside diameter to indicate the position for an elbow angle of 10°, required for motorcycle test set up, as specified in ISO 13232-6. This prevents over centre locking of the elbow joint, which would distort dummy torso motion.

Except for the scribe marks on the elbow bushings and the use of grippable motorcyclist dummy hands, the motorcyclist arms are the same as the HIII. Specifying HIII arm mass properties will eliminate a potential difference between test dummies.

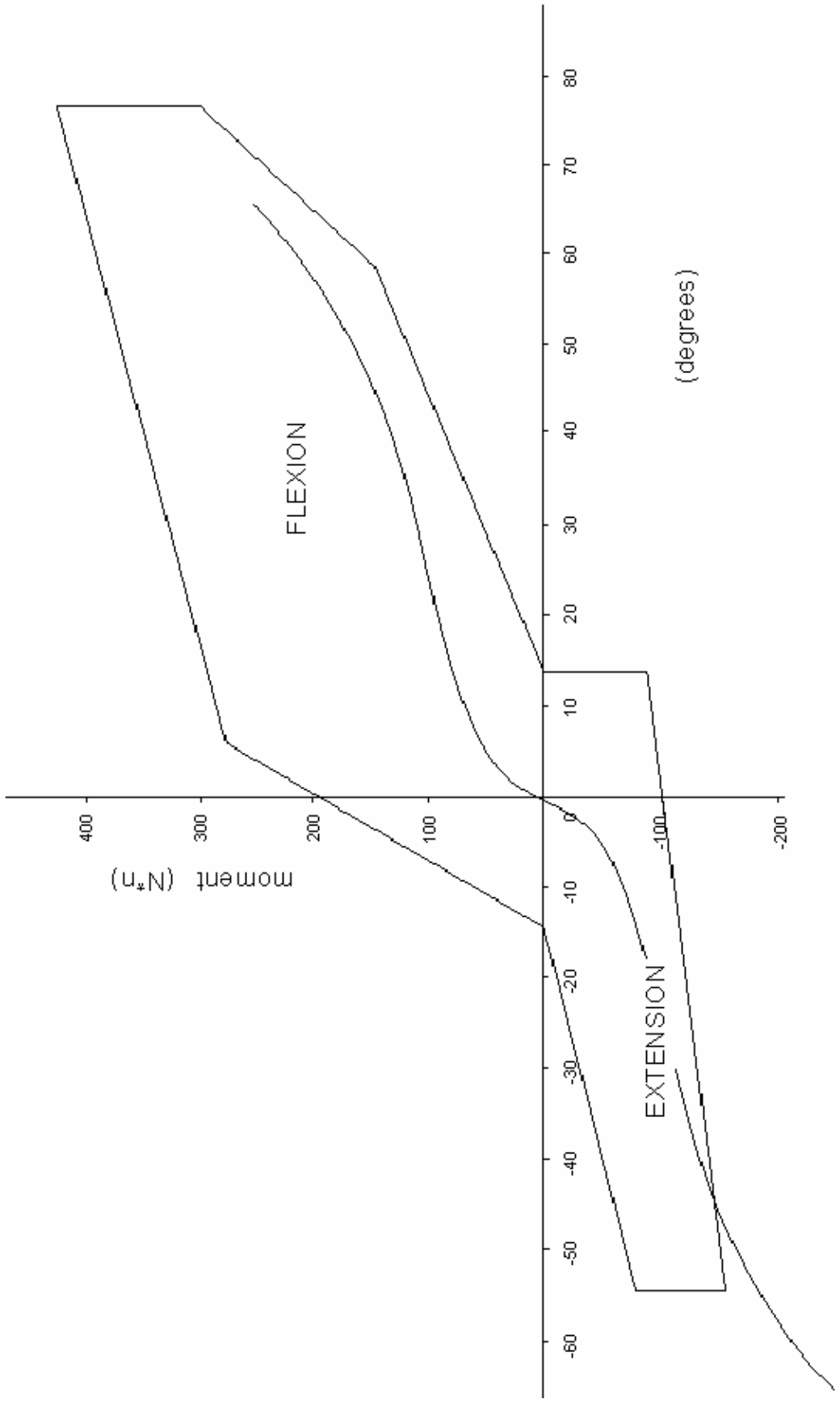

Figure B.5 — Human response corridor and modified lumbar spine response of static moment vs. thoracic angular displacement

B.2.14 Motorcyclist dummy hands (see 4.7)

The dummy hands are necessary in order to provide realistic seating position and dummy to handlebar force properties. The hands are anthropomorphic and are constructed of deformable aluminum wires covered with a silicon skin material. They are designed to wrap around the hand grips as described in ISO 13232-6; to hold the dummy in position in a realistic manner during the run up to impact; and to allow release of the hands under inertial loads after impact.

B.2.15 Motorcyclist dummy upper leg components (see 4.8)

A specified mass for this assembly will eliminate a potential difference between test dummies. The 4,89 kg mass is based on the existing feasible design.

B.2.15.1 Frangible femur bone and mounting hardware (see 4.8.1)

Frangible leg bones which have human-like stiffness and strength are necessary in order to provide: human-like (biofidelic) impact force magnitudes up to the fracture level; human-like trajectory after fracture; and continuous monitoring for fracture potential along the length and around the circumference of the bone. In addition, such a bone should have adequate repeatability and be compatible with the mechanical, geometric, and mass properties of the crash dummy. The ability to measure, electronically, the loads at several points should be included, not as an injury indicating means (for which such electronic sensors are inadequate, as discussed below), but as a means to trace sources of fractures.

For these reasons, frangible leg bones have been utilized in past and current motorcyclist and pedestrian research (Uto, 1975; Nyquist, et al., 1985; Tadokoro, et al., 1985; Miyazaki, et al., 1989; Sakamoto, 1989; St. Laurent, et al., 1989a; Newman, et al., 1991; Rogers, 1991a; Gibson, et al., 1992; Mayer and Hochgeschwender, 1993). These have varied in their material composition and the axes in which they simulate human bone stiffness and strength. The bones incorporated in ISO 13232 are the composite bones described by St. Laurent, Newman, Rogers, and Gibson, cited above.

Leg bones for car crash dummies are rigid and non-frangible (e.g., the metal bones used in the Hybrid III dummy). These are inappropriate for motorcycle crash research because:

— they were designed for a different purpose and crash environment. In particular, Hybrid III leg bones are intended for frontal impacts, usually to the knees, against padded or relatively deformable car interiors, with a dummy which is usually restrained by lap and torso belts. Motorcyclist legs can be exposed to multiple frontal and lateral impacts to the knees, lower and upper legs; the impacted objects are often rigid; and the rider is typically not restrained.

— mid-span impacts to a fleshed metal Hybrid III lower leg bone with a rigid impactor result in greatly distorted (i.e., magnified) forces, compared to those recorded for a human cadaver lower leg or the feasible frangible lower leg design (see Figures B.6 to B.10). This rigid/rigid interaction can result in more than 100% overestimation of impact forces, and therefore, of fracture potential.

— the fact that the metal leg bone does not fracture can distort, in some cases, the dummy motion compared to the motion with frangible human or dummy leg bones. This distortion was measured by Tadokoro (1987) and Miyazaki, et al., (1989). Another occurrence of this is illustrated in Figures B.11 to B.16, which are from an Articulated Total Body (ATB) three-dimensional computer simulation of an impact to the rider's knee by the front corner of a car, with and without frangible femur and tibia leg bones, as defined in 4.8.1 and 4.11.1, with all other parameters held constant. As can be seen, there are large differences in the head, shoulder, hip, knee, and ankle trajectories when frangible vs. non-frangible bones are used. This large difference in trajectory is verified by the full-scale test pelvis trajectory results shown in Figure B.17, for an offset frontal impact with Hybrid III legs and with composite frangible leg bones, defined in 4.8.1. and 4.11.1.

— force monitoring with load cells only measures the loads at the specific load cell location, and not at other potential fracture sites. This may be suitable for monitoring knee frontal impact in cars; but is not adequate for the multiple impacts and impact directions in motorcycle crash tests. This method can result in underestimation of fracture potential in many cases. An example is the three point loading impact to the lower leg, illustrated in

Figure B.18. The lower leg is supported near the upper and lower tibia load cells, while the 50 kg mass impacts the mid-tibia. A practical example of this would be an impact to the mid- tibia by a car bumper, while the lower leg is resting against the fuel tank at the upper end and engine case at the lower end. The sensed loads indicate little or no bending moment applied to the bone, whereas in fact, the loads are sufficient to fracture human or frangible dummy leg bones. The result is a nearly 100% underestimation of the bending moment, and therefore, injury potential.

The composite femur and tibia bones, geometry and performance requirements which are given in ISO 13232, have been validated against the Yamada (1970) and Martens, et al., (1980) cadaver data, as well as more recent cadaver testing. For example, Figure B.19 shows mid-tibia impactor force for three point dynamic tests with a sample of nine wet tibia specimens (mostly 55 years and older) as reported by Fuller and Snider (1989). As is typical, there is considerable scatter in the responses, but for most of the specimens, the fracture pulse is over within 0,001 s. Figure B.20 shows envelopes which bound the time responses for all nine specimens and for the weakest six specimens (after correction for support length variation). Also shown are impactor force time histories for two composite tibia bones. The latter show:

— a high level of reproducibility;

— a waveform which is similar to the envelopes for the cadaver data, and which lies between the weaker and the stronger specimens (closer to the stronger specimens). This is not unexpected since the design target, as noted below, was the young adult male cadaver properties described by Yamada (1970).

Another validation example is shown in Figure B.21, which is a two point (i.e., pivoted at the knee) impact test with fully fleshed wet cadaver lower leg, and fully fleshed composite dummy bone lower leg. Again, the time history waveform is similar; and the composite bone forces are somewhat higher than those for the embalmed and approximately 60 year old cadaver specimen.

The conclusion of the above is that frangible leg bones which have human like stiffness and strength are appropriate for use in motorcycle crash research; and standard Hybrid III rigid leg bones are not appropriate for use in motorcycle crash research.

The mounting of the frangible femur bone and the specification of its mass are intended to provide compatibility with the remaining Hybrid III leg components.

Static and dynamic performance tests are specified for leg bone design certification and quality control purposes (described in clause 6). Of these procedures, the dynamic laboratory tests provide conditions which are most relevant for the leg bone's intended use, while the static measurements are more convenient to perform.

The characteristics which are specified for the femur are bending, torsion, and axial characteristics, as these are the types of loads which have been observed in past motorcycle impact testing and in motorcycle clinical studies. The specified static and dynamic properties are for an existing feasible leg bone design which is consistent in its characteristics with the published biomechanical data, as defined below. The specified values are provided as references in order to standardize dummy component performance to those achieved in one feasible design. The feasible design is based upon (and achieves to within a few percent) published biomechanical data.

The biomechanical data for bending strength and stiffness are based upon data reported by Yamada (1970), measured by Motoshima (1960). The static bending deflection is based on static measurements of a sample of young adult male cadavers. The dynamic bending strength of the femur is also based on the Motoshima statically measured young adult male samples increased by a factor of 1,4 to account for dynamic stiffening. The 1,4 factor is based upon a literature review by St. Laurent, et al., (1989) which included the available biomechanical data of McElhaney (1966) and others. The static torsion deflection is based on the work by Martens, et al., (1980). The dynamic torsion strength is based on the Motoshima statically measured young adult male samples increased by a factor of 1,4, again to account for dynamic stiffening.

For axial loading, the upper leg stiffness and strength properties are heavily dependent on the bending properties, due to the presence of eccentricity in the human and dummy hip joints. The static axial peak strength is specified so as to maintain consistency with the available biomechanical data and also to assure similarity to the existing feasible leg bone design.

B.2.16 Femur load cell simulator (see 4.8.2)

This component is specified in order to provide for proper leg dimensions and weight when the optional femur load cells are not used.

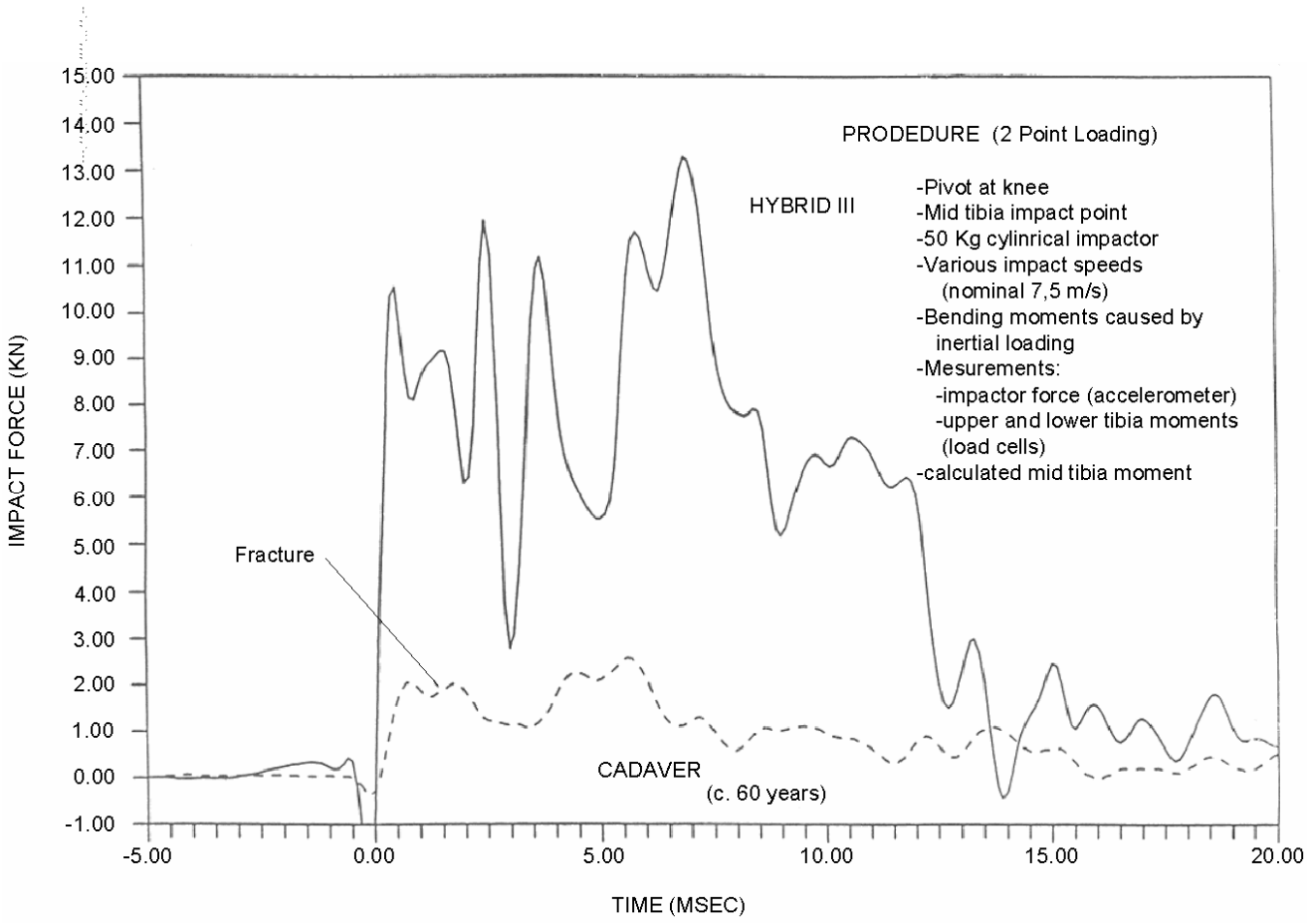

Figure B.6 — Lower leg dynamic impact tests impact force vs. time: Hybrid III and cadaver legs

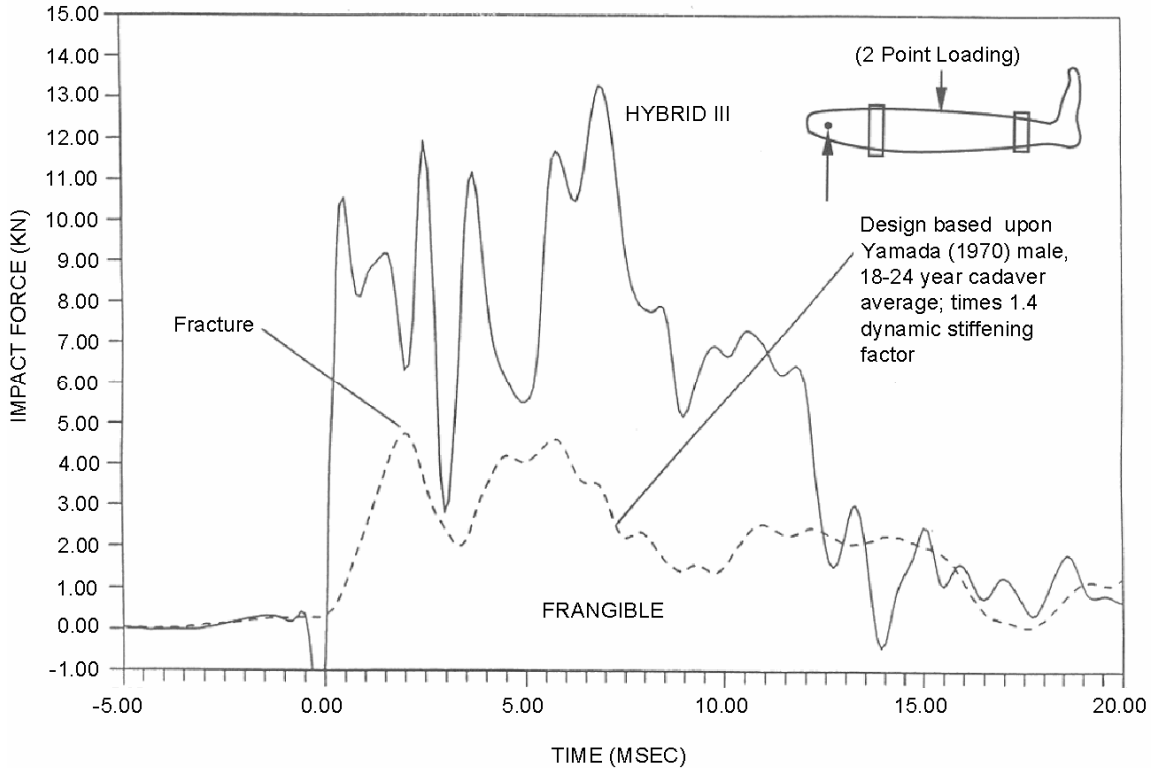

Figure B.7 — Lower leg dynamic impact tests impact force vs. time: Hybrid III legs and frangible leg, as defined in 4.11.1

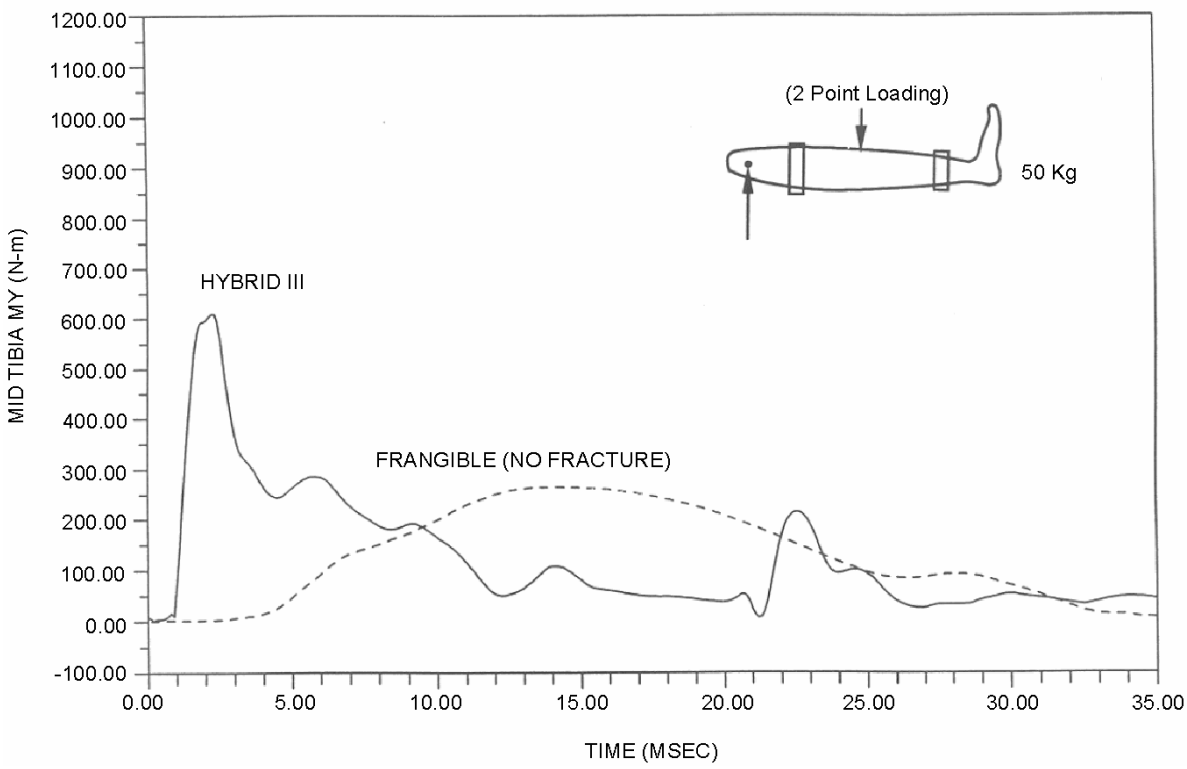

Figure B.8 — Instrumented lower leg impact tests mid-tibia moment vs. time for drop height = 1,016 m: Hybrid III leg and frangible leg, as defined in 4.11.1

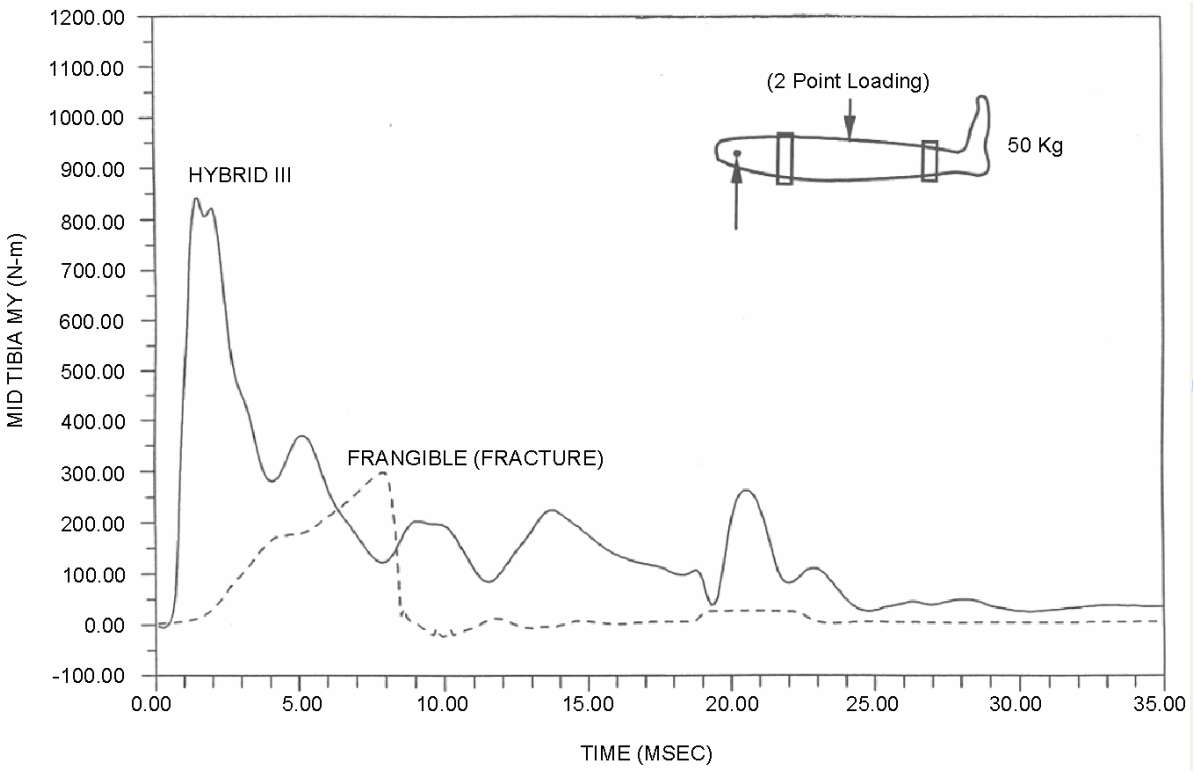

Figure B.9 — Instrumented lower leg impact tests mid-tibia moment vs. time for drop height = 1,778 m: Hybrid III leg and frangible leg, as defined in 4.11.1

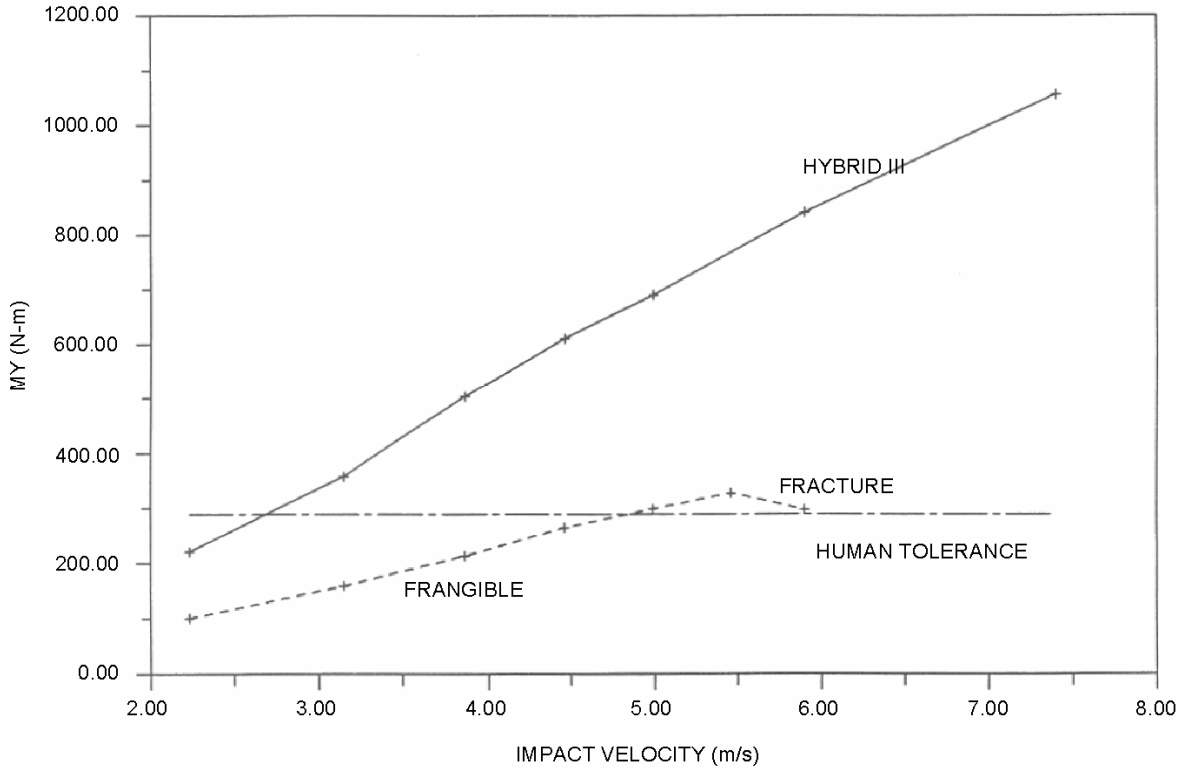

Figure B.10 — Lower leg impact tests mid-tibia bending moment M_y vs. impact velocity: Hybrid III leg and frangible leg, as defined in 4.11.1

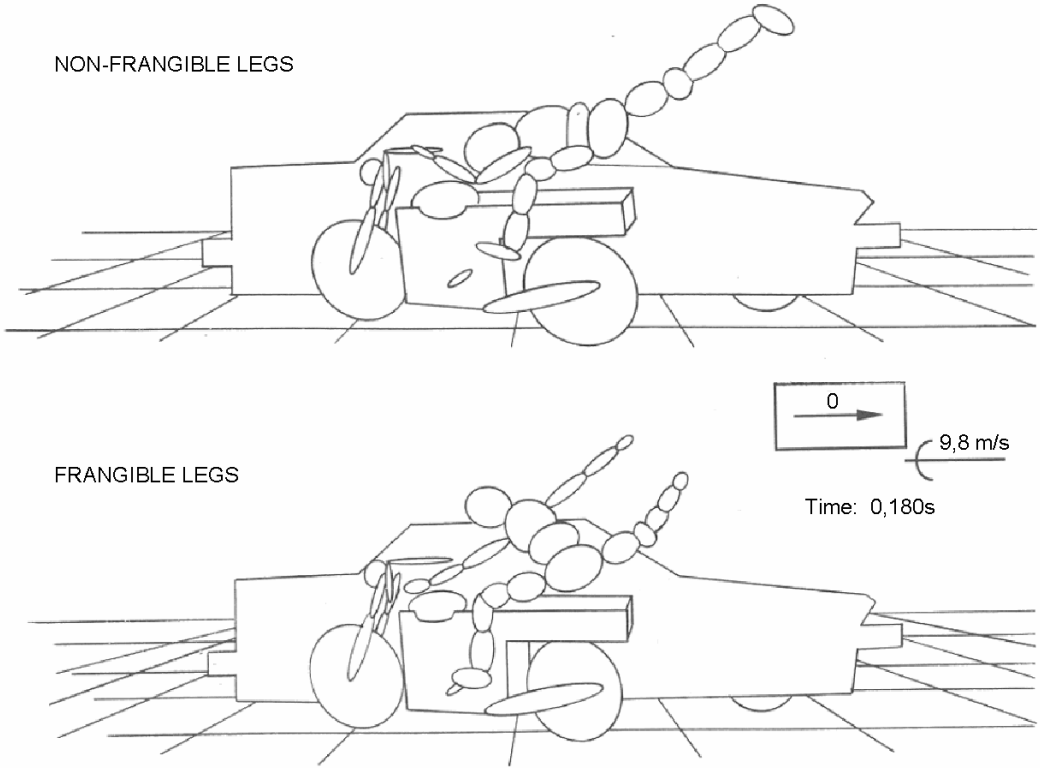

Figure B.11 — View of ATB simulated offset frontal impact, medium conventional motorcycle, with and without frangible leg bones, as defined in 4.8.1 and 4.11.1

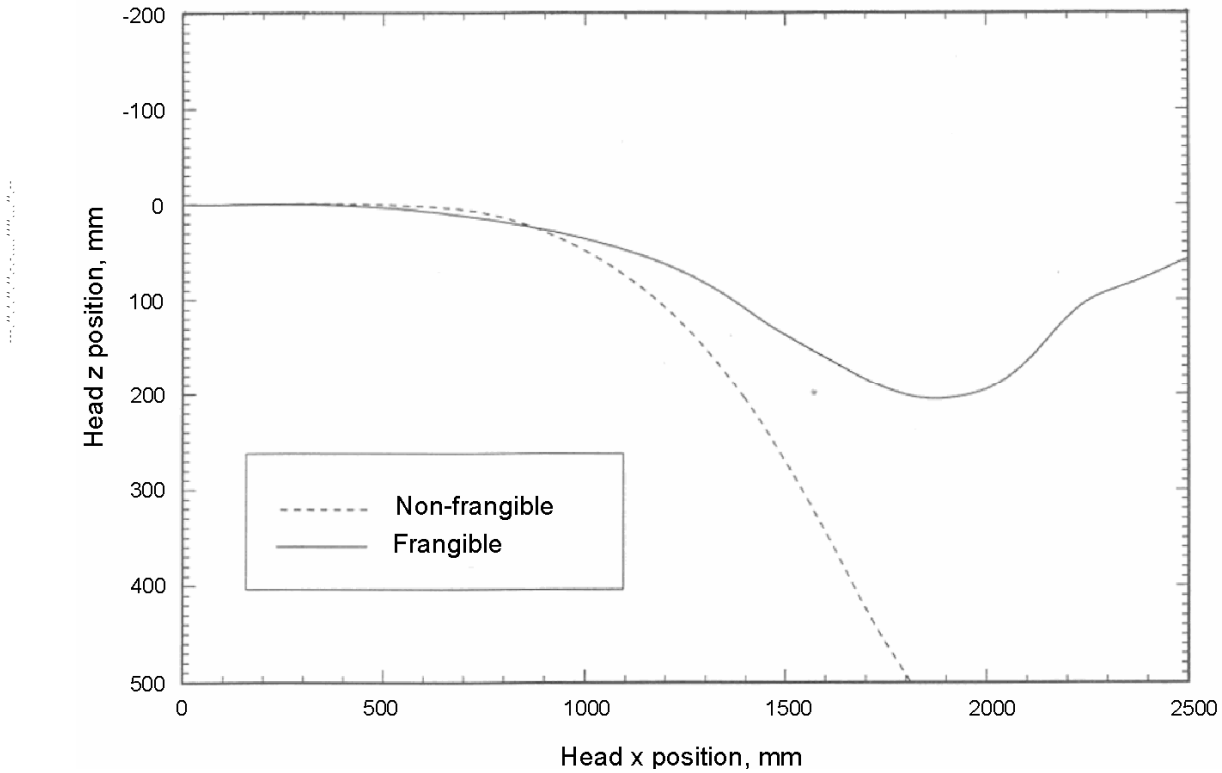

Figure B.12 — Head trajectory comparison of frangible and non-frangible legs

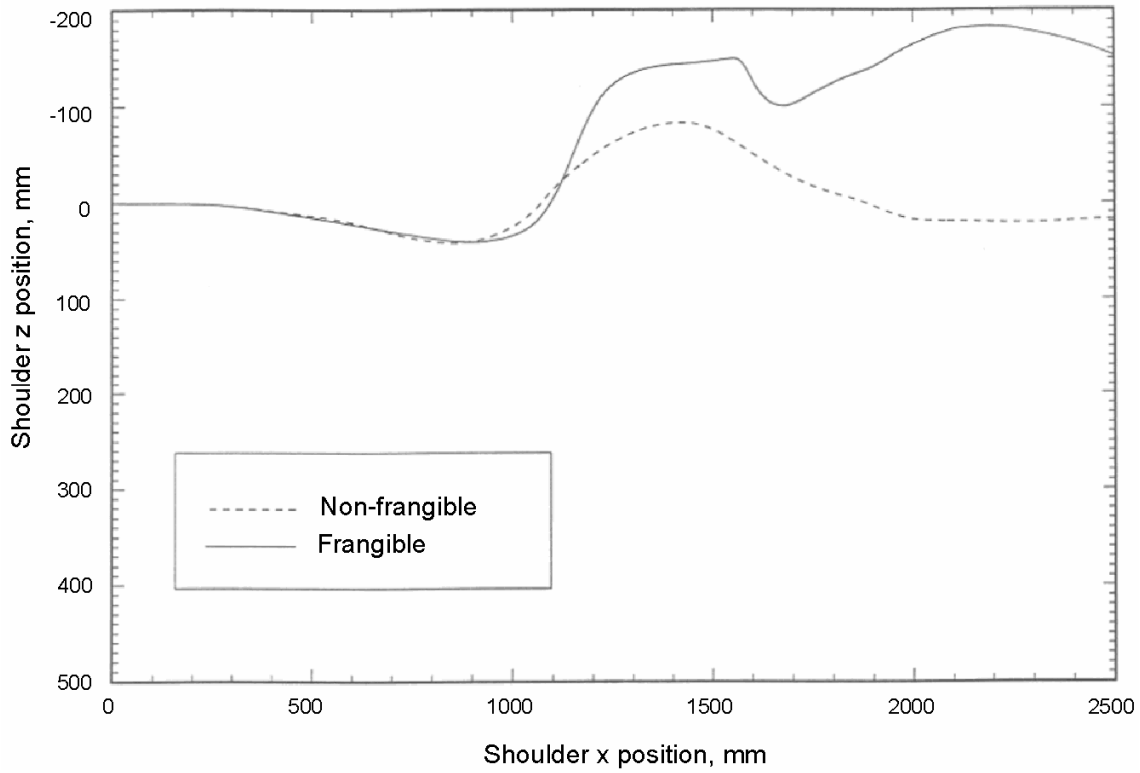

Figure B.13 — Shoulder trajectory comparison of frangible and non-frangible legs

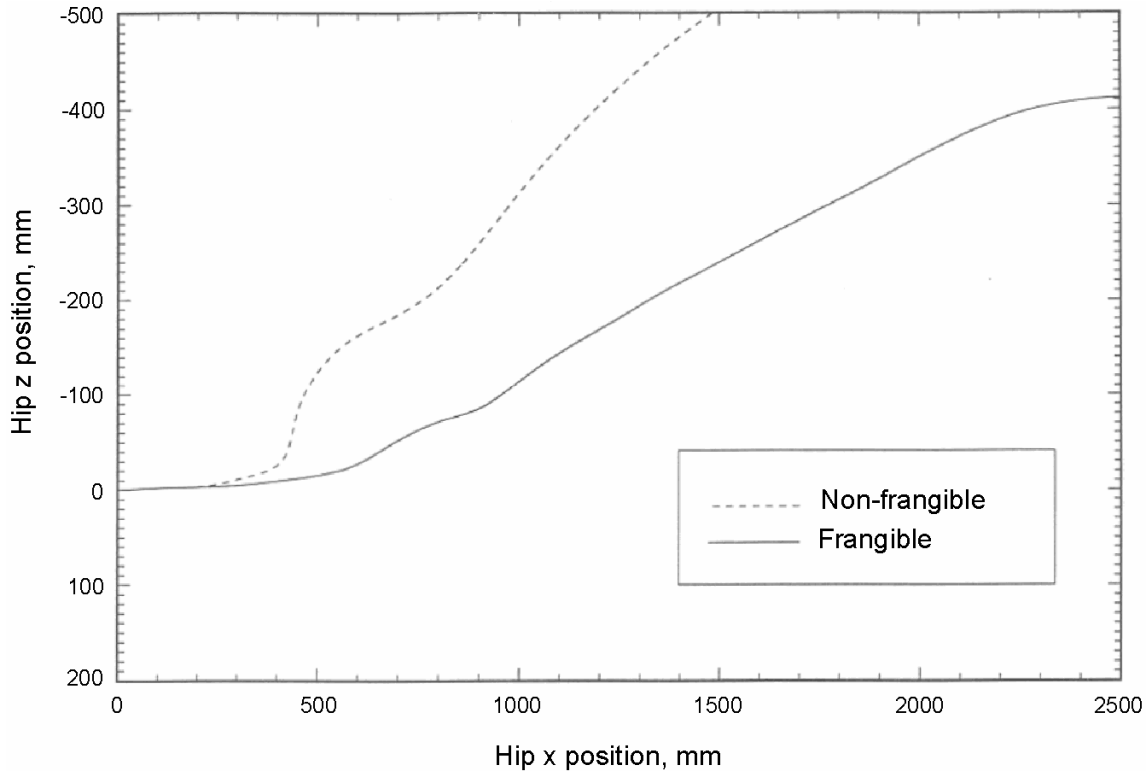

Figure B.14 — Hip trajectory comparison of frangible and non-frangible legs

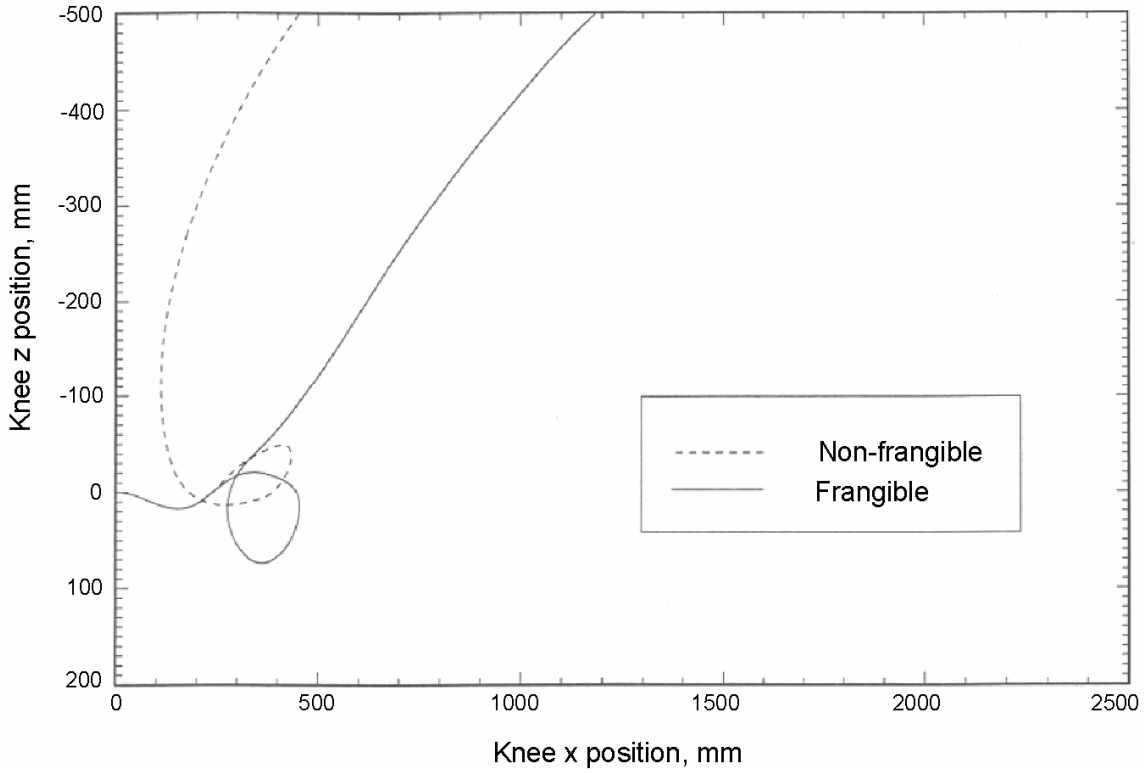

Figure B.15 — Knee trajectory comparison of frangible and non-frangible legs

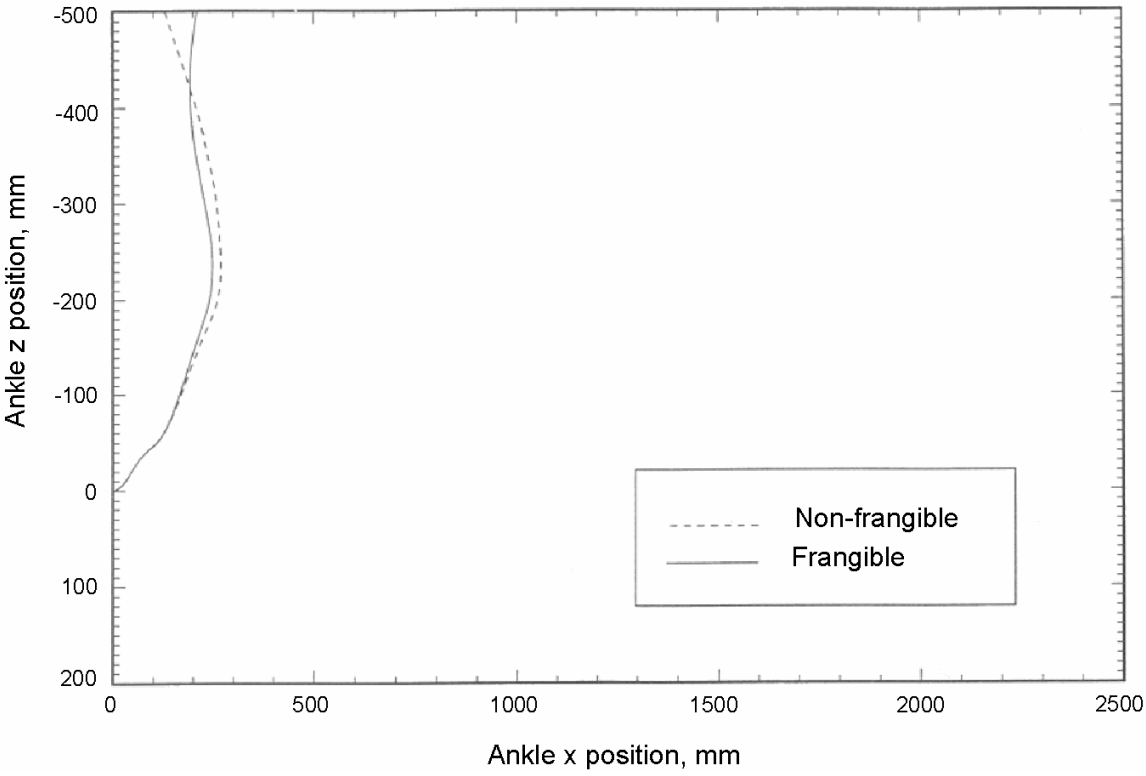

Figure B.16 — Ankle trajectory comparison of frangible and non-frangible legs

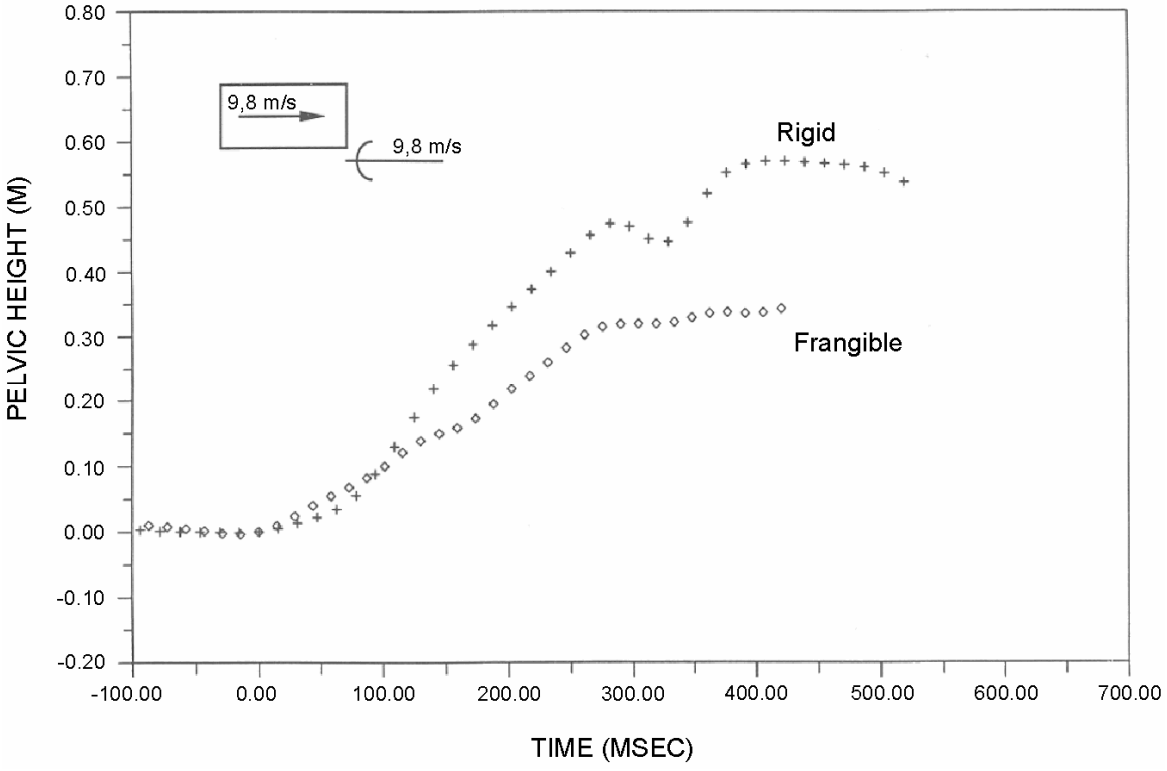

Figure B.17 — Pelvis trajectory comparison of frangible and non-frangible bones, full-scale test, offset frontal impact, large conventional motorcycle

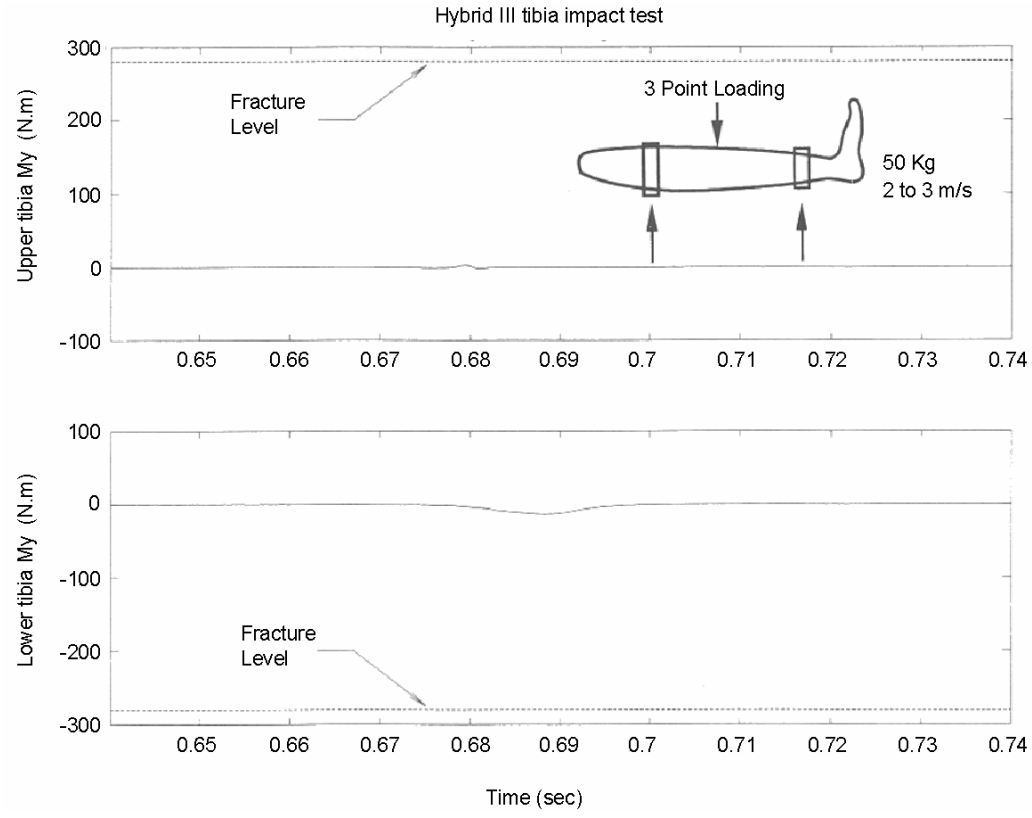

Figure B.18 — Sensed upper and lower tibia bending moments vs. time in Hybrid III tibia, for three point impact test sufficient to fracture human tibia

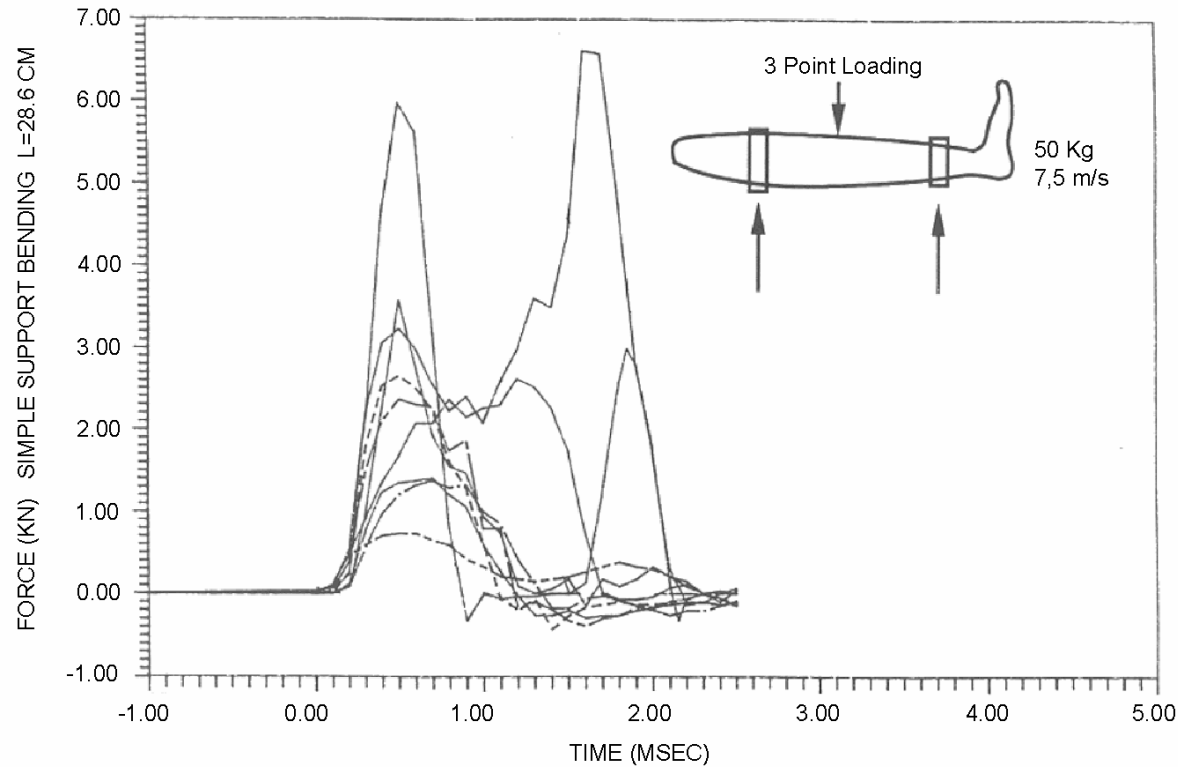

Figure B.19 — Impactor time histories for nine cadaver tibia specimens from Fuller and Snyder, 1989

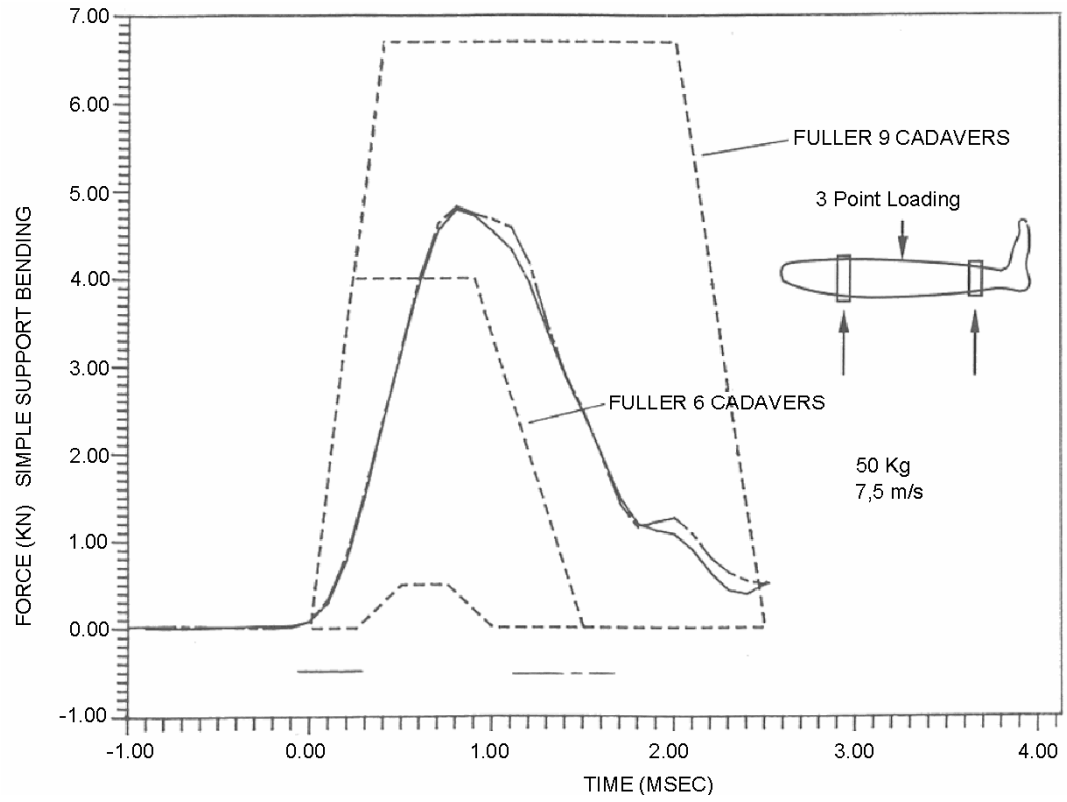

Figure B.20 — Comparison of composite tibia fracture force response with envelopes of cadaver tibia fracture force response

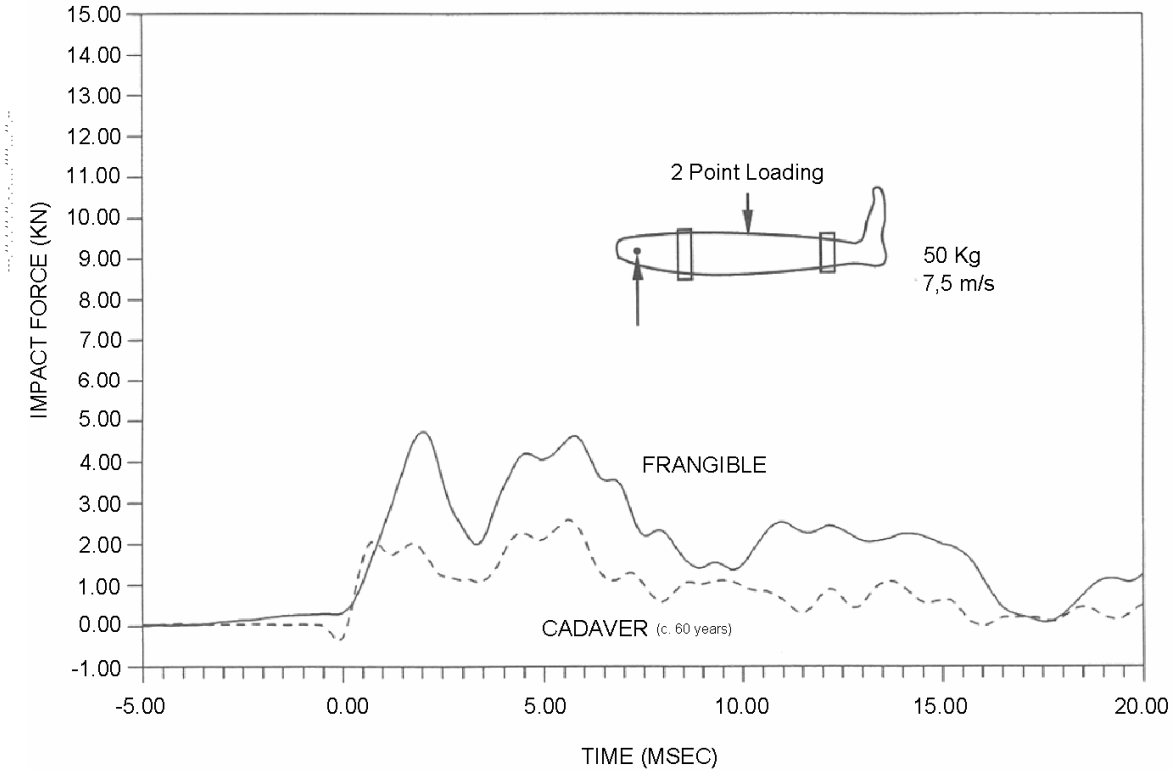

Figure B.21 — Lower leg dynamic impact tests impact force vs. time: frangible and cadaver legs

B.2.17 Motorcyclist dummy frangible knee assembly (see 4.9)

A frangible knee assembly has been specified in order to monitor for knee ligament injuries in lateral bending and torsion relative to the tibia (M_x, M_z); to provide for appropriate knee joint rotations and dummy motions when the lower leg is restrained; to provide appropriate forces and structural "fusing" between the lower and upper legs (i.e., realistic rotations and moments); and to be compatible with existing biomechanical data (St. Laurent, et al., 1989). In addition, prior research (Tadokoro, et al., 1985) had indicated the potential for large torsional loads in the femur. The frangible knee was intended to provide enhanced biofidelity in this regard.

The frangible knee assembly has been specified to be compatible with the remaining Hybrid III leg components and masses.

Static tests are used to confirm knee designs and provide quality control for frangible knee components because the existing biomechanical data is static in nature. The pre-failure and at failure moment and rotation values for varus valgus (lateral bending) and torsion are based on cadaver measurements (St. Laurent, et al., 1989), and upon the measured properties of the existing feasible knee design which are consistent with these biomechanical data.

For this frangible knee concept, a failure of an internal shear pin is interpreted as an injury of the respective knee ligaments, according to 5.2.3.2 of ISO 13232-4. "Pre-failure" (in Table 3) refers to a loaded condition prior to fracture of the shear pin.

B.2.18 Leg retaining cables (see 4.10)

Retaining cables are necessary to prevent the separation of dummy legs from the dummy upon fracture of the frangible element. Loss of a leg during a test could affect overall dummy motion. Traumatic loss of a limb is a rare event in accidents, and in any case the dummy leg does not otherwise have sinew, muscle, and other tissues which retain the limb. The cable has a weight limit and is installed with slack so as not to affect the fracture force of the bone itself.

B.2.19 Motorcyclist dummy lower leg components (see 4.11)

A specified mass for this assembly will eliminate a potential difference between test dummies. The 5,29 kg mass is based on the existing feasible design.

B.2.19.1 Frangible tibia bone and mounting hardware (see 4.11.1)

The same considerations apply here as in the case of the frangible femur bone and mounting hardware noted above, with the exception of the tibia axial characteristics, as these were judged to be unimportant for typical motorcycle impact situations. For both the upper and the lower leg bones, the specified static deflections are approximately 50% of the deflection at peak strength, to provide a measurement in the linear material behavior range. The static and dynamic characteristics of the tibia bones in Table 4 are based upon the corresponding Yamada (1970), Martens, et al., (1980) and McElhaney (1966) data for tibia bone samples.

B.2.20 Modified lower leg skin (see 4.11.2)

Modified lower leg skins are specified in order to provide for installation and removal of the skin from the frangible leg bones, which is not feasible with the standard Hybrid III leg skins. The internal contour of the leg skin has been modified to conform to the frangible knee assembly. The masses are consistent with the standard Hybrid III specification.

B.2.21 Complete motorcyclist dummy (see 4.12)

A specified mass for the entire dummy assembly will eliminate a potential difference between test dummies. The 75,84 kg mass is based on the existing feasible design.

B.3 Sampling of frangible components

B.3.1 Initial conformity of production (see 5.1)

The purposes of frangible component sampling and measurement are to: allow for performance specification of potentially different frangible component designs and to ensure that the variability in frangible components is controlled to a feasible minimum.

A sample of 10 frangible components is specified because this is the approximate minimum number needed to establish a usable mean and standard deviation. Since the tests are destructive in nature, separate samples of 10 are needed for each characteristic. A relatively tight bound of 5% for the sample mean for specified strengths (and abdominal insert static forces) is given because these values are crucial in injury assessment. Also, this number is relatively small compared to run-to-run variability in other dynamic measurements such as maximum resultant head acceleration, for example. A broader range of 20% for the static deflections is specified because these values affect injury assessment in a more indirect manner. Likewise, a relatively tight specification on the allowable standard deviation is given in order to control variation of leg samples used in evaluating injuries. A standard deviation less than 7% of the sample mean is specified for all strengths (and abdominal insert static forces) and less than 10% for all static deflections because this reflects the relatively tight bounds that have been achieved with the existing feasible designs. Data in Tables B.6 to B.13 and B.17 for the feasible designs of the femur and tibia indicate that these bone designs meet the criteria. Data in Tables B.14, B.15 and B.16 indicate that the feasible designs of the abdominal insert and knee compliance elements meet the criteria.

B.3.2 Subsequent conformity of production (see 5.2)

The purpose of the subsequent conformity of production (CoP) tests is for lot checking and quality control of components, once the bone design, material, and manufacturing processes have been certified by the manufacturer. Here a compromise between the cost of quality control sampling and the reliability of the sampling process has been reached. For typical past production runs of 30 to 60 bones, a sample of three bones represents 5% to 10% destructive sampling, which is relatively costly. For a sample of three bones, assuming a normal distribution and the same mean, it would be expected that one of the bones would exceed one standard deviation

in its properties. Therefore, if none of the components deviates by more than two standard deviations (14%) the lot is considered to be normally distributed and acceptable for impact testing. If one or more of the samples deviates by more than two standard deviations, this exceeds the bounds of a normal distribution, and a larger sample is then used to improve the reliability of the estimate. This involves three more components from the same lot. Then, again, if one third of the total test sample (of six components) deviates by more than two standard deviations from the established means, the lot is considered to exceed the bounds of a normal distribution and is rejected for full-scale impact testing purposes.

Table B.6 — Sampled static bending stiffness of composite femurs

Specimen number	Mid-span deflection mm
1	4,98
2	5,33
3	4,91
4	5,26
5	5,06
6	4,90
7	4,94
8	5,59
9	5,23
10	5,17
NOTE 1 Bending span = 341 mm	
NOTE 2 Mid-span load = 1 366 N	
NOTE 3 Mean: 5,13 mm	
NOTE 4 Standard deviation: 0,23 mm (4,5%)	

Table B.7 — Sampled static torsional stiffness of composite femurs

Specimen number	Rotation rad
1	0,099
2	0,103
3	0,108
4	0,108
5	0,094
6	0,093
7	0,103
8	0,110
9	0,105
10	0,095
NOTE 1 Torque = 67 Nm	
NOTE 2 Mean: 0,102 rad	
NOTE 3 Standard deviation: 0,0062 rad (6,0%)	

Table B.8 — Sampled dynamic bending strength of composite femurs

Specimen number	Peak bending moment Nm
1	360
2	359
3	367
4	363
5	374
6	358
7	357
8	365
9	350
10	357
NOTE 1 Mean: 361 Nm	
NOTE 2 Standard deviation: 6,7 Nm (1,8%)	

Table B.9 — Sampled dynamic torsional strength of composite femurs

Specimen number	Peak bending moment Nm
1	227
2	196
3	210
4	194
5	196
6	208
7	211
8	197
9	211
10	214
NOTE 1 Mean: 206 Nm	
NOTE 2 Standard deviation: 10,4 Nm (5,0%)	

Table B.10 — Sampled static bending stiffness of composite tibias

Specimen number	Mid-span deflection mm
1	3,56
2	3,46
3	3,92
4	3,80
5	4,37
6	3,66
7	3,86
8	3,73
9	4,27
10	3,70
NOTE 1 Bending span = 286 mm	
NOTE 2 Mid-span load = 1 470 N	
NOTE 3 Mean: 3,84 mm	
NOTE 4 Standard deviation: 0,28 mm (7,2%)	

Table B.11 — Sampled static torsional stiffness of composite tibias

Specimen number	Rotation rad
1	0,119
2	0,128
3	0,120
4	0,128
5	0,124
6	0,127
7	0,126
8	0,123
9	0,126
10	0,122

NOTE 1 Torque = 45 Nm

NOTE 2 Mean: 0,124 rad

NOTE 3 Standard deviation: 0,0032 rad (2,6%)

Table B.12 — Sampled dynamic bending strength of composite tibias

Specimen number	Peak bending moment Nm	Specimen number	Peak bending moment Nm
1	286	16	276
2	281	17	289
3	281	18	285
4	267	19	282
5	279	20	265
6	282	21	280
7	287	22	277
8	288	23	294
9	281	24	267
10	281	25	286
11	277	26	266
12	279	27	283
13	281	28	286
14	282	29	279
15	280	30	288

NOTE 1 Mean: 281 Nm

NOTE 2 Standard deviation: 7 Nm (2,5%)

Table B.13 — Sampled dynamic torsional strength of composite tibias

Specimen number	Peak torsional moment Nm
1	180
2	159
3	166
4	174
5	168
6	149
7	177
8	192
9	172
10	171
NOTE 1 Mean: 171 Nm	
NOTE 2 Standard deviation: 11,6 Nm (6,8%)	

Table B.14 — Sampled deflection of abdominal inserts

Specimen number	Force at 20 mm displacement N	Force at 40 mm displacement N	Force at 60 mm displacement N
1	1 012	1 897	3 036
2	1 044	1 897	3 004
3	1 075	1 897	2 973
4	1 012	1 866	2 846
5	980	1 897	2 783
6	1 012	1 929	3 036
7	1 012	1 866	2 783
8	1 012	1 866	2 751
9	1 012	1 866	2 909
10	1 044	1 897	2 973
Mean	1 021	1 889	2 909
Standard deviation	26,1 (2,56%)	21,1 (1,12%)	110,6 (3,80%)

Table B.15 — Sampled static torsion strength and deflection of knees

Specimen number	Rotation at 35 Nm deg	Maximum torque Nm	Rotation at maximum torque deg
1	23,00	91,38	40,00
2	22,00	93,90	40,30
3	21,40	91,38	40,30
4	18,20	87,11	36,80
5	19,44	88,82	37,08
6	19,70	88,82	37,98
7	21,06	90,95	40,95
8	21,06	89,67	40,68
9	19,44	87,11	37,98
10	19,80	87,11	39,40
Mean	20,51	89,62	39,15
Standard deviation	1,44 (7,01%)	2,27 (2,54%)	1,55 (3,95%)

Table B.16 — Sampled static valgus strength and deflection of knees

Specimen number	Rotation at 89 Nm deg	Maximum torque Nm	Rotation at maximum torque deg
1	20,88	133,22	25,50
2	20,70	129,81	25,74
3	20,20	129,38	24,91
4	20,60	134,08	25,92
5	20,88	131,09	25,81
6	20,08	128,10	25,49
7	19,75	135,36	24,48
8	20,88	129,81	25,92
9	20,88	130,66	26,82
10	20,64	128,53	26,19
Mean	20,55	131,00	25,68
Standard deviation	0,40 (1,95%)	2,44 (1,86%)	0,65 (2,53%)

Table B.17 — Sampled static axial strength of composite femurs

Test number	Load at failure N
1	32 671
2	36 113
3	34 107
4	32 639
5	34 579
6	34 588
7	36 856
8	34 663
9	36 109
10	34 592
Mean	34 692
Standard deviation	1 390 (4,0%)

B.4 Test methods

B.4.1 Frangible bone static bending deflection test (see 6.1)

The distance between support points defined in Table 7 corresponds approximately to the values defined by Yamada (1970). The applied radial loads correspond to about 50% of the ultimate load of each of the bones to provide an index of deflection in the linear force/deflection region.

B.4.2 Frangible bone static torsional deflection test (see 6.2)

The applied torsional loads of 69 N · m and 48 N · m correspond to about 50% of the ultimate load in torsion of each of the bones to provide an index of the linear torsion-deflection properties.

B.4.3 Frangible bone dynamic bending fracture test (see 6.3)

The defined impactor properties and conditions correspond approximately to conditions which ensure a bone fracture and are similar to those used by Kress, et al., (1990) in conducting cadaver tibia tests with 26 specimens. The mass and the speed are sufficient to ensure fracture.

The measurement procedures use commonly available sensor and data acquisition procedures which are compatible with ISO 6487:1987 and other measurement procedures defined in ISO 13232-4.

Extensive dynamic testing of the frangible bones has indicated that the forces measured in the CoP test procedures (while very consistent from run-to-run and along the length of the bone) are quite sensitive to differences in the details of the test apparatus. This sensitivity can be controlled by specifying the existing apparatus in great detail, so that all laboratories will be able to reproduce the required tests more accurately.

The details of the apparatus principally involve the features of the impactor used to develop the original CoP data including the impactor rails and bearings, the bone extensions, and the specimen supports.

B.4.4 Frangible bone dynamic torsional fracture test (see 6.4)

A load cell rather than an accelerometer is used on the impactor to eliminate the inertial effects present in the acceleration of the torque arm component. The use of a 0,025 m ± 0,003 m diameter impactor ensures precise definition of the impact point. Otherwise, the procedures are analogous to those for the frangible bone dynamic bending failure test.

B.4.5 Frangible femur bone static axial load fracture test (see 6.5)

The frangible femur static axial strength criterion is similar to that reported by Yamada (1970). Use of the criteria is intended to prevent axial failure of the bone at unrealistically low or high axial forces. The latter obviously could inappropriately influence the design of a protective device.

B.4.6 Frangible knee static strength and deflection test (see 6.6)

The frangible knee uses manufactured components to model the elastic and strength properties of cadaver knees in both the varus valgus and torsional directions. Compliant spring blocks are used to mimic the elastic properties of cadaver knees, and brass shear pins are used to mimic the ultimate failure loads of the knee complex. Representative testing of the manufactured frangible knee elements is required to ensure that the frangible knee responds in accordance with the cadaver knee performance data.

B.4.6.1 Apparatus (see 6.6.1)

The mechanical structure of the frangible knee constrains the induced rotation to occur about designed pivot point. As such, torque can be applied to the frangible knee of the MATD using the simple lever arm apparatus shown in Figure A.26.

The minimum length of 0,5 m was specified for a lever arm so that the magnitude of the load required to fracture the frangible knee elements would be limited to a level that can be applied manually.

The applied load and the rotation of the knee in the varus valgus and the torsional directions are measured with a load cell and a rotational potentiometer, respectively. These transducers allow for continuous monitoring and recording of the loads and displacements during the certification tests. The peak load and the corresponding rotation can be extracted from the recorded data and the loading rate can be determined from the slope of the applied load vs. time data.

B.4.6.2 Procedure (see 6.6.2)

Due to the strain rate sensitivity of the spring blocks used in the knee design, a quasi-static load application rate was chosen to ensure consistency in the frangible knee element certification results. A loading rate of 30 N · m/s ± 5 N · m/s was considered quasi-static in attaining the peak loads of 87 N · m to 132 N · m required to fracture the frangible knee shear pin elements. It is also a rate that was compatible with the apparatus used to test the frangible knee components.

B.4.7 Frangible abdomen test (see 6.7)

A 25 mm crushing anvil was used for the abdominal certification tests because it allowed the results to be compared directly to existing force/deflection corridors proposed by Cavanaugh, et al., (1986). Cavanaugh's corridors were derived from dynamic abdominal impacts on cadavers using a 25 mm diameter steel bar as an impacting anvil. The 25 mm anvil is also representative of the likely intrusive surfaces the abdomen would contact, namely, the motorcycle handle bars.

The force/deflection response of the polystyrene material used for the frangible abdominal insert is almost completely velocity independent. A quasi-static loading rate could, therefore, be used for the frangible abdomen certification test, and the results could still be compared to Cavanaugh's dynamic abdominal force/deflection corridors. A quasi-static loading rate of 450 N/s ± 150 N/s was chosen because it was a rate that could be applied with the test apparatus used during the development of the abdominal insert certification tests.

B.4.8 Motorcyclist neck dynamic axial torsion test (see 6.8)

The neck torsion test apparatus is designed to measure the axial stiffness of an impact test dummy neck in torsion. One end of the neck is twisted at a steady rate while the resistive torque is measured at the other end by a load cell. The power required to twist the neck dynamically is supplied by using a small amount of energy from a swinging pendulum. The pendulum has a mass of 40 kg $\pm$ 0,5 kg and moves at 4,2 m/s $\pm$ 0,2 m/s at the bottom of its swing, providing available energy of 352 J. Only about 35 J of energy are required to twist the neck, so using this amount from the swinging pendulum has negligible effect upon its speed.

The pendulum is connected by a wire rope to a 40 cm diameter disk that is mounted on a spindle. The spindle is restrained by a thick bushing and has a universal joint in line with it before being rigidly attached to the base of an inverted impact test dummy neck. The top of the neck, which is facing downward, is connected to an upper neck load cell mounted as a universal joint, as well. In this fashion, the neck experiences a pure torque in a pinned-pinned configuration without its bending stresses in torsion influencing its behaviour. At the bottom of its swing, the pendulum causes the rope to tighten and pull the disk into a circular motion. This causes the neck to twist at a rate proportional to the constant speed of the pendulum. The rope loops over a hook on the disk and disengages when the disk has turned approximately 115°. This allows the pendulum to continue its swing uninterrupted. A stop is provided to arrest the disk in rebound. A schematic of this test apparatus is shown in Figure A.28.

B.5 Marking (see 7.1)

The purpose of marking all frangible components is to enable tracing of the manufacturing process and conformity of production data.

B.6 Annex A (normative) Drawings for motorcyclist anthropometric impact special components

These are the drawings required to reproduce the modified Hybrid III components such that they comply with the specifications stated in clause 4 and the test methods described in clause 6.

Annex C
(normative)

Motorcyclist neck subsequent conformity of production test procedures

C.1 Flexion-bending and head forward displacement static test

Perform the procedure given in Table C.1.

Table C.1 — Procedures for flexion bending and head forward displacement static tests

Sequence	Procedure
1	Attach the neck load cell simulator shown in Figure C.1 and the neck calibration test fixture shown in Figure C.2 to the top of the motorcyclist neck. Total mass of the load cell simulator plus neck calibration test fixture, head pivot pin, and instrumentation shall be 850 g ± 50 g.
2	Shim the nodding blocks as needed to eliminate any gaps between the nodding blocks and the lower surface of the neck load cell simulator.
3	Verify that the neck load cell simulator is free to rotate with respect to the neck.
4	Note: If the neck pin is too tight rotation may be inhibited.
5	Attach the upper half of a HIII lower neck serrated mount[a] and a HIII bib simulator[a] to the bottom of the neck.
6	Adjust the mid neck angle adjustment to the full forward (flexion) position.
7	Mount the lower half of a HIII lower neck serrated mount to a vertical surface with the serrations facing in a downward direction.
8	Adjust the apparatus such that vertical surfaces of the lower mount are 90° ± 1° from horizontal.
9	Adjust the apparatus such that horizontal surfaces of the lower mount are 0° ± 1° from horizontal.
10	Mount the neck assembly with the lower neck serrated mount set at about 7° extension (head back).
11	Adjust the apparatus such that the top surface of the neck load cell is 90° ± 2° from horizontal.
12	Prepare to hang 20 kg ± 1 kg (total weight including the weight hanger and any required straps or cables) on the test fixture at the load application point designated in Figure C.4.
13	Press down on the back of the neck slider and release to remove any slack in the slider and spring.
14	Rock and rotate the neck load cell with respect to the neck to equalize the compression in the nodding blocks.
15	Measure the initial angle (in degrees) of the top surface of the neck load cell from horizontal.
16	Measure the initial x axis position (in mm) of the neck slider with respect to a fixed portion of the neck.
17	Slowly apply the weight to the neck assembly. The applied load shall increase from 0 kg to the full weight in no less than 3s and no more than 8s.
18	Measure the deflected angle of the top surface of the neck load cell from horizontal 15s ± 1s after the first application of weight.
19	Measure the deflected x axis position of the neck slider with respect to the same fixed portion of the neck used for the initial position measurement 30s ± 5s after the first application of weight.
20	Remove the weight from the neck.
21	Calculate the change in the angle of the neck load cell simulator.
22	Calculate the change in the x axis position of the neck slider.
23	Repeat the weight application and measurement process (C.1.11 to C.1.21) a total of five times, allowing 5 ± 1 min between applications.

Sequence	Procedure
24	Calculate the average change in angle and the standard deviation of the last three measurements as a percentage of the average.
25	Calculate the average change in x position and the standard deviation of the three measurements as a percentage of the average.

[a] A list describing one or more example products which meet these requirements is maintained by the ISO Central Secretariat and the Secretariat of ISO/TC 22/SC 22. The list is maintained for the convenience of users of ISO 13232 and does not constitute an endorsement by ISO of the products listed. Alternative products may be used if they can be shown to lead to the same results.

C.2 Extension-bending test

Perform the procedures given in Table C.2.

Table C.2 — Procedure for extension-bending static test

Sequence	Procedure
1	Attach the neck load cell simulator shown in Figure C.1 and calibration test fixture shown in Figure C.2 to the top of the neck. Total mass of the load cell simulator plus neck calibration test fixture, head pivot pin, and instrumentation shall be 850 g ± 50 g.
2	Shim the nodding blocks as needed to eliminate any gaps between the blocks and the lower surface of the neck load cell simulator.
3	Verify that the neck load cell simulator is free to rotate with respect to the neck.
4	Note: If the neck pin is too tight rotation may be inhibited.
5	Attach the upper half of a HIII lower neck serrated mount[a] and a HIII bib simulator[a] to the bottom of the neck.
6	Adjust the mid-neck serrated joint to the full forward (flexion) position.
7	Mount the lower half of a HIII lower neck serrated mount to a vertical surface with the serrations facing in the upward direction.
8	Adjust the apparatus such that the vertical surfaces of the lower mount are 90° ± 1° from horizontal.
9	Adjust the apparatus such that horizontal surfaces of the lower mount are 0° ± 1° from horizontal.
10	Mount the neck assembly with the lower neck serrated mount set to 3.5° extension (head to rearward).
11	Adjust the apparatus such that the top surface of the neck load cell is 90° ± 2° from horizontal.
12	Prepare to hang 20 kg ± 1 kg (total weight including the weight hanger and any required straps or cables) on the test fixture at the designated load application point.
13	Rock and rotate the neck load cell with respect to the neck to equalize the compression in the nodding blocks.
14	Measure the initial angle (in degrees) of the top surface of the neck load cell from horizontal.
15	Slowly apply the weight to the neck assembly. The applied load shall increase from 0 kg to the full weight in no less than 3s and no more than 8s.
16	Measure the deflected angle of the top surface of the neck load cell from horizontal 15s ± 1s after the first application of weight.
17	Remove the weight from the neck.
18	Calculate the change in the angle of the neck load cell simulator.
19	Repeat the weight application and measurement process (C.2.11 to C.2.17) a total of five times, allowing 5 ± 1 min between applications.
20	Calculate the average change in angle and the standard deviation of the last three measurements as a percentage of the average.

[a] A list describing one or more example products which meet these requirements is maintained by the ISO Central Secretariat and the Secretariat of ISO/TC 22/SC 22. The list is maintained for the convenience of users of ISO 13232 and does not constitute an endorsement by ISO of the products listed. Alternative products may be used if they can be shown to lead to the same results.

C.3 Lateral-bending test

Perform the procedures given in Table C.3.

Table C.3 — Procedures for lateral-bending static test

Sequence	Procedure
1	Attach the neck load cell simulator shown in Figure C.1 and calibration test fixture shown in Figure C.2 to the top of the neck. Total mass of the load cell simulator plus neck calibration test fixture, head pivot pin, and instrumentation shall be 850 g ± 50 g.
2	Shim the nodding blocks as needed to eliminate any gaps between the blocks and the lower surface of the neck load cell simulator.
3	Verify that the neck load cell simulator is free to rotate with respect to the neck (if the neck pin is too tight rotation may be inhibited).
4	Attach the upper half of a HIII lower neck serrated mount and a HIII bib simulator to the bottom of the neck.
5	Adjust the mid neck serrated joint to the full forward (flexion) position.
6	Mount the lower half of a HIII lower neck serrated mount to a vertical surface with the right side of the fitting up.
7	Adjust the apparatus such that vertical surfaces of the lower mount are 90° ± 1° from horizontal.
8	Adjust the apparatus such that horizontal surface of the lower mount are 0° ± 1° from horizontal.
9	Mount the neck assembly with the lower neck serrated mount set at 0 degrees.
10	The top surface of the neck load cell should be 87° ± 2° from horizontal.
11	Prepare to hand 20 kg ± 1 kg (total weight including the weight hanger and any required straps or cables) on the test fixture at the designated load application point.
12	Rock and rotate the neck load cell with respect to the neck to equalize the compression in the nodding blocks.
13	Measure the initial angle of the top surface of the neck load cell from horizontal.
14	Slowly apply the weight to the neck assembly. The load applied to the neck shall increase from 0 kg to the full weight in no less than 3 s and no more than 8 s.
15	Measure the deflected angle of the top surface of the neck load cell from horizontal 15s ± 1s after the first application of weight.
16	Remove the weight from the neck.
17	Calculate the change in the angle of the neck load cell simulator.
18	Repeat the weight application and measurement process (C.3.11 to C.3.17) a total of five times, allowing 5 ± 1 min between applications.
19	Calculate the average change in angle and the standard deviation of the last three measurements as a percentage of the average.

C.4 Torsion test

Perform the procedures given in Table C.4

Table C.4 — Procedures for torsion static test

Sequence	Procedure
1	Verify that the torque extension arm shown in Figure C.3 weighs 920 g ± 10 g and has a c.g. location 348 mm ± 4 mm from the centre of the neck load cell simulator (when attached to the neck load cell simulator).
2	Verify that when attached to the neck load cell simulator as shown in Figure C.4, the torque extension arm has a load application point 700 mm ± 5 mm from the centre of the neck load cell simulator.
3	Verify that when attached to the neck load cell simulator, the load application point on the torque extension arm is 18 mm ± 5 mm above the centre of the head pivot pin.
4	Attach the neck load cell simulator and calibration test fixture to the top of the neck. Total mass of the load cell simulator plus neck calibration test fixture, head pivot pin, and instrumentation shall be 850 g ± 50 g.
5	Shim the nodding blocks as needed to eliminate any gaps between the blocks and the lower surface of the neck load cell simulator.
6	Verify that the neck load cell simulator is free to rotate with respect to the neck (if the neck pin is too tight rotation may be inhibited).
7	Attach the upper half of a HIII lower neck serrated mount[a] and a HIII bib simulator[a] to the bottom of the neck.
8	Adjust the mid neck serrated joint to the full forward (flexion) position.
9	Mount the lower half of a HIII lower neck serrated mount to a vertical surface with the right side of the fitting up.
10	Adjust the apparatus such that the vertical surfaces of the lower mount are 90° ± 1° from horizontal.
11	Adjust the apparatus such that the horizontal surfaces of the lower mount are 0° ± 1° from horizontal.
12	Mount the neck assembly with the lower neck serrated mount set at 0°.
13	Adjust the apparatus such that the flat edge on the back of the of the neck load cell is 90° ± 2° from horizontal.
14	Prepare to hang 3.2 kg ± 0.2 kg (total weight including the weight hanger and any required straps or cables) on the extension arm at the designated load application point.
15	Rock and rotate the neck load cell with respect to the neck to equalize the compression in the nodding blocks.
16	Measure the initial angle of the flat edge on the back of the neck load cell from horizontal.
17	Install the torque extension arm (without the extra 3,2 kg weight) such that the rod is forward from the neck.
18	Slowly apply the 3.2 kg weight to the extension arm 700 mm from the centre of the neck load cell. The additional load applied to the neck shall increase from 0 kg to the full weight in no less than 3 s and no more than 8 s.
19	Measure the deflected angle of the flat edge on the back of the neck load cell from horizontal 15 s ± 1 s after the first application of 3,2 kg weight.
20	Remove the weight from the extension arm.
21	Remove the extension arm.
22	Calculate the total change in angle due to the weight of the extension arm and the additional 3,2 kg.
23	Repeat the attachment of the extension arm, weight application and total angle measurement process (14 to 22) a total of five times, allowing 5 ± 1 min between applications.
24	Calculate the average total change in angle and the standard deviation of the last three measurements as a percentage of the average.

[a] A list describing one or more example products which meet these requirements is maintained by the ISO Central Secretariat and the Secretariat of ISO/TC 22/SC 22. The list is maintained for the convenience of users of ISO 13232 and does not constitute an endorsement by ISO of the products listed. Alternative products may be used if they can be shown to lead to the same results.

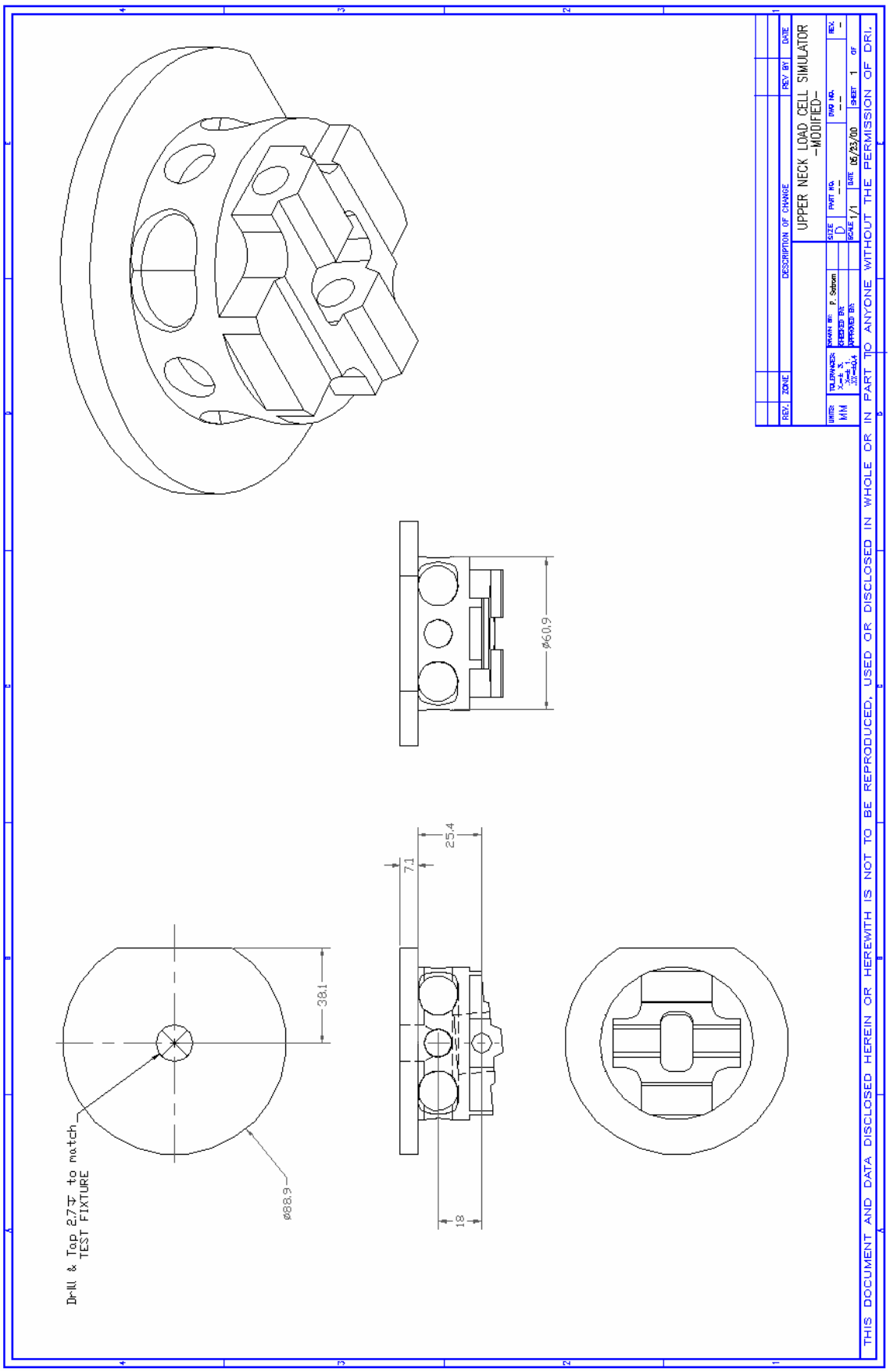

Figure C.1 — Neck load cell simulator

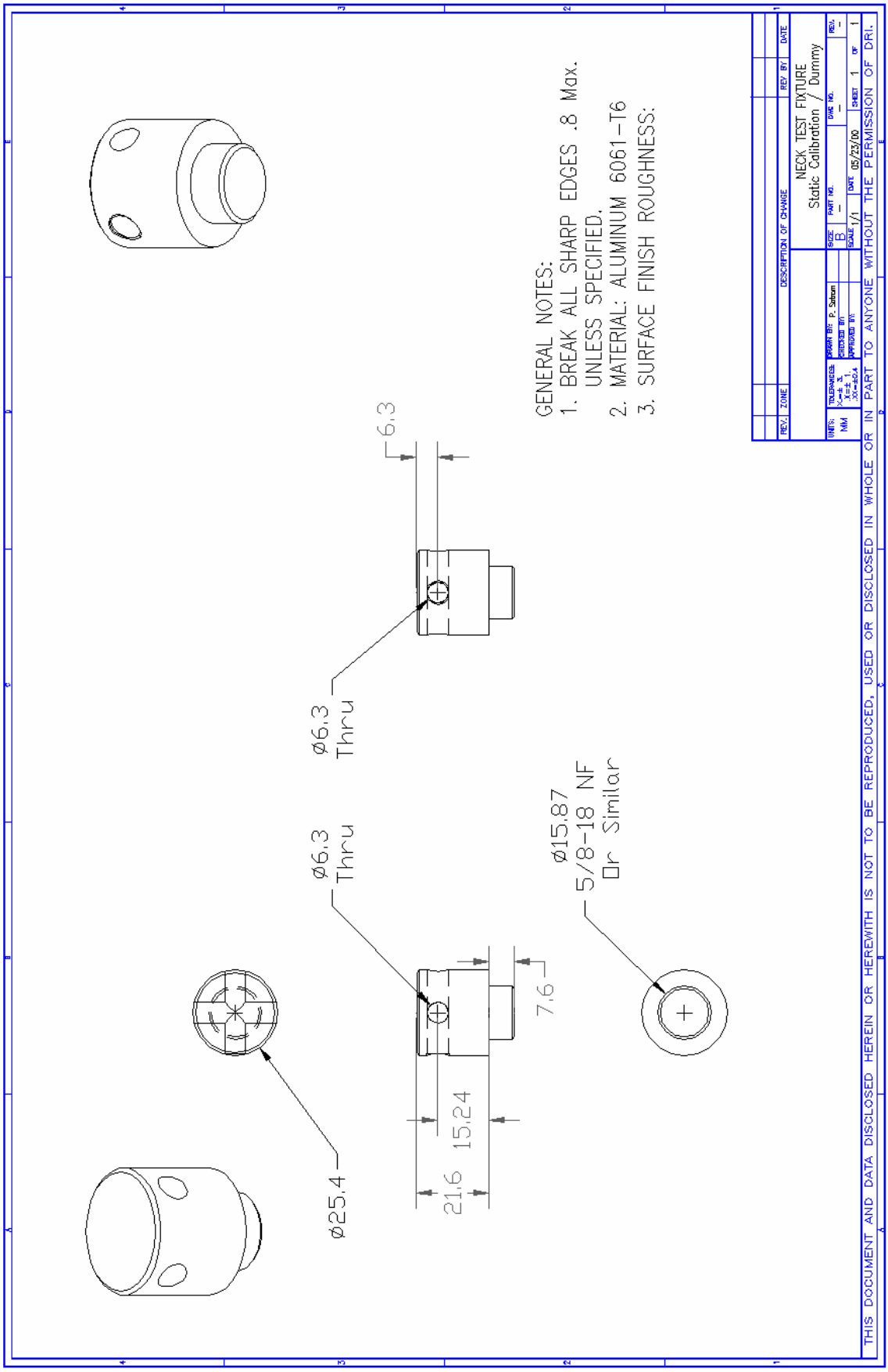

Figure C.2 — Neck calibration test fixture

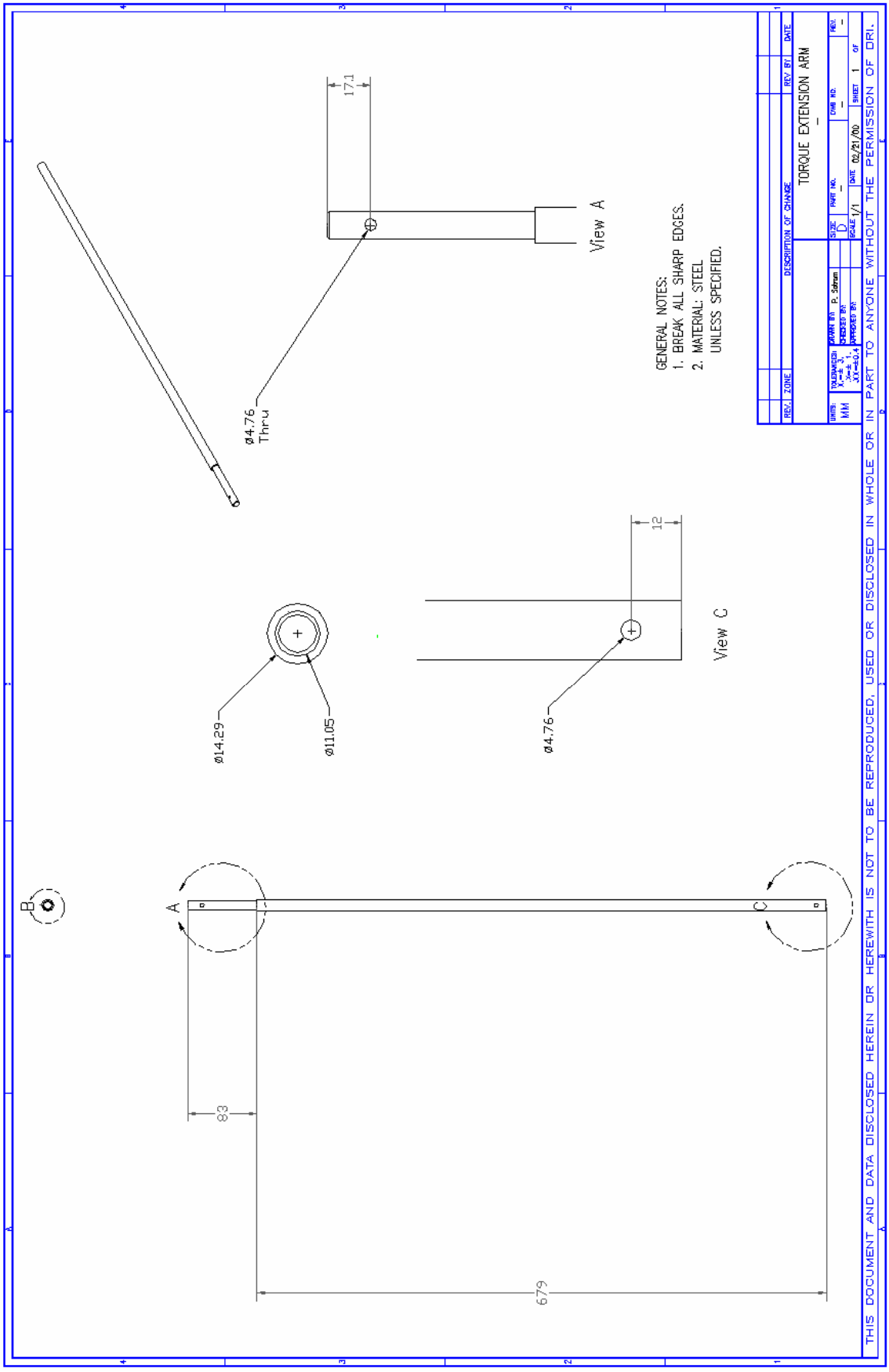

Figure C.3 — Neck calibration torque extension arm

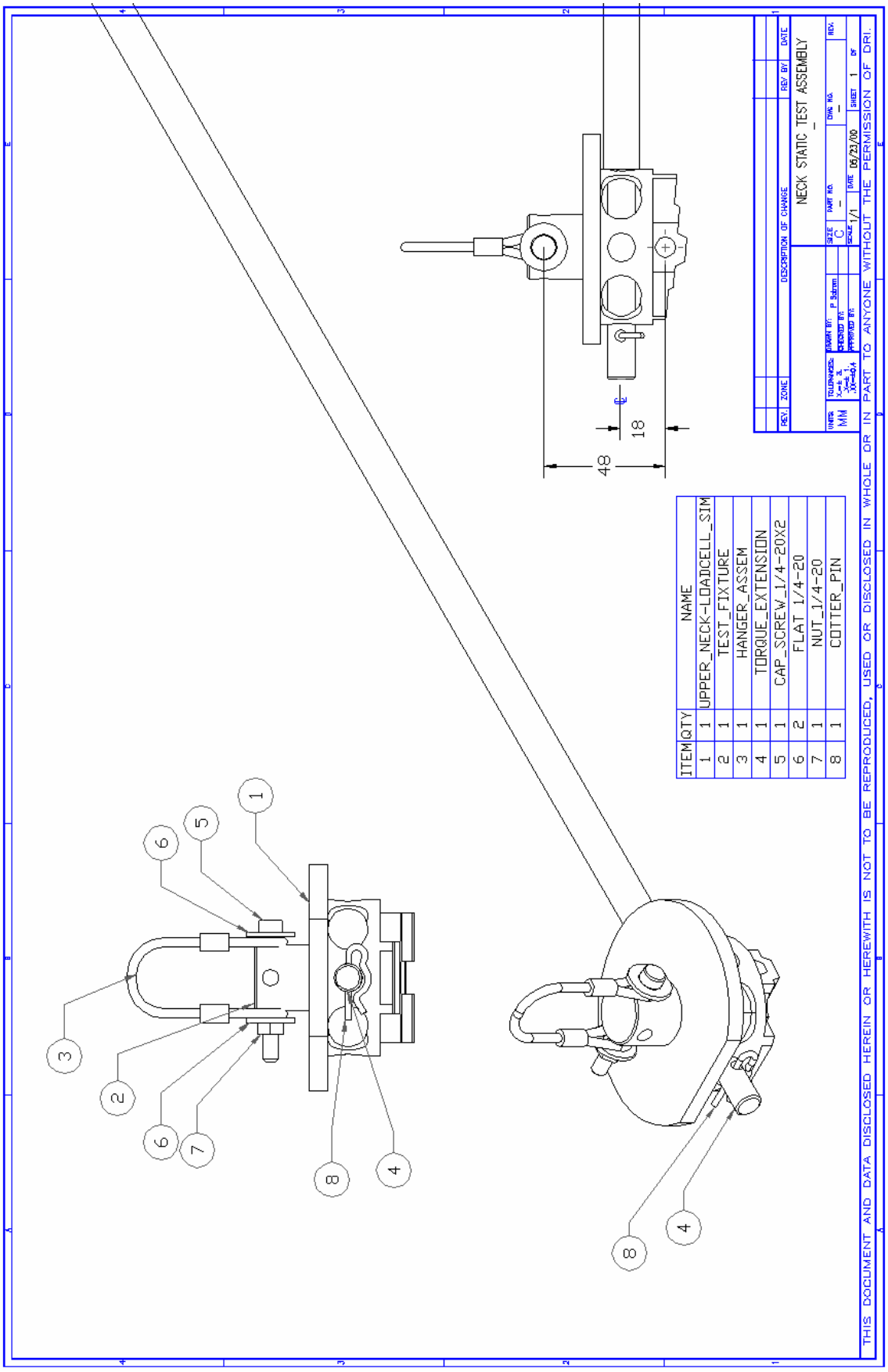

Figure C.4 — Neck calibration assembly

ICS 43.140

Price based on 88 pages